REX NORMAN BAYLISS, M.Sc.

THE TOUGHNESS OF A HOT WORK DIE STEEL.

Re-Submitted for  :  Doctor of Philosophy Degree.
November 1974.

# SYNOPSIS.

The literature dealing with the practical use of fracture mechanics
in the better understanding of crack propagation characteristics of
industrially used steel products, with particular reference to hot work
die steels, has been reviewed.

The effect of forging reduction and heat treatment on the fracture
toughness of B.S.S. 224 No. 5. nickel-chromium-molybdenum hot work die
steel has been determined in the ambient to $500^{o}$C. temperature range.

Arising from these tests the expected rise in fracture toughness from
ambient temperature to $100^{o}$C. occurs, which is maintained up to $300^{o}$C;
thereafter a decay takes place and the fracture toughness at $500^{o}$C. is
nearly identical to that at room temperature. Temper embrittlement and
the possibility of dynamic strain ageing appear to contribute to the
loss of elevated temperature toughness.

Stereoscan fractrographic analysis showed little variation between maximum
and reduced toughness when examined at relatively low magnifications.
However, at high resolutions it was observed that a cleavage pattern was
present with maximum toughness, whilst a dimple structure surprisingly was
associated with falling toughness.

Upset forging appears to offer superior fracture toughness and mechanical
properties compared to direct forged die block material. Increasing
forging reduction did not affect properties measured in the longitudinal
direction : transverse properties were impaired by heavier amounts of
forging.

Drop forge Works trials of No. 5. die steel inserts, used in
conjunction with a 4-ton counter-blow hammer, manufacturing
crankshafts, were assessed for die production life.  The insert
which produced the largest number of drop forgings also possessed
superior fracture toughness at room temperatures.

It was unfortunate that in assessing toughness, validity criteria
were not met. However, comparison between inserts was still possible.

A possible practical and economic consideration has arisen from these
results in that the drop-forger, by selecting a die block pre-heating
temperature of $100^{\circ}$C. (this being the temperature at which maximum
crack resistance occurs), and then by the judicious application of
coolant to ensure that the die block temperature does not exceed $300^{\circ}$C.
a more consistent and improved die life may result.

The use of fracture toughness data to predict the most suitable
operating temperature conditions has demonstrated the limitations of
using conventional notch toughness assessment, which should now be
replaced by substituting crack propagation testing techniques.

Additionally, any die steel development should take cognizance of the
fracture toughness parameter which should be included in any property
assessment requirement for hot work die steels.

# CONTENTS.

# CONTENTS.

# GLOSSARY AND SYMBOL DEFINITION.

Plane Stress.                      a condition of loading in that all stresses acting at the crack tip are in one plane.

Plane Strain.                     a condition of loading in that all deformation strains acting at the crack tip are in one plane.

Stress Intensity Factor.         the value which determines how much a stress intensifies at a sharp crack tip.

Plane Strain Critical Stress Intensity Factor, $K_{1c}$.    the particular value of the critical stress intensity factor where loading is under plane strain conditions.

Plane Stress Critical Stress Intensity Factor, $K_c$.    the value of critical stress intensity factor where loading is under plane stress conditions.

| | | |
|---|---|---|
| $a$ | $=$ | crack length. |
| $B$ | $=$ | test piece thickness. |
| $W$ | $=$ | test piece width. |
| $P$ | $=$ | applied force. |
| $P_Q$ | $=$ | particular value of P. |
| $Y$ | $=$ | stress intensity co-efficient. |
| $\sigma y$ | $=$ | 0.2% proof stress. |
| $K$ | $=$ | stress intensity factor. |
| $K_1$ | $=$ | plane strain stress intensity. |
| $K_{1c}$ | $=$ | a critical value of $K_1$. |
| $K_Q$ | $=$ | a provisional value of $K_{1c}$. |

$$\left\{ \begin{array}{l} K_1 \\ K_{11} \\ K_{111} \end{array} \right. \quad = \quad \text{stress intensity factor for different modes.}$$

<u>INTRODUCTION</u>.

## 1. TOUGHNESS OF A HOT WORKING DIE STEEL.

Little fundamental work contributing to the better understanding of crack propagation in hot work die steels has been reported, and the aim of this thesis is to explore the subject more fully.

The toughness of die steels has been considered difficult to measure and, until recently, only the Izod or Charpy notch bar tests allowed toughness values to be compared. This Izod or Charpy test, however, does not separate the two mechanisms contributing to a fracture process – the initial generation and the subsequent propagation of a crack. Consequently, these notch bar tests seldom relate to service performance, even if they are carried out at elevated temperatures. The distinction must be drawn between die materials that crack superficially, but still have a useful service life, and those that fail in a brittle manner. With the introduction of fracture toughness testing a more meaningful measurement of the crack resistance of die materials, (a function which conventional notch bar tests cannot accomplish) could be of scientific and commercial importance. The fracture toughness characteristics of commercially produced carbon and alloy steels have only recently been actively studied, whilst little information is available for die steels.

### 1.1 FACTORS AFFECTING DIE LIFE.

The two major factors governing the performance of hot work die steel tools are in the manufacture of the die block itself and in the methods of use within the metal-forming industries. In the first instance, the die block manufacturer can alter his hot working and thermal treatments thereby affecting the performance of the block and, in the second case,

the process variables within the metal forging industries also have a similar effect. These variables can exert a significant influence upon the performance of a hot work die tool with consequent economic implications for the drop forger who expects die blocks to produce a specified minimum number of drop forgings before the die tool must be re-machined or scrapped. Failure to achieve this minimum number of components can result in production and financial loss.

## 1.2 THE PRODUCTION OF DIE BLOCKS.

Direct forging and upset forging are the two methods used for manufacturing die blocks. The object of upset forging is to minimise the differences between the longitudinal plane mechanical properties from those existing in the transverse plane. Therefore after the conversion of the ingot into a billet (by either forging or rolling) individual slices are sectioned from the billet. To further consolidate the original longitudinal grain fibre, hot working should be continued by forging to the desired dimensions. For example, with a cube-shaped die block hot working should be continued by forging each of the six sides of the die block.

Increased forging deformation with the direct hot working method produces inferior transverse tensile ductility and notch toughness, particularly when forging reductions are greater than 5:1.          (1).

In the heat treatment of die blocks even though closely controlled thermal cycles are employed marked variations in hardness occur in which required specification hardness ranges are not achieved.   No satisfactory explanation for this re-treatment situation was advanced by Bayliss (1), as steelmaking specifications, together with Jominy hardness and grain size, are controlled.

Table 1. indicates these hardness ranges which constitute the basis of die block sales.

## TABLE NO. 1.

### HARDNESS CONVERSION TABLE.

showing standard hardness ranges of heat treated die blocks.

| 3000 Kg. load. Diameter Brinell impression. mm. | | 10 mm. ball. Brinell Hardness Number. | TENSILE STRENGTH. | | Rockwell "C". |
|---|---|---|---|---|---|
| | | | tonf/in$^2$ | MN/m$^2$ | |
| 2.95 | A | 429 | 94 | 1452 | 45.5 |
| 3.00 | | 415 | 91 | 1408 | 44 |
| 3.05 | | 401 | 88 | 1359 | 43 |
| 3.10 | B | 388 | 85 | 1314 | 41.5 |
| 3.15 | | 375 | 82 | 1266 | 40 |
| 3.20 | | 363 | 80 | 1236 | 38.5 |
| 3.25 | C | 352 | 77 | 1191 | 38 |
| 3.30 | | 341 | 74 | 1143 | 36 |
| 3.35 | | 331 | 73 | 1130 | 35.5 |
| 3.40 | D | 321 | 71 | 1098 | 34 |
| 3.45 | | 311 | 68 | 1050 | 32.5 |
| 3.50 | | 302 | 66 | 1019 | 31.5 |

## 1.3     VARIATIONS AFFECTING PERFORMANCE IN THE DROP FORGE.

The practice adopted by the drop forger with his forging procedure can exert a profound influence upon the performance of die blocks. Such practices include :-

(a) Preheating of the die block.
(b) Die Design.
(c) Lubricants used.
(d) Re-heating of the stock bar from which drop-forgings are produced.
(e) Mechanical damage.

In their studies of the life of drop forging dies Aston & Muir (2) found that a significant factor in determining the minimum life of a die block is the weight of the drop forging itself as increasing weight decreases life. Also draft angle and fillet radii are important factors to be considered. They found that the use of a correct size forging unit for any particular drop forging was important in achieving optimum die life. Forging units possessing excessive driving energy contribute to an inferior die life.

Die blocks are normally withdrawn from service because of damage from one of the following :

(a) Gross cracking.
(b) Thermal fatigue cracking.
(c) Mechanical fatigue cracking.
(d) Metal removal by deformation.
(e) Erosion.

It has been observed in the metallurgical examination of used die tools, which apparently possess similar metallurgical and mechanical properties, that varying die life has been obtained. No truly satisfactory explanation can be given for these variations, as the drop forger reports that similar orthodox workshop practices have been employed.

The drop forging industry has long sought the ideal low priced die

material which incorporates high wear resistance together with freedom from premature cracking, and which presents no difficulties in the die sinking process. The No. 5. grade of die steel is favoured by drop-forgers for use as a general-purpose hot work die steel which, whilst not possessing the ideal conditions previously noted, at least is regarded as a useful substitute. The crack resistance of die steels, particularly at changing sections within the die impression face, has long since been of interest to the drop-forging industry: in consequence, the toughness parameters of die steels have special significance.

2. <u>LITERATURE SURVEY</u>.

## 2.1      FRACTURE MECHANICS.

From the research data published the following survey is representative
of general aspects on this subject.

Before the acceptance of fracture mechanics being relevant to failure
analysis, Tipper (3) concluded in her paper that after fifteen years devoted
to the study of testing methods, and their application to the selection of
m aterial to resist brittle fracture, there was no general agreement
on what test should be applied or what standards should be set.

Wells (4) surveyed the published work on fracture mechanics, and gave a
historical review. At the same 1959 Conference, Irwin (5) commented that the
subject of fracture mechanics had been of interest for the past twelve years,
but more than half of that time was required merely to earn the right to
such a respectable title.

The joint authorship of Irwin & Wells (6) gave a comprehensive survey of the
progress in fracture mechanics citing investigators who assessed various
test piece shapes and sizes: starting with Griffith who, in 1920, developed the
concept that a pre-existing crack can only extend when the amount of elastic
strain energy released upon growth of the crack equals or exceeds the surface
energy of the new-formed crack.   Griffith assumed that brittle amorphous
materials, such as glass, contained many small invisible cracks and that
fracture resulted when the applied stress caused these fine cracks to grow
to macroscopic size. Griffith's reasoning, whilst not strictly applicable
in metals, was the basis for development of the concept of fracture
toughness.

Griffith (7) used the stress analysis of Inglis (8) in considering the
energy distribution around an elliptical crack in a thin plate of infinite

length and width. Griffith considered the condition when the ellipse
was transformed into a thin crack that could extend when the total energy
in the system remained unchanged as the crack grew. The Inglis formula
provided a solution for the stress distribution around an internal crack
with the maximum stress being given by

$$G \text{ max.} = 2 G_0 \sqrt{C/P}.$$

Where $G_0$ is the applied stress remote from the crack, 2C is the crack
length, Whilst P. is the radius of curvature at the ends of the major axis
of the elliptical crack. Because $G$ max. can be indeterminate without
knowing the generally unmeasurable quantity P., Griffith developed an
analysis based upon energy considerations. From the stress distribution
around an elliptical crack he calculated the elastic energy per unit of
volume stored in the material and obtained for a plate of uniform thickness :

$$U = \pi C^2 G_0^2/E.$$

Where U. is the elastic energy stored in the plate ahead of the crack
front: E. is Young's modulus. The other terms being the same as those
previously used. The above expression is applicable to thin plates only,
where the thickness direction stress is zero. For thick plates, wherein
thickness direction stresses develop as a consequence of a non-uniform
Poisson's ratio contraction at the apex of a notch, the thickness direction
strain is considered to be equal to zero. This reasoning led to the
familiar Griffith formula $- G_0^2 = \dfrac{2 \propto E}{\pi C}$

where $G_0$. is the applied stress, E. being the elastic modulus,

$\propto$ the surface energy.

The previous analysis, involving the application of classical elastic theory, applies only to isotropic materials that behave in a linear elastic manner.

Irwin (9) and Orowan (10) stated that a plastic term should be added to the surface tension in the Griffith equation as, even with a very brittle material, using the formula had shown that the calculated strength values for known crack lengths erred considerably.

Irwin's desire was to find a reliable design criterion for predicting the stress at which rapidly propagating fracture will occur. This is essentially a macroscopic theory that is concerned with cracks that are a tenth of an inch in length or greater. The crack extension force G. measured in units of in.-lb/in$^2$ is the quantity of stored elastic strain energy released from a cracking specimen as the result of the extension of an advancing crack by a unit area. When this quantity reaches the critical value Gc. the crack will propagate rapidly and represents the fraction of the total work expended on the system, which is irreversibly absorbed in local plastic flow and cleavage to create a unit area of fracture surface. Thus, Irwin's "Gc" factor can be considered to be equivalent to Orowan's factor "P" in the modification of the Griffith formulae. Incorporating the factor "P" expressed the condition of extending the crack by plastic work, the difference being that the Irwin's modification factor Gc. is experimentally determined.

The energy absorbed in plastic flow has been called by various names, such as crack propagation energy or plastic surface work, but the term generally used is "fracture toughness". The symbols used to designated fracture

toughness "Gc" or "Glc" are due to Irwin. It has been demonstrated that the value of Gc. is many orders of magnitude larger than the surface tension      : therefore, the Griffith equation was modified to include the process involving plastic flow :

$$\mathcal{G}_{c.} = EGc / \pi C.$$

where $\mathcal{G}_{c.}$ is the value of the gross stress remote from the crack necessary to cause an internal crack of length 2C. to propagate.

The approach adopted by Irwin led to the hope that the fracture toughness parameter Gc. would be a unique value for a given material which could be evaluated by progressively loading any test specimen of suitable geometry, and observing the onset and subsequent crack propagation characteristics until rapid fracture occurred in the material under test.

The concepts of fracture toughness of metals were surveyed by Barnby (11) and others (12 & 13), who provided Materials Scientists with a sound introduction to fracture mechanics and explained how such knowledge could be applied to engineering problems without over-emphasizing the mathematical background.

A similar lucid explanation on toughness testing was given by Steigerwald (14), who dispensed with involved mathematics and gave an admirable simple, straight-forward review of the fracture toughness theory, together with a discussion on test piece geometry used with fracture toughness testing.

The application of fracture toughness techniques was studied by Winne & Wundt (15) in the testing of large notched steel discs. High rotational

speed was used to propagate fracture. These laboratory tests simulated
the working environment of large rotor forgings in which catastrophic
failure had been reported from the U.S.A. in the period 1954–1956.
From the investigational work carried out during this period better
understanding of the inspection and permissible defect orientations
was postulated for these large generator rotor forgings. The laboratory
data obtained clearly showed, when compared to actual service failures,
that the starting cracks had propagated to a size of several inches before
rapid and catastrophic failure took place.

Similarly, concerning himself with the toughness of a large industrial
forging, Wessell (16) used large flat notched and un–notched specimens
selected from a 36" diameter x 38'-0" long (915 mm x 9 metres approximately)
forging, manufactured to a .25% carbon, 3.0% nickel, .25% chromium,
.50% molybdenum, 0.08% vanadium composition, being air hardened and
tempered to 260 B.H.N.   The relationship between cracked notch to plain
tensile properties was studied in association with the fracture
appearance transitional characteristics in similar temperature regions
in which the grade of steel under discussion was in everyday use.  The
presence of pre–existing cracks, and the geometrical size, was shown to
exert an influence upon brittle fracture; thus an increase in the crack
size in a constant thickness ratio decreased the fracture strength in
proportion to the inversed square root of the crack length.

A great deal of work has been accomplished, using relatively small section
material, in the study of fracture resistance.  Yen & Pendleberry (17)
used two steels, of the following analyses, to establish a relationship
between hardness and fracture resistance.

| Analyses. | H.11. % | A.I.S.I. 4340. % |
|---|---|---|
| Carbon | 0.40 | 0.42 |
| Silicon | 0.97 | 0.28 |
| Sulphur | 0.011 | 0.008 |
| Phosphorus | 0.006 | 0.012 |
| Manganese | 0.21 | 0.77 |
| Nickel | – | 1.82 |
| Chromium | 5.08 | 0.85 |
| Molybdenum | 1.24 | 0.24 |
| Vanadium | 0.58 | – |

It was found when these two steels had been heat treated to achieve 265–285 k.s.i., that shallow cracks less than 0.020" long (·508 mm) and 0.010" deep (.254 mm) did not adversely affect the toughness but larger cracks did reduce toughness significantly.

The influence of non-metallic inclusions upon the toughness of steels has been studied by Birkle, Wei & Pellissier (18) who investigated the plane strain fracture toughness of a series of steels containing – .45% carbon, 2% nickel, 1% chromium, .40% molybdenum with differing sulphur contents –(such steels having slightly higher nickel and molybdenum contents than No. 5. die steel). The onset of plane strain fracture instability on their series of specimens was controlled by the reduction of sulphide inclusions, and that other parameters being satisfactory the level of $K_{1c}$ is determined by the density and distribution of such sulphide inclusions. The lowest sulphur content of 0.008% gave the highest fracture toughness.

The influence of impurities and cleanliness was also considered by Cottrell and Langstone (19) who determined $K_{1c}$ values by using single-edge notch fatigue cracked specimens of a 3% chromium-molybdenum steel and .18% nickel, 1.2% titanium mar-ageing steels. Included in the study was the effect of varying the forging reduction, heat treatment and melting

processes. $K_{1c}$ values were also determined from material adjacent to the failure of a 36" diameter rocket case, wherein it was shown that the failure stress can be predicted from the knowledge of defect size and the material $K_{1c}$. Toughness values were improved when the material received a greater amount of hot working. Additionally, vacuum induction melted steels possess superior $K_{1c}$ values to those present when air melting had been carried out, but the greatest improvement of all was noted when impurity contents of sulphur, arsenic and tin were reduced to a low content.

The literature survey has failed to reveal any information on the fracture toughness of No. 5. die steel or similar hot work tool steels, although a considerable amount of testing has been done at ambient temperature using 5% chromium, 1% tungsten, .50/1.0% vanadium, 1% molybdenum steels, because such an alloy has found use in the nuclear and space programmes in addition to its long-standing use in the metal forming industries.

Of data published concerning fracture toughness of engineering materials the following four investigations have been directly concerned with hot work die steels.

## 2.2     FRACTURE TOUGHNESS OF HOT WORK DIE STEELS.

Two well-known die steels were examined by Barnby and Bayliss [20] who showed that differences in toughness exist between the following materials :-

(a)                                           %

    Carbon                          0.40
    Sulphur                         0.040 maximum.
    Phosphorus                      0.040 maximum.
    Manganese                       0.60
    Nickel                          0.30
    Chromium                        3.25
    Molybdenum                      1.00
    Vanadium                        0.20

(b)

    Carbon                          0.20
    Sulphur                         0.025 maximum.
    Phosphorus                      0.025 maximum.
    Manganese                       0.65
    Nickel                          2.9
    Chromium                        0.90
    Molybdenum                      2.9

It was found that at ambient temperature the $K_{1c}$ values are sensitive to structural variations through the thickness of the material and that the resistance of these steels to the propagation of sharp internal cracks can bear no relationship to the toughness measured by Izod impact tests.

Alloy additions to the nickel–molybdenum die steels were studied by Holloway & Hopkins (21), who investigated the addition of up to 10% cobalt in die material (b) used by Barnby & Bayliss. It was found that 3% cobalt was the optimum addition, and slight benefit to ambient temperature fracture toughness was evident, but amounts over this impaired toughness.

The 5% chromium grade of hot work die steels was assessed by Firth & Garwood (22), who compared the fracture toughness of a die steel possessing a chemical compositional range –

                                                    %
    Carbon                          0.34/0.37
    Chromium                        5.03/5.24
    Molybdenum                      1.29/1.40
    Vanadium                        0.08/1.12

in the air and vacuum re-melted steelmaking conditions to those present
with an alloy containing –

|            | %    |
|------------|------|
| Carbon     | 0.44 |
| Chromium   | 5.42 |
| Molybdenum | 2.08 |
| Vanadium   | 0.53 |

This latter steel gave toughness values superior to the previous type
of alloys which constitute the commercially produced range of 5% chromium
hot work die steels. It was observed that if the heat treated structure
contained uniformly distributed carbides, $K_{1c}$ values showed no
directionality, although conventional mechanical properties demonstrated
that tensile ductility in the transverse direction was inferior to that
existing in the longitudinal plane.

The vacuum re-melted material offered no significant improvement in
fracture toughness over the air melted steels.

The only instance of the fracture toughness of cast rather than wrought
hot work die steel was reported by Younkin & Jacobson, (23), who assessed
two cast forging dies possessing 5% chromium, 1.5% tungsten,
1.5% molybdenum, on which production data had been obtained : one die
block achieving an increase in useful working life of 50% over the other.
By using fatigue pre-cracked Charpy specimens a significant difference
in fracture toughness was found. The die which had given the worst
service performance also possessed the lowest fracture toughness.

These four investigations of hot work die steels measured the
fracture toughness at room temperature, which is of limited value if the
actual die tools are operating at elevated temperatures within their normal
working environment.

In drop-forging, the effect of heat transfer from the stock material
being hot worked to the die impression surface must be taken into
account. Any study of crack propagation of die materials must therefore
be measured at temperatures up to $500^{o}C$. which is near to the
hot working conditions, although in certain small parts of the die
impression, temperatures in excess of $500^{o}C$. have been reported (24).
It should be recalled that the alloy compositions of the 5% chromium grade
of die steel are superior to the standard $1\frac{1}{2}$% nickel-chromium-molybdenum
No. 5. die steel.Even though the 5% chromium alloy content steel is
used within the drop-forging industry, its application is normally
limited by size and cost.

The literature survey has failed to reveal any information concerning
fracture toughness parameters at temperatures in excess of $120^{o}C$.
The aim of this investigation is to remedy these deficiencies by
comparing the fracture toughness of the nickel-chromium-molybdenum
steel at a variety of temperatures, so that a better understanding of
crack propagation of hot work die tools can be made.

Many industrial engineers still regard with suspicion the application
of fracture mechanics to everyday engineering problems despite the
amount of data presented to them concerning fracture toughness.

A similar unconnected relationship between materials and everyday
service conditions arises with AISI 4340 and H.11, in which their toughness
has been assessed on applications other than die tools.

3. <u>LINEAR ELASTIC FRACTURE MECHANICS.</u>

3.1    <u>PHILOSOPHY OF TESTING.</u>

The three basic modes of failure treated by fracture mechanics relate

to the way in which the direction of the fracture process, with

corresponding crack surfaces move under applied loads. (Fig 1).


Mode 1.    is the opening mode, the crack surfaces move
           opposite and perpendicular to each other.

Mode 11.   is the forward sliding mode. The two crack surfaces
           move in approximately the same plane and in a
           direction perpendicular to the line of the crack
           tip.

Mode 111.  this is called the tearing mode. The two corresponding
           crack surfaces move in approximately the same plane
           and in a direction which is parallel to the line of
           the crack front.


Mode 1. is the most important mode from the point of view of low stress

fracture and, consequently, has been studied in greater detail than the

other two modes.

## 3.2   CRACK PROPAGATION CRITERIA.

It will be recalled that it was Griffith, in the early 1920's, who
observed for the first time the difference between the theoretical
fracture strength of crystals to those obtained by experimentation.
His original theory was applicable only to brittle solids, such as
glass, and stated that crack propagation will take place when the
elastic strain energy is decreased, and is at least equal to the
energy required to create the new crack surface.

From these early beginnings many sophisicated theories of crack
propagation criteria have been advanced in order that the study of
brittle fracture can be more fully understood. Various test piece
geometries and associated differing stressing systems have been
quantitatively assessed.  However, all these theories are based upon
a simple property of the material termed Kc. which is called the
fracture toughness or the critical stress intensification value at the
crack tip, at which fast crack propagation will occur in the
material being assessed. This Kc value is a material property, just
in the same way as engineers today consider that yield and tensile
strengths are material properties.

The understanding of the material constant Kc. can be furthered by
considering the local stress distribution at the tip of a crack. For a
two-dimensional example of crack propagation, based upon the plane
theory of elasticity, the following illustration, (Fig 2A) will
suffice.

If a uniform applied stress $\sigma$ a is applied to the specimen the local
tensile stress   $\sigma$ y at the notch root is theoretically infinite at the
actual notch root where x equals 0, and rapidly decreases as x increases.

The mathematical relationships developed by Irwin in the advancement of
fracture mechanics was based upon restricting considerations to the
region very close to the crack tip : this is where x is small and is the
important area as far as crack propgation is concerned. The local stress
then decreases according to the equation :

$$\sigma\, y = \frac{K_1}{\sqrt{2\pi}\ x}$$

(1)

$K_1$ is designated the stress intensification factor and describes the level of local stress distribution.

$K_1$ depends on the applied stress $G_a$ and if the applied stress is increased then the $K_1$ stress intensity factor increases: in consequence, the local stress distribution increases as shown in Fig 2A.
Finally $K_1$ attains a critical value $K_{1c}$, at which the local stress is high enough to allow the crack tip to propagate forwards.
Thus, $K_{1c}$ represents the maximum value of the local stress distribution which the material being evaluated can withstand at the point of fracture. Since $K_1$ increases with the applied stress $G_a$, the degree that the stress intensity factor rises with the applied stress is expressed :

$$K_1 = Y \quad G_a \quad \sqrt{c} \tag{2}$$

Y. being a geometrical constant and c. is the depth of notch, (Fig 2A).

From this equation it can be seen in principle how the material constant $K_{1c}$ can be measured because if Y. and c. are constant for the notched specimen, all that remains to incorporate in the equation is when the particular critical value of a. is reached, this being the point at which fracture occurs.

In some situations three-dimensional considerations must be taken into account. Cracks may be partially or fully embedded in a plate and have a simple geometry: stresses are generated in the x and z directions as well as in the y direction. Such stresses are of great importance in considering crack propagation.

## 3.3   THREE-DIMENSIONAL STRESSES BELOW A NOTCH ROOT.

Let us consider a specimen, Fig 2B, where an entirely elastic situation applies. The uniform applied stress $G$ a is concentrated to a large local value of $G$ y at the notch root. The presence of the concentrated stress $G$ y, associated with the notched geometry, produces constraint stress in the x and z directions. These arise because of the Poisson effect, which demands large contractions in both the x and z directions, corresponding to the large longitudinal stress $G$ y close to the notch root.

The cross-hatched areas of Fig 3A. represent the area which is outside the region of highly concentrated stress, in which only small Poisson contractions are required. The material shaded restrains the notch root material from contracting in the x and z directions and generates $G$ x and $G$ z constraint stresses. Generally the $G$ x follows the $G$ y stress in its distribution, but the former stress will always be less than $G$ y. The shape of the notch and its elastic displacements influence the $G$ x stress and so it cannot be entirely specified by the Poisson effect. The $G$ z stress tends to follow the $G$ y and $G$ x stresses and is given by :

$$G \text{ z} = V(G \text{ y} + G \text{ z}).$$

As the $G$ x and $G$ z stresses are generated by geometrical constraints they must be zero af the free surfaces of the specimen. In consequence, they tend to follow $G$ y but deviate from $G$ y and fall to zero at the free surfaces as shown in Fig.3B.

Linear elastic fracture mechanics have quantitatively assessed the relationship between the $G$ x, $G$ y and $G$ z stresses. Two conditions arise

which greatly affect the stress distribution: these depend upon the

plate thickness. Plates of thickness $B_1$ develop $G$ y and $G$ z stresses

in the manner previously described and, if they possess sufficient

thickness that the $G$ z stress is constant over most of the thickness,

then this situation approximates to one of a plane strain.

This condition of plane strain is one in which all strains or

displacements would lie in one plane. For the specimen, (Fig 3B) all

displacement would lie in the xy plane, as there would be no

displacements through the thickness direction apart from very close to

the surfaces where $G$ z becomes too small to prevent the displacements.

The critical stress intensity factor $K_{1c}$ is the designation afforded

to plane strain conditions. The second condition is an alternative

extreme situation in which a plate possesses a thickness $B_2$. In this

instance, the thickness is too small to allow the $G$ z stress to develop,

In consequence this $G$ z stress is approximately zero through the thickness

direction: this situation approximates to one of a plane stress condition.

In a plane stress situation all the stresses lie in the single Oxy

plane, (Fig 3B). There is, however, a significant difference between

plane strain and the plane stress condition. This becomes apparent at

the point at which local plastic yielding occurs as the notch root

is approached. With plane strain there are three prevailing stress systems

to consider. With plane stress this is not the case, because one of these

three principal stresses is essentially zero.


3.4   CRACK PROPAGATION ENERGY.

The Griffith theory of fracture postulated that the decrease in stored

elastic energy in a specimen provides the increasing surface energy

required as the area of the crack faces increase.

The condition for crack propagation derived by Weiss & Yukawa (25)

is that the applied stress should attain the value –

$$\sigma a = \left( \frac{2 Ey}{\pi (1 -v^2)c.} \right)^{\frac{1}{2}}$$

assuming that plane strain conditions for a through crack in a plate

applies. (Fig 4).   Where the energy per unit area of crack surface is

y, E being Young's modulus and v Poisson's ratio, whilst the crack is a

central crack of length 2c. or an edge crack of length c. With metals

the concentrated stresses at the crack tip induce plastic yielding

which takes the form of a small plastic zone.

This plastic yielding, according to Orowan (10) produced a large

increase in the consumption of elastic strain energy which is transformed

into plastic work per unit increase in the crack face area and is

therefore equivalent to an increase in surface energy.


Irwin generalised upon Orowan's work by introducing the constant Gc.

which represents the total work consumed in producing unit area of a

non crack surface.


For a plane strain situation the work is –

$$G_{1c}$$

whilst for plane stress it is Gc.

According to Irwin the relationship with $K_{1c}$ for plane strain is :

$$K_{1c} = \left( \frac{G_{1c} E}{1 -v^2} \right)^{\frac{1}{2}}$$

The term $G_{1c}$ has, in the past, been termed as the critical driving force

or the critical strain energy release rate. Currently toughness is specified

in the terminology of the $K_{1c}$ value, which eliminates the need for

considering different allowances for elastic modulus conditions.

### 3.8 PLASTIC YIELDING.

The size of the plastic zone at the crack tip is dependent upon whether plane strain or plane stress conditions exist. A formal representation of the plastic zone at the front of a through thickness crack is shown schematically in Fig 4A, for a situation in which plane stress predominates at the surface and plane strain in the central regions. The influence of the free surface extends into the thickness of the specimen for a distance proportional to the characteristic dimension $(K_{1c}/\sigma YS)^2$. Generally a large plastic zone denotes a desirable degree of fracture toughness. (Equation 1. predicts that at the crack tip where x is zero the local stress is infinitely high). In real situations this cannot apply as the localised stress cannot exceed the yield stress. If the stress distributions are cut off at the level of the yield stress, (Fig 4B) this represents schematically the radius of the yielded region. In practical terms the shape and size of the plastic zone depends upon material properties and on the stress system.

In considering plane strain where there are three non-zero principal stresses near the crack tip the Tresca conditions for plastic yielding show that $\sigma y$ will be higher than the uniaxial yield stress in tension $\sigma YS$. The $\sigma YS$ must satisfy.

$$\sigma YS = \sigma y - \sigma z$$

as $\sigma z$ is the minimum and $\sigma y$ the maximum principal stress.

In consequence, the normal stress at the crack tip rises to the given value –

$$\sigma_y = \sigma_{YS} + \sigma_z$$

This normal stress is greater than the yield stress and, in consequence, can do work in opening the crack and is a basic condition in determining whether good or bad crack propagation characteristics apply at the notch which generates a triaxial stress system because of geometrical constraints.

Irwin (6) states that under plane strain conditions :

$$ry = \frac{1}{5.6\pi} \left(\frac{K_{1c}}{\sigma_{YS}}\right)^2$$

whilst for plane stress –

$$ry = \frac{1}{2\pi} \left(\frac{K_{1c}}{\sigma_{YS}}\right)^2$$

During the fracture process the crack tip is preceded by this plastic zone which for plane stress is larger than when plane strain conditions apply. With thick plates the plastic zone is small in the central region in which plane strain conditions arise, but is larger at the side surface where plane stress is present. A specimen, Fig 5, prepared from a thick plate demonstrates the effect that the plastic zone (plane strain) is small in the central region but larger at the wide surface in which plane stress predominates. The depth below the side surfaces at which plane strain situations apply is approximately equal to ry. The smaller plane strain plastic zone consumes the minimum energy in the form of plastic work.

The specimen fracture appearance change relative to plate thickness is noted by the thin section possessing plastic flow, whilst with the thick specimen, constraint gives rise to plane strain : thus, with a reducing plate thickness the situation approaches plane stress in which energy is consumed as plastic work increases: therefore, toughness increases. (Fig. 6).

The mathematical content of the fracture mechanics concept, although being refined and extended to meet particular needs, is now unquestionably accepted as fulfilling a definite need in the better understanding of crack propagation characteristics. This is a far cry from the early unrecognized beginnings associated with fracture mechanics.

At the Risley Conference in 1969 (25A), it was stated that the application of fracture toughness to engineering problems seemed unlimited as was the flow of literature. It was felt to be advantageous if all concerned fully appreciated not only the advantages but also the limitations of linear elastic fracture mechanics.

## 3.6    DEVELOPMENT OF TESTING TECHNIQUE.

### 3.6.1.    The Traditional Assessment of Toughness.

Fracture and brittle toughness information was initially based upon the philosophy of using test methods in which the ductile/brittle transition temperature assessment was extensively used. This method relied on the premise that a material such as steel plate used in ship construction has a temperature range below which it is susceptible to low stress brittle failure, whilst above this temperature, freedom from brittle fracture can be expected. Many test methods using this ductile/brittle transition temperature approach have been devised and numerous attempts have been made to correlate the results. An example of assessing such methods was examined by Pellini, Steel & Hawthorn (26) who investigated the drop weight and explosion bulge test as a means of measuring the fracture resistance of materials.

The nil-ductility test has broader implications than Charpy impact testing, as it defines the temperature at which material loses its capacity for plastic deformation in the presence of an existing crack. The explosion test method is based on applying a hard surface bead weld on the centre of a plate of 14" x 14", which serves as an initiator of cracking. An explosive force is then directed on to the plate, sufficient to cause bulging at elevated temperatures. The test is repeated as the temperature is successively lowered, and the temperature at which the plate cracks with no notable deformation is identified as the nil-ductility transition temperature (N.D.T). Similarly, with the drop weight test, a welded bead is used to initiate failure. A weight is dropped on the mid-position of a $3\frac{1}{2}$" x 14" square specimen, the welded bead being placed on the tensile side. N.D.T. is the highest temperature at which fracture takes place within a $5^{o}$ bend.

Investigations have attempted to correlate such ductile/brittle philosophy

with fracture toughness parameters. Pellini & Loss (27) concerned themselves with the integration of metallurgical and fracture mechanics concepts of transition temperature factors whereby fracture safe design for structural steels could be undertaken. This comprehensive work introduced a fracture analysis diagram (F A D) procedure in which flaw size/stress relationships for fracture initiation in the transition range could be determined.

Differing test procedures have been developed to establish fracture toughness parameters, so that rapid crack propagation with no gross deformation could be fully explored. In the past design philosopy has placed over-emphasis upon the importance of various notch tests in the avoidance of service failure of engineering components. For example, if a Charpy or Izod test result is established from material from which a pressure vessel is to be constructed, the strength of the vessel in the presence of a flaw cannot in any way be calculated from the energy absorption factor determined in the Charpy or Izod test. In many cases the Design Engineer seems to assume these notch tests do possess such meaningful information. Nevertheless, conventional notch tests serve a useful function for the quality control evaluation of applied heat treatment of fabricating procedures.

The work of Irwin developed fracture toughness parameters which can successfully evaluate brittle fracture which has practical significance in design. Furthermore, fracture mechanics has an advantage of taking into account section size effects, a function which the conventional notch tests cannot perform. Fracture mechanics makes it possible to define the conditions of applied load, crack size and temperature into one single parameter in which separation from slow ductile to fast brittle fracture is evaluated.

### 3.6.2. Present-day Approach to Toughness Evaluation.

The stress/strain distribution in the vicinity of a crack or
notch is now adopted as being more meaningful to predict the
characteristics for low stress fracture.    A standard reference work
compiled by Brown & Srawley (28) presented a state of the art survey
on factors necessary to determine the fracture toughness of metallic
materials. The contents ranged from the fundamentals of specimen
design, testing and K. calibration curves, to the instrumentation methods
used to evaluate toughness parameters.

The stress intensity $(K_1$ factor) of a crack tip in a specimen is
equal to the load multiplied by some function of the selected specimen
dimensions plus the crack length which has dependence upon the type of
specimen used. So that the relationship between load and crack
length parameters can be reduced to a more simplified form, a K. calibration
factor is used. These K. calibrations are required to allow for
stress field intensity modifications, due to the particular  loading
imposed by the design of a particular test specimen. Such K. calibrations
have been experimentally or mathematically determined for each sample type.

The calculation procedure for determining the plane strain fracture
toughness from the specimen geometry and applied loads was reviewed by May
& Walker (29).  The complex compliance functions required to calculate
$K_1$ values were simplified and presented in tabular form for seven of the
more popular types of fracture toughness specimens, ranging from the centre
cracked plate, edge notched specimens, to the wedge open-loaded type.
These tables have been of extreme benefit for the technologist undertaking
toughness testing, as calculation time has been greatly reduced.   In the
use of any test specimen cited it is presumed that linear fracture mechanics

generally require a sharp crack defect with a fracture stress below the yield stress of the material.

The specimen geometry most suited to meet individual testing requirements was studied by Brothers & Yukawa (30) and others (31 & 32) who considered that notched three-point bend test bars are applicable for large sample testing where fracture toughness is moderate, and further demonstrated that a circumferentially notched round specimen, when tension tested, has advantages in examining material associated with round bar form, particularly when considering plane strain toughness. They also showed that a surface cracked tension test piece has the ability to demonstrate everyday service defect orientation, and additionally reported that the single edge notch test specimen has a decided advantage of indicating the combined tension and bending stress at the notch which allows reduced loading requirements compared with other testing methods.

The selection of the type of specimen most suited to meet special needs was also discussed by Wessell (33) who gave a broad and detailed survey on the approach and use of fracture mechanics data to the better understanding of some everyday practical engineering problems associated with the American Westinghouse products, such as thick walled pressure vessels and large rotating machinery parts. Because of the relatively low ratio of fracture toughness to yield stress with some of these engineering components, the absolute specimen size, required to induce valid $K_{1c}$ values became too large for everyday testing purposes and, therefore, the author concentrated upon assessing the usefulness of various small specimens. It was found that the Manjoine or wedge open-loading type, with slight mpdification, considerably increased the measurement capacity of all specimens. Fracture toughness measurements were carried out using the modified

WOL specimen over a testing temperature band of $-70^\circ$ to $+80^\circ$C., and a broad range of $K_{1c}/G$ ys levels obtained. It was demonstrated conclusively the suitability of using the wedge open-loaded type specimen to meet standard testing conditions when the yield stress is moderate. However, whatever type of test piece is selected to measure $K_{1c}$ values, such factors as the cross section of the material to be tested, the associated load compatibility, and the degree of simulation of defects encountered in everyday engineering environments, have to be considered before final specimen geometry is selected to fulfill a particular testing requirement.

After specimen selection, preparation of fracture toughness test pieces has to be undertaken with much greater care than, for example, when producing a Charpy or Izod test bar. This is particularly true concerning the influence of notch sharpness and root radius of fracture toughness specimens. Whether bend or tension specimens are selected, care must be exercised in machining the crack notch. Various methods can be used to produce the original notch from which fatigue cracking originates; a notch root radius must be less than 0.005 inches. The use of a milling cutter, accurately dimensioned at the notch cutting face, is presently favoured. The number and hardness of the specimens requiring to be machined will dictate the amount of actual tool wear and related notch accuracy. If this presents problems the spark erosion technique can be used to produce the notch. It must be recognised that the use of standardized test pieces to ensure that testing conditions conform to specification criteria (34) cannot be solely guaranteed by calculation, and that practical sample experimentation is necessary. This is one of the unusual features of toughness testing.

Not all investigators agree that the concise specification measurement requirements are totally necessary to obtain meaningful data. For example, Cottrell & Langstone (19) in reviewing the current literature, indicated that specimen geometry, when kept within fairly narrow limits, does not vary greatly with $K_{1c}$ if original crack extension takes place before yielding and the plastic zone size of the initial cracking is small compared with the crack depth and specimen cross section. It was also reported that no significant effect on $K_{1c}$ was noted in the method of fatigue cracking when the number of fatigue cycles was greater than 2000. This differs from the recommended procedure for plane strain fracture

toughness testing of ASTM E.24 (35) who proposed that the last 0.050 inches (1.27 mm) of fatigue crack growth should take place in not less than 50,000 stress cycles.

From the earliest traditional attempts to quantify the parameters of brittle fracture, using the ductile/brittle transition temperature characteristics, there has now developed, whatever the variation on specimen geometry or testing conditions, a more meaningful situation in which the use of linear elastic fracture mechanics forms the modern basis for the better understanding of the brittle fracture process.

## 3.7     SOME PRACTICAL USES OF $K_{1c}$ FRACTURE TOUGHNESS.

Reference has already been made in the literature survey on the usefulness of assessing a material's resistance to brittle fracture by measuring the fracture toughness. Some of the surveyed published literature was concerned with evaluating fracture toughness of general engineering components and with the use of fracture mechanics calculations, studying more closely design criteria (36).

Other investigations were applicable to the better understanding of some of the mathematical concepts embodied in the various parameters associated with fracture toughness testing.

The relevance of fracture mechanics in solving some of the toughness problems associated with the production and use of general engineering components can be illustrated with the following examples, which are representative of the type of work undertaken by using linear elastic fracture mechanics.

The manner in which fracture mechanics could be applied to general everyday engineering applications was indicated by Hofer (37). An investigation was carried out on a pressure vessel which, examination showed, had a through crack of known dimensions. The fracture mechanics calculations showed that failure occurred about one-third of the stress rating as compared to conventional failure design criteria. A further illustration of the use of applying fracture toughness calculations was undertaken when the safe operating stress for a component possessing an edge crack in grade 4349 steel was determined, and it was found that conventional safe design theory, which stipulated 260 k.s.i. erred by nearly 100%.

Pook (38) illustrated engineering failures. One was a drilling rig which collapsed in the North Sea with catastrophic effects, and another a ship's anchor which parted company from the vessel. The author showed how the steelmaker and designers may be drawn finally into fracture mechanics through the formulation of design codes.

On the basis of obtaining data on industrially used power generation components, Thornton (39) determined the fracture toughness of turbo-generator

materials whose chemical composition ranged from alloys containing 3.5% chromium, .5% molybdenum, 1.0% vanadium to 12.0% chromium, 5.0% nickel, 1.0% molybdenum with niobium additions. Toughness values were obtained by using both linear elastic and general yield fracture mechanics. It was further stated that the ASTM criterion (35) from which it will be seen both specimen thickness and crack length should not be less than $2.5 \left(\dfrac{K_{1c}}{\sigma_{ys}}\right)^2$ was too conservative and, with more data becoming available, could be relaxed. In the case of conventional stress analysis and metallurgical inspection on rotor forgings for non-metallic inclusions in the critical bore area of such forgings, present acceptance standards could tolerate inclusions approximately .25" long (6.3 mm) having a radial depth of approximately 0.030" (.702 mm). Using fracture mechanics, it was noted that even at the proof stress of these heavy generator forgings the critical defect size for rapid fracture could be so very much in excess of the new permitted values. Caution was expressed that relaxation of acceptance standards can only successfully be undertaken after much more work which, of necessity, must include evaluation of non-destructive testing methods, such as ultrasonic flaw detection, so that defect size can be accurately monitored.

Two frequently used constructional alloy steels were studied by Logan and Crossland (40) who compared the fracture toughness. One steel, contained 0.33% carbon, 2.5% nickel, 0.60% chromium, 0.54% molybdenum and the other 0.31% carbon, 3.42% nickel, 1.00% chromium, 0.58% molybdenum and 0.17% vanadium. The material used was 102 mm. diameter, being oil hardened and tempered at various temperature levels ranging from 200 to $650^\circ$C., in which the proof stress varied from 53 to 93 tonf/in$^2$. (0.82 – 1.4 GNm$^{-2}$). Single edge notched and compact tension specimens were used to assess toughness, as one of the objects of the work undertaken was to ascertain which sample (which transpired to be the compact tension type), was most satisfactory to obtain transverse fracture toughness when the available test material was limited.

A linear relationship between $K_{1c}$ and notch impact strength over the energy range from 0 – 30 J. was reported. If a similar situation exists with other steels, differing in compositional and structural properties, this would be of significant practical importance.

The important issue voiced by Nichols(41) at the 1971 Pressure Vessel

Conference concerned the limitation of extropolating Charpy notch data
outside the environment from which such data was obtained. He
showed that in some cases the Charpy vee notch test can grade materials
in the incorrect order of fracture resistance.

An attempt to correlate various toughness parameters was made by Susukiea,
Ando, Tsuji and Hibarn (42) who determined the fracture toughness of alloy
steel plates used in the construction of reactor vessels containing 3.0/4.0%
nickel and approximately 1.4% chromium and .5% molybdenum. They used four
test specimens comprising smooth round tension test bar, the Charpy vee notch
specimen, the drop weight test and the WOL (test method developed by
Westingham Electric Company, U.S.A) termed "wedge opening loading". The
authors considered that some correlation might be possible in comparing the
results obtained between the WOL, Charpy V. and drop weight tests which could
give rise to the establishment of safe design criteria. Additionally, attentio
was drawn to manufacturing procedures which could significantly influence
toughness characteristics.

Fracture mechanics has presented a means for evaluating structural
reliability. The contribution of engineering geometry to notch strength can no
be predicted. Traditionally, the transition temperature and impact strength,
together with the strength value between notched or un-notched test conditions
was the only means of assessing the ability of materials to arrest a crack
that could be the cause of sudden failure. Plane strain calculations allow,
for the first time, a means of predicting reliability in that the toughness
measured confirms material constants unaffected by specimen geometry. It
has been shown that fracture mechanics can be of extreme importance in the
design calculations and in the better understanding of the brittle failure
phenomena that plagues everyday engineering materials.

Beniszewaki & Rendall (43) stated that now science of fracture toughness
has been established it will be necessary for specialists to simplify
involved mathematics. They should present data in a very practical manner,
otherwise design engineers would refrain from using the concepts of
fracture mechanics.

To allow such a situation to develop would be asinine.

4. <u>EXPERIMENTAL METHODS AND MATERIALS</u>.

## 4.1 PRODUCTION OF DIE BLOCKS.

There are two methods of using wrought die blocks.

1.      By using inserts in which the die impression is produced in relatively thin section of die steel which, when worn out, cannot be re-machined.

2.      From a solid block which can be re-machined, perhaps more than once, when the impression becomes worn by use, so that forging can continue until the block is too thin to allow the operation of re-sinking to be carried out again.

The mechanical properties of fully heat treated solid die blocks to those existing in the smaller insert form are not, in any way, comparable. Martensitic transformation times, associated with heat treating larger solid blocks, will vary considerably to those present in quenching small insert material. In consequence, the smaller insert section thus possesses a more satisfactory level of as-quenched hardness which, after tempering, produces superior tensile and notch toughness to that present with the larger solid die block even though identical heat treatments were given.

4.2.     WORKS TRIALS ON DIE TOOLS.

To evaluate the properties including fracture toughness of No. 5.
die steel, after the useful die life had been obtained, a controlled
industrial experiment using 12" x 5" x 31.5" (305 mm. x 127 mm x
800 mm) inserts was carried out.

Eight inserts were supplied to Ambrose Shardlow & Company Limited, with
the object of studying production characteristics and assessing die life.
A crankshaft impression was machined into the inserts, a 4-ton counterblow
hammer being used to hot form the crankshafts.  During the period of
time in which the trials were undertaken, additional technical
control was exercised in the drop forge to ensure that only approved
procedures were adopted.

It is acknowledged (2) that of the top and bottom forming tools, either
in insert or solid die block form, the bottom impression die form
invariably receives the more severe amount of wear and tear.
Two selected bottom inserts were withdrawn from production because of
different reasons in which localised cracking was present with one die
tool whilst thermal wear was evident with the other.
The insert which had locally cracked, necessitating rejection, produced
4231 drop-forgings, whilst the other bottom insert achieved a production
rate of 4633 drop-forgings before the impression became distorted and
produced forgings which were oversize to dimensional requirements.

The inserts, which produced the 4231 and 4633 drop forgings, were designated
"A" and "B" respectively, and are shown in Figs. 7. and 8., which indicate
some areas of the impression which have locally cracked or thermally
distorted.

The investigation will deal with the properties of these nickel-chromium-
molybdenum inserts and, in addition, the effect on toughness of a No. 5.
die steel upset forged test block utilising a different hot working
procedure and incorporating in the heat treatment practice a water quenching
operation. Such production variations being totally dissimilar to those
carried out in manufacturing the trial inserts.

## 4.3     FORGING AND HEAT TREATMENT OF STEEL FOR TRIAL INSERTS.

Forgings having a cross section of 12" x 5" (305 x 127 mm) were forged from electrically melted vacuum degassed 5-ton 10-cwts (6188 Kg) octagonal ingots, possessing the following chemical composition and having a girth size of $27\frac{1}{4}$" x 23" (692 x 585 mm).

|            | %     |            | %    |
|------------|-------|------------|------|
| Carbon     | 0.54  | Manganese  | 0.73 |
| Silicon    | 0.29  | Nickel     | 1.77 |
| Sulphur    | 0.032 | Chromium   | 0.74 |
| Phosphorus | 0.018 | Molybdenum | 0.27 |
|            |       | Aluminium  | 0.01 |

A re-heating cycle was used in which the ingot was charged into a furnace at $700^{\circ}$C. After allowing a 35 minute period for heat conduction the ingot was rapidly heated to $1220^{\circ}$C. in 7 hours. A further 6 hours was allowed at $1240^{\circ}$C. to equalise the temperature throughout the ingot before forging took place.

A two-stage forging operation was carried out : the ingot being converted to a 15" square (381 mm) after which the impure discard material was removed. The 15" bloom (381 mm) at a minimum temperature of $850^{\circ}$C. was then re-charged into a furnace, and heated to $1200^{\circ}$C. in 5 hours. This temperature of $1200^{\circ}$C. was maintained for 4 hours, after which a further forging was carried out to achieve the desired dimensions of 12" x 5" x 31.5" long (305 x 127 x 800 mm).

The 15" bloom, being converted into multiple inserts received a total hot forging deformation of 8 : 1, after which the bar inserts were immediately charged into a heat treatment furnace, and the following thermal cycle applied. Held at $650^{\circ}$C. for 8 hours. The inserts were then withdrawn from the furnace, air cooled to $400/300^{\circ}$C. and re-charged into a furnace and heated to $850^{\circ}$C. in 8 hours, allowing 7 hours at $850^{\circ}$C. for temperature equalisation. The forgings were then cooled to $650^{\circ}$C. in 6 hours, held at $650^{\circ}$C. for 7 hours and furnace cooled.

The object of carrying out this heat treatment was to ensure that the remnant Widmanstatten structure was refined and, more importantly, hydrogen diffusion had been accomplished whereby the die steel would have freedom from hairline cracks. Pieces, 12" x 5" x 31.5" (305 x 127 x 800 mm) were then cold sawn, and were finally heat treated in one batch by oil quenching from $850-870^{\circ}$C. followed by tempering at $600/620^{\circ}$C. for 6 hours.

## 4.4    FORGING AND HEAT TREATMENT OF UPSET FORGED TEST BLOCK.

It was decided to combine upset and two different forging reductions in a
larger test block in order to assess any effect upon toughness.
Unfortunately, in processing this upset two–stage deformation, or stepped
test block, it was not possible to use the same cast material as that
selected for the insert forgings, as a much larger ingot was required,
the chemical composition being :-

### TABLE NO. 2.

| C. % | Si. % | S. % | P. % | Mn. % | Ni. % | Cr. % | Mo. % | Al. % |
|------|-------|------|------|-------|-------|-------|-------|-------|
| .52  | .28   | .038 | .020 | .75   | 1.62  | .88   | .32   | .01   |

which conforms to the required melting specification for No. 5. hot work
die steel.

An 8–ton electrically melted vacuum degassed ingot, having a chemical
composition as given in Table 2, and possessing an octagon girth size
of $35\frac{1}{4}$" x $30\frac{1}{4}$" (896 x 769 mm) was selected. The pre–heating schedules
previously noted in paragraph 4.3 were, in the main, used : the only
difference in the re–heating cycle being that the 35–minute period for
heat conduction was followed by a further holding period at $650^{\circ}$C. for
90 minutes, whilst time at the actual forging temperature of $1240/1250^{\circ}$C.
was 8 hours.

The ingot was then converted to a 14" square (356 mm) bloom which
received a reduction from the ingot in a ratio of 3.1/1. The bloom
was then transferred to a heat treatment furnace and received a similar
initial thermal cycle to that outlined in paragraph 4.3. From the 14"
square a piece, 21" long (534 mm), weighing 1180 lbs. (539 Kg) was cold
sawn. This block was then re–heated, the furnace temperature being $850^{\circ}$C.
A period of 30 minutes for heat conduction by the cold block was allowed.
The furnace charge was then raised to $1200^{\circ}$C. in 5 hours, and held at this
temperature for 4 hours. Upset forging was then instituted, after which
shaping the block to dimensions of 16" x 16" x 14" (407 x 407 x 356 mm)
was carried out. The block was then re–charged into a furnace and maintained

at 1200°C. for 4 hours, after which a two-stage forging deformation was carried out to the following dimensions :
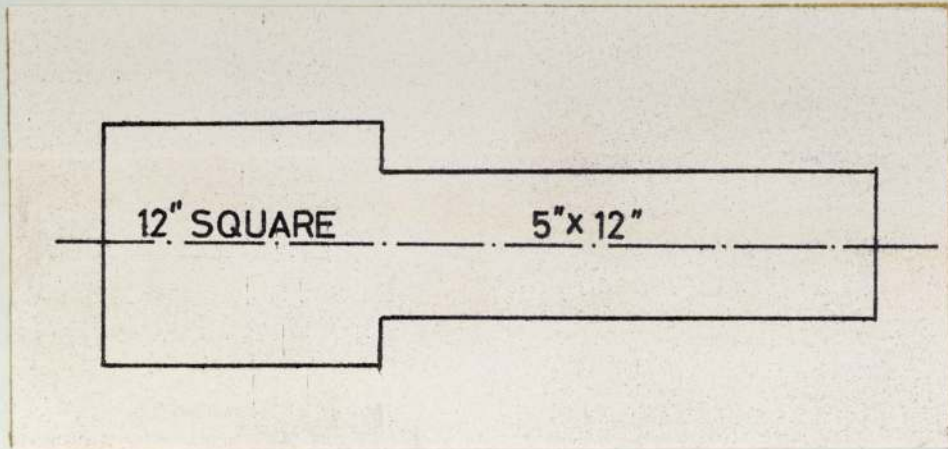


The total forging reduction for the 12" square (305 mm) section was 6.8 :1, whilst the 5" section (127 mm) received a forging deformation of 17 :1.

The block, Fig 9, was then heat treated by including in the hardening process a water/oil quenching operation.
After being austenitized at 850/870°C. the block was water quenched for 10 minutes, transferred to an oil bath for hardening to be accomplished in 30 minutes, followed by tempering at 600°C. for 9 hours.

## 4.5.  ULTRASONIC EXAMINATION.

This form of non-destructive testing consists of energy waves being
transmitted through the section under examination : any imperfections
lying within the path of this energised beam can be detected. The pioneer
and subsequent studies by the International Authority, Dr. Krautkramer,
on the practical use of ultrasonic energy in the testing of forgings
are referred to in his standard work (44).

On the areas away from any changing impression section which would affect
the sound wave beam, examination of the two inserts was undertaken using a
Krautkramer USIP 10 instrument.  A 4 M/Hz. power frequency was selected
for assessing the internal soundness of the die tools. The oscillogram
traces, together with frequency details, are shown, Figs. 10. and 11.
The Oscillogram reflections of sample "B", Fig 10, indicate the
presence of non-metallic inclusions, whilst at the same frequency of
testing sample "A", Fig 11, shows no such inclusions. The stepped test
block showed near identical results denoted with the oscillogram pattern
of sample "A", Fig 11.

The interpretation of the characteristics of various metallurgical
defects, and their correlation to ultrasonic examination, requires
careful judgment and lengthy operator experience (45).

## 4.6.  HARDNESS TESTING AND MECHANICAL PROPERTIES.

### Brinell Hardness.

Hardness testing, using a Jackman radial arm machine with a
3000 Kg. load and a 10 mm. ball was employed to ascertain the hardness on
four selected areas of each insert. Insert "A" gave a hardness of 363/352
B.H.N. and insert "B" - 341/321 B.H.N. The stepped test block hardness
was 388/363 B.H.N.

### Mechanical Tests.

From the two inserts, and the stepped test block, tensile and notch
toughness specimens were selected, Figs. 9 & 12. Tensile test pieces with a
diameter of 0.564" (14.33 mm) were prepared in accordance with appendix
D. of British Standard 970. Tensile loading up to the 0.2% proof stress

level was carried out at a constant rate of 2 tons per minute (3.1 Kg. per square mm). Thereafter the loading was increased to 6 tons per minute, (9.3 Kg. per square mm). The Izod and Charpy notch bar test pieces were also prepared in accordance with appendix D. of B.S.970. The 10 mm. square Charpy specimen using a 2 mm. vee notch, and the round 0.45" (11.5 mm) three-notch Izod samples being selected. These tensile and notched bar impact tests were carried out at room temperature.

## 4.7 CONSTRUCTION OF THE HIGH TEMPERATURE FURNACE.

It was decided that a furnace and ancillary equipment should be constructed in order that the fracture toughness at elevated temperatures could be examined. The furnace unit to be capable of attaining and accurately controlling temperatures up to $500^{o}$C., which would be representative of temperatures attained in the surfaces of industrial metal forming die tools.

To meet different specimen design and, additionally, so that the largest complete unit could be accommodated within the Instron testing machine, a welded stainless steel furnace lining, $5\frac{1}{2}$" x $4\frac{1}{2}$" x 14" long, (140 mm. x 115 mm. x 356 mm) was constructed with asbestos furnace openings connected by 4 mild steel tie rods, Fig 13. Four 750 watt 240 volt high Inconel hot-foil coil heating elements were assembled to the four faces of the stainless steel inner furnace lining: the elements being minerally insulated by magnesium oxide. The furnace was covered with aluminium sheet. A furnace support table, constructed of mild steel, (Fig 14A) allowed the ancillary testing arm extensions to be mounted in a truly vertical position.

At an early stage in manufacture it was necessary to prove temperature uniformity of the furnace. Therefore, a block of mild steel of similar dimensions to the W.O.L. test piece was drilled in order that thermocouples could be inserted. To simulate the possible scaling effect that the actual test jaws could exert two samples of identical section in mild steel were placed adjacent to the test block, and the unit heated to various temperatures up to $500^{o}$C. The results are shown in Fig. 15(A). A uniformity within $20^{o}$C. can be observed which is sufficiently accurate for the purpose as temperature fluctuations which occur within a die block in service is greater than $20^{o}$C.

To transmit the crack propagation extensions from the hot test pieces to the clip gauge, (Fig 16), and to apply the load, it was necessary to design an apparatus which could cater for the effects of temperatures up to $500^{o}$C. Materials capable of withstanding this high temperature condition had to be used, the general arrangement of such components is shown (Fig 17).

Nilo 50 material was used for constructing the extension legs attached

to the hot specimen in order to reduce the effects of thermal
expansion on clip gauge readings.     The complete unit, attached to
the Instron machine, is shown in Fig 18.

Tne tension bars, jaws and pins were manufactured from a hot work
die steel having the following chemical analysis, similar to the
H.12 grade, but with a higher molybdenum content :-

|  | % |
|---|---|
| Carbon | 0.41 |
| Manganese | 0.61 |
| Silicon | 0.32 |
| Chromium | 5.13 |
| Molybdenum | 2.35 |
| Vanadium | 0.48 |

and salt bath heat treated to achieve a B.H.N. of 388/415.

As a differential heat treatment technique was required for the tension
bars the salt bath method was preferred. By positioning the tension
bars in the bath the larger head areas could be locally re-tempered and
softened, thus facilitating easier machining, as final alignment,
which required an accurate drill location hole in the head could only
be determined after all the components had been assembled.

## 5.   RESULTS.

## 5.1.  METALLOGRAPHY.

Sulphur Printing.

Transverse slices, 1" thick, were sectioned from the two inserts.
Sulphur prints, etched in sulphuric acid, Figs. 19. & 20. were
taken, and revealed normal sulphide distribution associated with
satisfactory electrically melted killed steel.

Microstructure.

Specimens were prepared by wet surface grinding on successively
finer grades of emery paper, final polishing being accomplished with
diamond paste of 1/8 micron particle size. The unetched examination
was carried out at a magnification of x 100. The inclusions present
are shown in Figs. 21 & 22.

Manganese sulphides predominate over oxide and silicate inclusions.
The microstructure was viewed at magnifications of x 100 and x 650
respectively after etching with 5% Nital. The general structure
consists of tempered bainite and martensite.  In addition, a degree of
banding is present, more pronounced on sample "A" than sample "B",
whilst the benefit of including a combined water/oil quenching cycle
in the heat treatment of the stepped test bar is evidenced by the
more acicular condition of the tempered martensite/bainite. These
structures are considered normal for everyday commercial use, Figs. 23-26.

Inclusion Counts – Quantitative Television Microscope.

The Q.T.M. instrument projects an image from a normal metallurgical
microscope into a television camera and, subsequently, to a television
monitor. The image characteristics can then be assessed and counted.

Careful sample preparation is necessary with micro-specimens. It is
possible with the Q.T.M. to area count oxides and sulphides individually
or collectively. These inclusions have different optical reflectivities
from the matrix and, if an examination for MnS. is required, the
selected sulphide area is produced on the television monitor, the
instrument being adjusted so that only the oxides are viewed.  A meter
indicates the percentage of these oxide inclusions, and the instrument
is then adjusted so that the field indicates the total inclusions present,
which again is indicated by a meter reading. The difference between

these two meter readings indicates the volume of MnS. inclusions.

These samples were examined with the Q.T.M. in order to assess total inclusion area density. A minimum of 300 area field counts were carried out on each specimen so that a statistical total percentage inclusion could be calculated.

| Sample. | % Oxide. | % Sulphide. | % Total Inclusion. |
|---------|----------|-------------|--------------------|
| Insert "A" | 0.011 | 0.105 | 0.116 |
| Insert "B" | 0.022 | 0.168 | 0.190 |
| Stepped test bar | 0.105 | 0.132 | 0.237 |

The results from microscopically examining the unetched metallographic specimens must be considered in the light of these area inclusion contents : the significant feature being that sample "B" contains approximately double the oxide content to that present in specimen "A".

## 5.2.   MECHANICAL PROPERTIES.

The results embodied in Table 3. demonstrate the marked difference
between the tensile data of the inserts compared to the test block,
even allowing for ingot heterogeneity, and are the outcome of applying
a different forging technique in addition to using a differential
quenching operation in the heat treatment cycle.

The tenuous empirical relationship between tensile stress
            and indentation hardness values has already been reported
(1) regarding No. 5. die steel.

Notch Toughness.

Longitudinal Charpy notched bar impact tests were carried out and the
toughness assessed in the temperature range of $-20/+400^{\circ}C$. The
resultant curves (Fig 27) demonstrate that insert "B" has significantly
superior notch strength to sample "A".

Hot Tensile Data.

Sufficient spare test material was not available to obtain elevated
temperature tensile data from the two inserts. However, longitudinal
specimens were prepared from the small section of the upset forged
test block and were prepared in accordance with Fig. 28.

Tensile properties were assessed over a temperature range of 100 to
$500^{\circ}C$. The tests being performed at a strain rate of 2 tons per
square inch per minute (3.1 Kg. per sq.mm) until the proof stress was
attained. Thereafter, the loading was increased to 8 tons per square inch
per minute (24.8 Kg. per sq. mm).

The results are embodied in Table 4. The data shows that with the
increasing elevated temperature the expected decrease in tensile and
proof stress occurs. It is interesting to observe that the reduction
of area shows that a trough exists between 100 to $400^{\circ}C.$, thereafter
ductility improves, (Fig 29).

TABLE 3.

| Forging reduction. Sample. | Tons per sq.in. Yield. | N/mm². | Tons per sq.in. tensile stress. | N/mm². | Elong. % on 2" | R. of A. % | Izod. ft. lbs. | Joules. | B.H.N. |
|---|---|---|---|---|---|---|---|---|---|
| **INSERT "A".** | | | | | | | | | |
| 8:1 Longitudinal. | 60.0 | 927 | 76.0 | 1175 | 16 | 44.8 | 14. 14. 16 | 18.5 18.5 21.4 | 363-352 |
| Transverse. | 57.5 | 892 | 74.4 | 1148 | 11 | 18.4 | 2. 3. 1 | 2.7 4.05 1.35 | |
| **INSERT "B".** | | | | | | | | | |
| 8 :1 Longitudinal. | 57.5 | 892 | 70.4 | 1086 | 18 | 54.8 | 18. 20. 20 | 23.6 26.3 26.3 | 341-321 |
| Transverse. | 54.2 | 836 | 68.4 | 1054 | 11 | 24.8 | 6. 7. 9 | 8.1 9.45 12.1 | |
| **UPSET FORGED TEST BAR.** 12" (305 mm) section. | | | | | | | | | |
| 6.8 :1 Longitudinal. | 78.0 | 1202 | 84.8 | 1304 | 11 | 30.4 | 10. 8. 6 | 13.5 10.8 8.1 | 363-388 |
| Transverse. | 74.4 | 1148 | 84.8 | 1304 | 14 | 38.0 | 8. 8. 6 | 10.8 10.8 8.1 | |
| 4" (100 mm) section. | | | | | | | | | |
| 17:1 Longitudinal. | 80.4 | 1257 | 86.8 | 1360 | 14 | 43.6 | 12. 12. 12 | 16.2 16.2 16.2 | 363-388 |
| Transverse. | 75.4 | 1165 | 82.4 | 1272 | 6 | 16.8 | 2. 1. 2 | 2.7 1.35 2.7 | |

## ELEVATED TEMPERATURE TENSILE TESTS.
### STEPPED TEST BLOCK (SMALL END).

| Test temperature °C. | | 100 | | 150 | | 150 | | 200 | | 200 | |
|---|---|---|---|---|---|---|---|---|---|---|---|
| Time to reach test temp. (mins). | | 120 | | 160 | | 150 | | 150 | | 120 | |
| Soaking time (mins). | | 25 | | 35 | | 25 | | 35 | | 40 | |
| | | $N/mm^2$ | Tons per sq.inch. | $N/mm^2$ | Tons per sq.inch. | $N/mm^2$ | Tons per sq.inch. | $N/mm^2$ | Tons per sq.inch. | $N/mm^2$ | Tons per sq.inc. |
| Proof stress for extension % | 0.05 | 1104 | 71.5 | 1042 | 67.5 | 1012 | 65.5 | 911 | 59.0 | 849 | 55.0 |
| | 0.1 | 1143 | 74.0 | 1073 | 69.5 | 1050 | 68.0 | 958 | 62.0 | 911 | 59.0 |
| | 0.2 | 1174 | 76.0 | 1127 | 73.0 | 1081 | 70.0 | 996 | 64.5 | 965 | 62.5 |
| | 0.5 | 1205 | 78.0 | 1143 | 74.0 | 1120 | 72.5 | 1042 | 67.5 | 1027 | 66.5 |
| | 1.0 | 1228 | 79.5 | 1174 | 76.0 | 1151 | 74.5 | 1089 | 70.5 | 1073 | 69.5 |
| Tensile strength $N/mm^2$ | | 1305 | 84.5 | 1262 | 81.7 | 1242 | 80.4 | 1189 | 77.0 | 1185 | 76.7 |
| Elongation % on 5.65 $\sqrt{A}$ | | 12.8 | | 10.4 | | 11.2 | | 10.4 | | 10.0 | |
| Reduction of area % | | 42.5 | | 40.0 | | 40.0 | | 37.0 | | 39.0 | |

TABLE 4a.

ELEVATED TEMPERATURE TENSILE TESTS.
STEPPED TEST BLOCK. (SMALL END).

| | | 250 | | 250 | | 300 | | 300 | | 350 | |
|---|---|---|---|---|---|---|---|---|---|---|---|
| Test temperature °C. | | 250 | | 250 | | 300 | | 300 | | 350 | |
| Time to reach test temp. (mins). | | 75 | | 105 | | 180 | | 120 | | 165 | |
| Soaking time (mins). | | 15 | | 20 | | 20 | | 20 | | 20 | |
| | | N/mm2 | Tons per sq. inch. | N/mm2 | Tons per sq.inch. | N/mm2 | Tons per sq.inch. | N/mm2 | Tons per sq.inch. | N/mm2 | Tons per sq.inch. |
| Proof stress for extension % | 0.05 | 1019 | 66.0 | 981 | 63.5 | 973 | 63.0 | 896 | 58.0 | 954 | |
| | 0.1 | 1058 | 68.5 | 1035 | 67.0 | 996 | 64.5 | 942 | 61.0 | 1010 | 65.4 |
| | 0.2 | 1089 | 70.5 | 1081 | 70.0 | 1050 | 68.0 | 988 | 64.0 | 1072 | 69.4 |
| | 0.5 | 1143 | 74.0 | 1143 | 74.0 | 1104 | 71.5 | 1050 | 68.0 | 1115 | 72.2 |
| | 1.0 | 1197 | 77.5 | 1189 | 77.0 | 1143 | 74.0 | 1097 | 71.0 | | |
| Tensile strength N/mm² | | 1260 | 81.6 | 1262 | 81.7 | 1236 | 80.0 | 1189 | 77.0 | 1198 | 77.6 |
| Elongation % on 5.65√A | | 11.1 | | 12.0 | | 11.0 | | 12.5 | | 13.5 | |
| Reduction of area % | | 35 | | 37.0 | | 35.0 | | 36.0 | | 48.0 | |

TABLE 4b.

ELEVATED TEMPERATURE TENSILE TESTS.
STEPPED TEST BLOCK. (SMALL END).

| Test temperature °C. | | 350 | | 400 | | 450 | | 500 | |
|---|---|---|---|---|---|---|---|---|---|
| Time to reach test temp. (mins) | | 100 | | 195 | | 210 | | 185 | |
| Soaking time (mins). | | 35 | | 25 | | 35 | | 15 | |
| | | $N/mm^2$ | Tons per sq. inch. | $N/mm^2$ | Tons per sq.inch. | $N/mm^2$ | Tons per sq.inch. | $N/mm^2$ | Tons per sq.inch. |
| Proof stress for extension % | 0.05 | 857 | 55.0 | 819 | 53.0 | 788 | 51.0 | 710 | 46.0 |
| | 0.1 | 903 | 58.5 | 873 | 56.5 | 842 | 54.5 | 764 | 49.5 |
| | 0.2 | 950 | 61.5 | 927 | 60.0 | 880 | 57.0 | 819 | 53.0 |
| | 0.5 | 1012 | 65.5 | 996 | 64.5 | 934 | 60.5 | 865 | 56.0 |
| | 1.0 | 1058 | 68.5 | 1004 | 65.0 | 965 | 62.5 | 888 | 51.5 |
| Tensile strength $N/mm^2$ | | 1152 | 74.6 | 1104 | 71.5 | 1050 | 68.0 | 964 | 62.4 |
| Elongation % on $5.65\sqrt{A}$ | | 13.2 | | 15.0 | | 11.9 | | 13.8 | |
| Reduction of area % | | 43.0 | | 42.0 | | 50.0 | | 56.5 | |

TABLE 4c .

## 5.3    FRACTURE TOUGHNESS.

The theory used for measuring critical stress intensity factors,
and applying the result to predict maximum working stresses in the
presence of a given defect size, or maximum defect size for a given
working stress, is termed linear elastic fracture mechanics. The
theory rests on the foundation that overall stresses and strains in the
cracked body are approximately elastic in spite of localised plastic
behaviour near to the crack tip. In order that the theory and
methods are applicable, tests to determine Kc. must conform to linear
elastic conditions. These conditions are incorporated into the British
Standard for fracture toughness testing (34).

The first condition is that the test is carried out under approximately
elastic conditions. This is so if the crack tip plastic zone reaches
only about 1/50th of the distance across the ligament. A          (Fig 31)
practical test of this is performed on the load/crack opening
displacement trace. In principle, the plastic zone contribution to the
trace is non-linear from the origin.   The trace also becomes non-
linear eventually because of crack extension which produces a decrease
in the effective modulus of the specimen. Thus, if only crack
extension produces non-linearity, the load/C O D trace would return
on a straight line of less slope back to the origin on unloading.
In the practical case, both plasticity and crack extension contribute
to non-linearity. Their relative contributions are judged in the light
of experience in this way. If a 5% less slope than the original elastic
slope of the load/ C O D trace is drawn, then their intersection is
at the load PQ.  The deviation from linearity at PQ arises from both
plastic behaviour and crack extension. The deviation from linearity
at lower loads must contain a greater proportional contribution from

the plastic zone than from crack extension. If we step back to 0.8 $P_Q$ the cracking contribution is typically very small. Therefore, the British and American Standards for toughness testing require that the deviation from linearity at 0.8 $P_Q$ (mostly plastic zone effects) shall be less than 0.25 of the deviation from linearity at $P_Q$ (combined plastic zone and cracking effects). If this is so the test passes the first validity criterion and the $K_Q$ measured is a linear elastic quantity and may be termed Kc.

The second validity criterion required by Standards is only applied if a minimum value of Kc. , namely $K_{1c}$, is required to be measured. Thus, the Kc. value is appropriate to calculating critical defect sizes for through wall defects in material as thick as the test specimen. Since Kc. falls as the specimen thickness increases, it is important to test at the thickness appropriate to actual service conditions. Further comparisons of different materials are in order so long as the Kc. values are for the same specimen thickness. Beyond a certain thickness the Kc. does not fall further. This is the thickness at which the fracture surface produced is more than 95% flat and normal to the applied tension. This fracture is termed plane strain because it results from rupture through a plane strain plastic zone at the crack tip. Thus a plane strain fracture is characterised by small shear lips. The Standards recommend that the test specimen thickness must be at least $2.5 \left(\dfrac{Kc}{\sigma ys}\right)^2$ before it is sure that the fracture is plane strain. The choice of the factor 2.5 is arbitrary but has been found to ensure plane strain conditions for most materials, though many fracture in a plane strain manner at thicknesses around $1.0 \left(\dfrac{Kc}{\sigma ys}\right)^2$

In this project the toughness was to be measured over a range of temperature such that the yield stress could conceivably fall by a factor of two. On this count alone the range of thickness required to maintain the thickness of $2.5 \left(\dfrac{Kc}{\sigma_{ys}}\right)^2$ would vary by a factor of four. Of course the Kc. would also be expected to change with temperature. Such a variation of specimen thickness was not possible, at the outset, in terms of the material available for testing. It was therefore decided to choose as great a thickness as possible in order to provide sufficient specimens from the material available; in order that plane strain conditions were met at room temperature, and further in order that the overall specimen size (which is scaled to the thickness) would fit within a furnace of reasonable dimensions. The tension specimen of Fig 32. was the final design chosen. After pre-fatigue cracking the notches, as recommended by the British Standard (34) two specimens of this design, in No. 5. die steel, were tested at room temperature in an Instron machine. The results conformed to both validity criteria and gave the following plane strain critical stress intensities -

Sample A.    $K_{1c}$    62 k.s.i. $\sqrt{\text{in.}}$

Sample B.    $K_{1c}$    60 k.s.i. $\sqrt{\text{in.}}$

The load/C O D traces for these specimens are shown in Fig. 33. This specimen design was subsequently adhered to and material cut from the die material as shown in Figs. 34 and 35.

Fracture toughnesses were measured over the temperature range from room temperature to $500^{o}$C. These tests, with only a single exception, (shown in Table 5) all gave valid Kc. values, since they were linear elastic tests according to the offset or deviation from linearity

criterion.    Though few of the elevated temperature tests met the
thickness criterion for a plane strain test, they are immediately
comparable from one material to another since we are comparing
Kc. values at the same material thickness at each temperature.
The value $2.5 \left( \frac{K_Q}{\sigma_{ys}} \right)^2$ is shown as $\beta$ in Tables 5, 6 and 7.
Thus, where the thickness B is greater than $\beta$ the test would be a
plane strain measurement. Unfortunately, accurate values of the
elevated temperature yield stresses were not measured and, therefore,
the $\beta$ values are based on room temperature yield values. The
validity tests on elevated temperature tests, other than at room
temperature are therefore of no real value.

In view of this lack of information on whether the Kc. values
were also $K_{1c}$ values macro-photographs of each fractured test piece
were taken. These are shown in Figs. 43, 44 and 45. The fractures
are flat plane strain fractures with almost no shear lips in all
cases with the exception of the tests on insert B. at $400^{o}$C. and
$500^{o}$C.        It is concluded that all the tests excepting specimen
1A6T provide valid Kc. values, that the room temperature Kc.
values are valid $K_{1c}$ values, and that the Kc's in all cases must be
very close to $K_{1c}$ values because the fracture surface is
predominantly of the plane strain type.

All tests were carried out on an Instron machine with the furnace
mounted on the machine.

Fig 38 shows values of Kc. for 1.25 inch thickness plotted against temperature separately, for longitudinal specimens and transverse specimens cut from Insert "A". Room temperature values are low in both cases. The rise to a maximum at $100^{o}$C. is followed by a significant fall in both cases also. In general the longitudinal specimens give a rather higher toughness than transverse specimens.

The results for longitudinal and transverse specimens of Insert "B" are shown in Fig. 39. Here the longitudinal specimens are also of a greater toughness in general, though the remarkable feature is the sustained high toughness of the longitudinal specimens up to $300^{o}$C.

Fig 40. shows the Kc. values for 1.25 inch thickness for the stepped block material. Since the results are not extensive the longitudinal and transverse specimens are plotted on the same graphs, which do not therefore reflect the true variation of Kc. with temperature. The large section maintains high toughness at least for the transverse specimens, whereas the smaller section, given greater forging reduction, shows low toughness except for the longitudinal specimen at $200^{o}$C.

A period of 20 minutes was allowed after the test temperature had been reached, in order to reach near equilibrium temperature conditions. Tests were carried out at a crosshead speed of 0.2 cm/min. Figs. 36. and 37. show typical load/C O D traces from the X-Y recorder. The results in terms of $K_{Q}$ are shown in Tables 5, 6 and 7. All but one of these values are valid Kc's., and so they are plotted as a function of test temperature in Figs. 38, 39 and 40.

## TABLE 5.

### ELEVATED TEMPERATURE FRACTURE TOUGHNESS TESTS – INSERT "A".

| Specimen. | Temp. °C. | B in. | a in. | W in. | a/w. | Y | $P_Q$ Kg. | $\sigma_y$ k.s.i. | $K_Q$ k.s.i. $\sqrt{\text{in.}}$ | $\beta$ | Comments. |
|---|---|---|---|---|---|---|---|---|---|---|---|
| 1A1L | R.T. | 1.25 | 1.625 | 2.50 | 0.650 | 16.78 | 2930 | 135 | 55 | 0.42 | Valid |
| 1A2T | R.T. | 1.25 | 1.645 | 2.50 | 0.659 | 17.50 | 2250 | 135 | 44 | 0.26 | Valid |
| 1A3L | 100 | 1.25 | 1.660 | 2.50 | 0.664 | 17.92 | 5250 | 130 | 110 | 1.80 | Invalid on $\beta$ |
| 1A4T | 100 | 1.25 | 1.530 | 2.50 | 0.612 | 14.22 | 4500 | 130 | 98 | 1.40 | Invalid on $\beta$ |
| 1A5L | 120 | 1.25 | 1.589 | 2.50 | 0.636 | 15.75 | 5500 | 130 | 105 | 1.63 | Invalid on $\beta$ |
| 1A5L | 200 | 1.25 | 1.760 | 2.50 | 0.704 | 21.87 | 3700 | 130 | 95 | 1.30 | Invalid on $\beta$ |
| 1A6T | 200 | 1.25 | 1.740 | 2.50 | 0.693 | 20.67 | 3000 | 135 | 73 | 0.73 | Invalid on offset. |
| 1A7L | 300 | 1.25 | 1.657 | 2.50 | 0.664 | 17.92 | 4120 | 135 | 87 | 1.04 | Valid |
| 1A8T | 300 | 1.25 | 1.695 | 2.50 | 0.678 | 19.17 | 3000 | 135 | 64 | 0.56 | Valid |
| 1A9L | 400 | 1.25 | 1.650 | 2.50 | 0.662 | 17.75 | 3938 | 130 | 82 | 0.99 | Valid |
| 1A10L | 400 | 1.25 | 1.545 | 2.50 | 0.618 | 14.58 | 6000 | 130 | 102 | 1.54 | Invalid on $\beta$ |
| 1A10L | 400 | 1.25 | 1.755 | 2.50 | 0.704 | 21.88 | 3312 | 130 | 86 | 1.10 | Invalid on offset. |
| 1A11T | 150 | 1.25 | 1.634 | 2.50 | 0.654 | 17.09 | 4030 | 135 | 81 | 0.90 | Valid |
| 1A12T | 250 | 1.25 | 1.580 | 2.50 | 0.632 | 15.48 | 4540 | 130 | 83 | 1.02 | Valid |
| 1A13L | 500 | 1.25 | 1.656 | 2.50 | 0.664 | 17.92 | 4380 | 130 | 92 | 1.25 | Valid |
| 1A14L | 500 | 1.25 | 1.652 | 2.50 | 0.662 | 17.75 | 4090 | 135 | 85 | 1.00 | Valid |
| 1A15T | 250 | 1.25 | 1.635 | 2.50 | 0.655 | 17.17 | 4000 | 130 | 81 | 0.97 | Valid |
| 1A16T | 350 | 1.25 | 1.595 | 2.50 | 0.639 | 15.96 | 4320 | 135 | 81 | 0.90 | Valid |
| 1A17L | 450 | 1.25 | 1.608 | 2.50 | 0.644 | 16.33 | 5100 | 130 | 98 | 1.42 | Invalid on $\beta$ |
| 1A18T | 150 | 1.25 | 1.600 | 2.50 | 0.640 | 16.04 | 4565 | 135 | 86 | 1.01 | Valid |

NO TEST MATERIAL WAS AVAILABLE TO DETERMINE THE ELEVATED .2% PROOF STRESS. IN CONSEQUENCE, THE $\sigma_{y.s.}$ VALUES HAVE BEEN CALCULATED FROM THE AMBIENT .2% PROOF STRESS.

58b-

## TABLE 6.

### ELEVATED TEMPERATURE FRACTURE TOUGHNESS TESTS OF INSERT "B".

| Specimen. | Temp. °C. | B in. | a in. | W in. | a/w. | Y. | $P_Q$ Kg. | $\sigma_y$ k.s.i. | $K_Q$ k.s.i. $\sqrt{\text{in.}}$ | $\beta$ | Comments. |
|---|---|---|---|---|---|---|---|---|---|---|---|
| 1B1L | R.T. | 1.25 | 1.674 | 2.50 | 0.670 | 18.44 | 5125 | 125 | 105 | 1.76 | Invalid on $\beta$ |
| 1B2T | R.T. | 1.25 | 1.626 | 2.50 | 0.651 | 16.86 | 4125 | 125 | 77 | 0.95 | Valid. |
| 1BD1 | R.T. | 1.25 | 1.706 | 2.50 | 0.683 | 19.66 | 3500 | 125 | 77 | 0.95 | Valid. |
| 1B3L | 100 | 1.25 | 1.630 | 2.50 | 0.653 | 17.01 | 5000 | 127.5 | 100 | 1.53 | Invalid on $\beta$ |
| 1B4T | 100 | 1.25 | 1.645 | 2.50 | 0.658 | 17.41 | 4750 | 127.5 | 97 | 1.45 | Invalid on $\beta$ |
| 1B5L | 200 | 1.25 | 1.625 | 2.50 | 0.650 | 16.78 | 5520 | 125 | 108 | 1.85 | Invalid on $\beta$ |
| 1B6T | 200 | 1.25 | 1.687 | 2.50 | 0.675 | 18.89 | 3440 | 125 | 76 | 0.92 | Valid |
| 1B7L | 300 | 1.25 | 1.614 | 2.50 | 0.047 | 16.35 | 5813 | 127.5 | 108 | 1.82 | Invalid on $\beta$ |
| 1B8T | 300 | 1.25 | 1.679 | 2.50 | 0.672 | 18.62 | 3625 | 127.5 | 76 | 0.90 | Valid |
| 1B9L | 400 | 1.25 | 1.654 | 2.50 | 0.662 | 17.75 | 4000 | 125 | 80 | 1.02 | Valid |
| 1B10L | 400 | 1.25 | 1.685 | 2.50 | 0.675 | 18.89 | 4500 | 125 | 95 | 1.45 | Invalid on $\beta$ |
| 1B13L | 500 | 1.25 | 1.707 | 2.50 | 0.682 | 19.56 | 3156 | 127.5 | 70 | 0.75 | Valid |
| 1B14T | 500 | 1.25 | 1.606 | 2.50 | 0.643 | 16.25 | 4710 | 123 | 86 | 1.18 | Invalid on offset. |
| 1B15T | 250 | 1.25 | 1.642 | 2.50 | 0.667 | 18.18 | 5285 | 126.5 | 108 | 1.82 | Invalid on $\beta$ |
| 1B16T | 350 | 1.25 | 1.632 | 2.50 | 0.654 | 17.09 | 4156 | 126.5 | 80 | 1.00 | Valid |
| 1B18T | 150 | 1.25 | 1.661 | 2.50 | 0.666 | 18.09 | 4219 | 125 | 83 | 1.105 | Valid |
| 1B19T | 150 | 1.25 | 1.621 | 2.50 | 0.648 | 16.63 | 4970 | 125 | 93 | 1.38 | Invalid on $\beta$ |
| 1B20L | 450 | 1.25 | 1.625 | 2.50 | 0.650 | 16.78 | 4938 | 126.5 | 93 | 1.35 | Invalid on $\beta$ |

NO TEST MATERIAL WAS AVAILABLE TO DETERMINE THE ELEVATED .2% PROOF STRESS. IN CONSEQUENCE THE $\sigma_{y.s.}$ VALUES HAVE BEEN CALCULATED FROM THE AMBIENT .2% PROOF STRESS.

## TABLE 7.

### ELEVATED FRACTURE TOUGHNESS RESULTS. STEPPED TEST BAR.

| Specimen. | Temp. °C. | B in. | a in. | W in. | a/w | Y. | $\sigma_y$ k.s.i. | $P_Q$ Kg. | $K_Q$ k.s.i. $\sqrt{in.}$ | $\beta$ | Comments. |
|---|---|---|---|---|---|---|---|---|---|---|---|
| | | | | | LARGE SECTION. | | | | | | |
| S1L | R.T. | 1.25 | 1.350 | 2.5 | 0.540 | 10.89 | 174.7 | 4750 | 57.6 | 0.27 | Valid. |
| S2T | 100 | 1.25 | 1.625 | 2.5 | 0.650 | 16.78 | 169 | 4625 | 83 | 0.59 | Valid. |
| S3L | 200 | 1.25 | 1.685 | 2.5 | 0.674 | 18.80 | 140 | 3970 | 83 | 0.87 | Valid. |
| S4T | 300 | 1.25 | 1.675 | 2.5 | 0.672 | 18.62 | 147 | 4125 | 86 | 0.85 | Valid. |
| S5L | 400 | 1.25 | 1.675 | 2.5 | 0.660 | 17.58 | 133 | 3250 | 64 | 0.50 | Valid. |
| S6T | 500 | 1.25 | 1.798 | 2.5 | 0.719 | 23.9 | 118 | 2530 | 67.5 | 0.60 | Valid. |
| | | | | | SMALL SECTION. | | | | | | |
| S8L | R.T. | 1.25 | 1.623 | 2.5 | 0.650 | 16.78 | 174.7 | 3125 | 59 | 0.28 | Valid. |
| S7T | 110 | 1.25 | 1.675 | 2.5 | 0.671 | 18.53 | 169 | 3000 | 62 | 0.50 | Valid. |
| S10L | 200 | 1.25 | 1.700 | 2.5 | 0.680 | 19.36 | 140 | 3960 | 85 | 0.92 | Valid. |
| S9T | 300 | 1.25 | 1.648 | 2.5 | 0.659 | 17.50 | 147 | 2625 | 52 | 0.31 | Valid. |
| S11T | 400 | 1.25 | 1.632 | 2.5 | 0.653 | 17.01 | 133 | 2950 | 56 | 0.52 | Valid. |
| S12L | 500 | 1.25 | 1.657 | 2.5 | 0.662 | 17.81 | 118 | 2665 | 52.8 | 0.50 | Valid. |

The $\sigma$ y.s. figures are calculated from the elevated temperature .2% proof stress.

These figures represent the variation of the Kc. for a fixed thickness, namely 1.25 inches, versus temperature for each material. From the fracture appearances of Figs. 43, 44 and 45 it would seem unlikely that the shape of these curves (Figs. 38, 39 and 40) would change significantly even if tests had been carried out at four times the thickness actually used. (Indeed had such a thickness been envisaged the furnace would not have been large enough nor the 5000 Kg. Instron load cell adequate to conduct the tests).

Fig. 41. shows traces of load / C O D for samples from the stepped test block, tested at $500^{o}$C. and room temperature. The vertical scale gives the load in thousands of kilograms. Thus the room temperature tests on the chosen specimen dimensions uses most of the 5000 Kg. capacity of the Instron. $K_Q$ values are calculated from -

$$K_Q = \frac{P_Q}{B W^{\frac{1}{2}}} \left[ 29.6 \left(\frac{a}{w}\right)^{\frac{1}{2}} - 185.5 \left(\frac{a}{w}\right)^{3/2} + 655.7 \left(\frac{a}{w}\right)^{5/2} - 1010 \left(\frac{a}{w}\right)^{7/2} + 638.9 \left(\frac{a}{w}\right)^{9/2} \right]$$

$$\text{Hence } K_Q = \frac{P_Q Y_2}{B W^{\frac{1}{2}}}$$

Where the stress intensity coefficient values of $Y_2$ for specific values of $\frac{a}{w}$ are obtained from standard reference tables (34).

### 5.3.1.   THICKNESS FOR PLANE STRAIN FRACTURE.

The American and British (34) Standards for toughness testing require

a minimum thickness, B, for plane strain value of Kc, namely $K_{1c}$, such

that —

$$B \text{ min.} = 2.5 \left( \frac{K_Q}{\sigma_{ys}} \right)^2$$

Irwin & McClintock (47) have shown that the radius ry of the plastic

zone under plane strain plastic behaviour is given by —

$$ry = 0.05 \left( \frac{K_{1c}}{\sigma_{ys}} \right)^2$$

The B minimum is therefore about 50 times the radius of the plastic

zone which would ensure small shear lips. The shear lips are

expected to extend inwards to a depth of about the plane stress plastic

zone radius at each side of the specimen. The plane stress plastic

zone (47) is about three times the radius of the plane strain plastic

zone. In fact tests on some materials show that the toughness Kc.

reaches a minimum value, $K_{1c}$, at smaller thicknesses than the B minimum

given above.   If this was true for the die steel examined here then

specimens of less than 1.25 in. thickness would still show the

same Kc. values.   These Kc. values for thinner specimens would then

be proved to be $K_{1c}$ values.     It was decided to test thinner specimens

in order to estimate the real thickness requirement for plane strain

fracture as distinct from the conservative thickness of $2.5 \left( \frac{K_{1c}}{\sigma_{ys}} \right)^2$

as specified by Standards.


Sufficient material was available for eight specimens only, and these

were prepared in accordance with Table 8.

TABLE 8.

| Specimen. | Size. | Notch. | Direction. |
|---|---|---|---|
| | | INSERT "A". | |
| A, B & D | $\frac{1}{4}$" x $\frac{1}{2}$" x $2\frac{1}{2}$" | 1/16" wide x .2" deep. | Longitudinal. |
| E1 & E2 | $\frac{3}{8}$" x $\frac{3}{4}$" x $3\frac{1}{2}$" | 1/16" wide x .2" deep. | Longitudinal. |
| TF & TG | $\frac{1}{2}$" x 1" x $4\frac{1}{2}$" | 1/8" wide x .3" deep. | Transverse. |
| | | INSERT "B". | |
| I | $\frac{1}{2}$" x 1" x $4\frac{1}{2}$" | 1/8" wide x .3" deep. | Longitudinal. |

The tests were conducted in accordance with the proposed method of test for plane strain testing (34). After fatigue cracking of the notch bend specimens values of $K_Q$ (candidate values of $K_{1c}$) were calculated, and checked against the validity criteria to determine whether or not they can be considered valid $K_{1c}$ results. The resultant properties are given in Table 9.

-62-

## TABLE 9.

SMALL SECTION THREE POINT BEND TESTS. FRACTURE TOUGHNESS DETERMINED AT ROOM TEMPERATURE.

| Specimen. | B in. | a in. | W in. | $a/w$ | Y | $\sigma_y$ k.s.i. | $P_Q$ k.s.i. | $K_Q$ k.s.i. $\sqrt{in.}$ | $\beta$ |
|---|---|---|---|---|---|---|---|---|---|
| | | | | INSERT "A" | - LONGITUDINAL TESTS. | | | | |
| A | 0.252 | 0.269 | 0.501 | 0.537 | 12.0 | 132.2 | 0.84 | 56.2 | 0.45 |
| B | 0.255 | 0.252 | 0.504 | 0.500 | 10.61 | 132.2 | 1.32 | 77.6 | 0.86 |
| D | 0.255 | 0.260 | 0.500 | 0.521 | 11.37 | 129.9 | 0.96 | 60.5 | 0.54 |

Specimen size $\frac{1}{4}$" x $\frac{1}{2}$" x $2\frac{1}{4}$" Notch 1/16" wide .2" depth.

| | | | | | | | | | |
|---|---|---|---|---|---|---|---|---|---|
| E1 | 0.382 | 0.411 | 0.753 | 0.546 | 12.37 | 132.2 | 2.0 | 75.3 | 0.83 |
| E2 | 0.377 | 0.415 | 0.753 | 0.552 | 12.64 | 132.2 | 2.02 | 78.7 | 0.88 |

Specimen size $\frac{3}{8}$" x $\frac{3}{4}$" x $3\frac{1}{2}$" Notch 1/16" wide .3" depth.

TRANSVERSE TESTS.

| | | | | | | | | | |
|---|---|---|---|---|---|---|---|---|---|
| TF | 0.506 | 0.424 | 1.00 | 0.424 | 8.44 | 129.9 | 4.18 | 69.7 | 0.72 |
| TG | 0.500 | 0.350 | 1.00 | 0.350 | 6.91 | 132.2 | 5.5 | 76.0 | 0.83 |

Specimen size $\frac{1}{2}$" x 1" x $4\frac{1}{2}$" Notch $\frac{1}{8}$" wide .3" depth.

INSERT "B" - LONGITUDINAL TEST.

| | | | | | | | | | |
|---|---|---|---|---|---|---|---|---|---|
| I | 0.504 | 0.404 | 1.00 | 0.404 | 7.98 | 132.2 | 4.14 | 65.5 | 0.61 |

Specimen size $\frac{1}{2}$" x 1" x $4\frac{1}{2}$" Notch $\frac{1}{8}$" wide .3" depth.

ALL THESE RESULTS FAILED TO MEET THICKNESS CRITERIA IN THAT IF $2.5\left(\frac{K_Q}{\sigma_y}\right)^2$ IS LESS THAN THE SPECIMEN THICKNESS (B) THE RESULT IS VALID.

$\sigma$ y.s. OBTAINED FROM DATA RELATING TO A HOUNDSFIELD TENSILE SPECIMEN TESTED AT ROOM TEMPERATURE.

The individual test results for the notch bend specimens are shown in Table 9, and the data for the various specimens are plotted in Fig 42, against specimen thickness. Included in Fig 42. is room temperature data obtained on 1.25 inch thick C.K.S. specimens from similar material. Superimposed on Fig 42 are lines indicating the limiting values of $K_Q$ which would satisfy the criteria of validity and be termed valid $K_{1c}$ tests. It can be seen from Fig. 42a, the figure with the most data, that at thicknesses below the limit of validity there is an apparent increase in the measured value of $K_Q$ and, although there is very little data, Fig 42b. reinforces this observation. The transition to plane strain conditions for the die steel does therefore appear to be complete only at a thickness of

$$2.5 \left( \frac{K_{1c}}{\sigma_{ys}} \right)^2 .$$

## 5.4 LOSS OF FRACTURE TOUGHNESS AT ELEVATED TEMPERATURES.

This loss of toughness was unexpected and contrary to the view that toughness is generally improved with increasing temperature. It was decided to examine the fracture surfaces of selected specimens by Stereoscan viewing. The fracture surfaces obtained in the series tests are shown in Figs. 43, 44 and 45.

Krafft (46) proposed a micro-mechanism for fracture in terms of the
linking of voids back onto the crack tip. The model allowed the
fracture toughness to be written in terms of the distance between
void centres, d, called the fracture process zone, the strain
hardening exponent, n, and Young's modulus, E. Thus :

$$K_{1c} = En \left(2 \pi d_T\right)^{\frac{1}{2}}$$

In order to investigate whether the toughness of the die steels
could be related to the spacing of the dimples on the fracture
surfaces specimens were examined in the scanning electron microscope
using a magnification of  x 300 for comparison purposes. Fracture
tests at temperatures above $300^{o}C$. produced, unfortunately, badly
oxidised fracture surfaces which could not be examined.  Since the
ductile dimples would characterize the material it was decided
to fracture round tensile bars at temperatures from $300^{o}C$. to $500^{o}C$
simply to produce fracture surfaces to examine. The tensile test
pieces were taken to fracture enclosed in a vacuum chamber.
The fracture surfaces, unoxidised, were therefore available for
examination.

Figs. 46 and 47 show fracture surfaces of die steel specimens from
insert "B".

Difficulty in assessing what constituted a true dimple formation was
encountered. The following results were considered representative –

| | | |
|---|---|---|
| 1A1L | Room temperature | 9 dimples. |
| 1A3L | $100^{\circ}$C. | 9 dimples. High toughness. |
| 1A5L | $200^{\circ}$C. | 8 dimples. High toughness. |
| 1A7L | $300^{\circ}$C. | 8 dimples. |
| 1B1L | Room temperature | 8 dimples. |
| 1B5L | $200^{\circ}$C. | 8 dimples. High toughness. |
| 1B7L | $300^{\circ}$C. | 7 dimples. |
| 1B9L | $400^{\circ}$C. | 7 dimples with colonies of ductile zones. |
| S2T | $100^{\circ}$C. | 7 dimples. |
| S3L | $200^{\circ}$C. | 7 dimples. High toughness. |

It is evident overall that no distinct discrimination between the
dimple size of specimens possessing superior fracture toughness to that
existing at elevated temperatures can be noted, and this is particularly
the case with insert "B" on which the largest number of specimens was
available for examination. Furthermore, determination of dimple size is
not easily interpreted using this particular examination method.
Surface specimen oxidation, which occurred during the elevated
temperature toughness testing, left only one sample – 1B9L – tested at
$400^{\circ}$C. for Stereoscan analysis. A definite change in structure can be
observed with this specimen, as colonies of very highly ductile flat
areas are present.

On selected fracture toughness specimens general Stereoscan examination
was undertaken on the transition area of pre-fatigue cracking and crack
propagation. The specimens were divided into five groups :–

1.   1B1L – 1B9L.
2.   1B2T – 1B6T.
3.   1A1L – 1A3L.
4.   1A2T – 1A6T.
5.   S3L – S2T.

1. B–L Series.

The specimens examined in this series were originally tested at –

        1B1L – room temperature.
        1B7L – 300$^o$C.
        1B5L – 200$^o$C.
        1B9L – 400$^o$C.

                                        see Fig 48.

Each of the specimens examined showed a transition in fracture ranging

from fatigue to ductile, then changing to cleavage as the ductile zone

became wider with increasing temperature. Specimen 1B9L possessed a

fully ductile fracture below the fatigue zone.

2. 1B–T Series.

The specimens examined in this series were originally tested at –

        1B2T – room temperature.
        1B4T – 100$^o$C.
        1B6T – 200$^o$C.

                                        see Fig 49.

There was a ductile zone immediately after the fatigue crack in specimen

1B2T, and then the remainder of the fracture was cleavage. In the case of

the 1B4T and 1B6T specimens the ductile zone extended throughout the

fracture face, i.e. there was no cleavage fracture. Inclusions are noted

in the ductile fractures of 1B4T and 1B6T.


3. 1A–L Series.

The specimens examined in this series were originally tested at –

        1A1L – room temperature.
        1A3L – 100$^o$C.
        1A5L – 200$^o$C.

                                        see Fig 50.

The 1A1L specimen had an almost completely cleavage type fracture – there

was a very small amount of ductile fracture in regions away from the

fatigue crack. Specimen 1A3L had a ductile fracture zone adjacent to the

fatigue crack but further away from the fatigue crack the fracture was the

cleavage type. Areas of cleavage fracture were observed within the fatigue

fracture of specimen 1A5L. The fracture immediately following the end of the

fatigue crack was cleavage but, further away from the fatigue crack the fracture was ductile.

4.  1A-T Series.

The specimens examined in this series were originally tested at —

1A2T — room temperature.
1A4T — $100^{\circ}$C.
1A6T — $200^{\circ}$C.

see Fig 51.

The fracture of the 1A2T specimen was almost 100% cleavage with a very small amount of ductile fracture in areas well away from the fatigue crack. Specimen 1A4T had a ductile zone adjacent to the fatigue crack, followed by an area of cleavage fracture, after which an area of mixed cleavage and ductile fractures, furthest away from the fatigue fracture can be observed. The fracture adjacent to the fatigue crack in specimen 1A6T was cleavage but this gave way to ductile type fracture further away from the fatigue crack.

5.  Stepped Test Block.

The specimens examined were S3L (at $200^{\circ}$C) and S2T (at $100^{\circ}$C), see Fig 52. The specimen S3L had a completely ductile fracture; the fracture adjacent to the fatigue crack in specimen S2T was ductile, but further away from the fatigue crack the fracture was cleavage.

Hot Tensile Specimen.

As the Stereoscan examination of the compact tension specimens was incomplete, because oxidised fracture surfaces tested in the $300-500^{\circ}$C. range could not be viewed, it was necessary to consider what type of fracture test, giving freedom from oxidation, would be of assistance. It was concluded that a round notched tensile test piece, enclosed in a vacuum furnace control unit, used in conjunction with the Mand tensile machine, would be acceptable.

In consequence the specimen size shown below was selected.
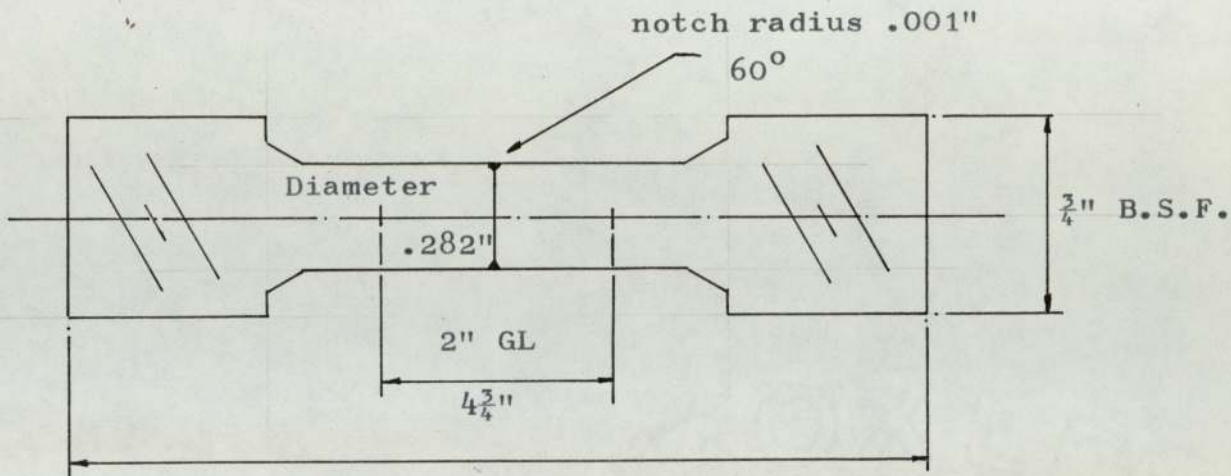


The tensile specimens were heated to the temperatures of 300/500°C.,
the vacuum furnace pressure being held at 2.4 x 10$^{-4}$ mm. Hg. A strain rate
crosshead speed of 0.033" (.84 mm) per minute was used to fracture the
specimens, after which slow cooling in the protective atmosphere unit took
place.


Stereoscan Viewing.

Specimens were subsequently prepared for Stereoscan viewing. It transpired
that no significant differences in examined surface structures could be
noted between the tensile and compact tension specimens when viewed at
low magnifications. To assess any possible structural variation six
samples were viewed at x  2,700  –

Compact tension sample 1A1L – originally tested at room temperature.
  "        "       "   1B1L –    "        "     "    "   "      "
  "        "       "   1B5L – originally tested at 200°C.
  "        "       "   1B7L – originally tested at 300°C.
  "        "       "   1B9L – originally tested at 400°C.
Round notched tensile sample tested at          500°C.


The structures are noted in Figs. 53 and 54.  A mixed mode of dimple,
but predominently cleavage, is noted with specimens 1A1L, 1B1L and 1B5L.
An entirely different dimple ductile structure is associated with the samples
tested in the 300/500°C. range. Surprisingly these dimple ductile structures

are associated with the decay of fracture toughness.

This feature of dimple fractures being observed with falling toughness is contrary to the popularly held view that dimple fracture is normally associated with ductile fracture whereas cleavage is representative of brittle conditions.

The highest fracture toughness for No. 5. die steel is associated with cleavage type structures, (Fig. 53), whilst reduction in toughness occurring at temperatures greater than $200^{o}C$, observed in Fig 54, indicates that a fine dimple pattern exists.

Thomason (48) showed that inclusions and second phase particles contribute in no small measure in determining the ductile-fracture process. They form sites for the nucleation of internal cavities; such cavities coalesce by a mechanism of internal necking to induce a fracture surface. The two systems whereby second phase particles are transformed to a nucleus cavity consists of :

1. The particles fracture under induced stress.
   or
2. The stress system associated with the geometry of the particle may cause a breakdown of the matrix/particle cohesion bond.

That the Stereoscan examination of No. 5. die steel specimens show a distinct change of structure from cleavage to a dimple pattern, and, furthermore, that cleavage is observed with improved toughness, should be reviewed in light of the work of Thomason in which the nucleation sites shown to be present with specimens tested above $300^{o}C$. would offer the least resistance to crack propagation.

The general Stereoscan examination for the steels shown in Figs. 48-52

exhibits a mixture of cleavage and ductile structures. Comparing

the room temperature structure for the inserts it should be

remembered that insert "A" possessed lower fracture toughness than

sample "B" and, furthermore, the structure observed with fracture

toughness specimens tested at room temperature possessed a

cleavage type structure.

## 5.5     HOT TENSILE DATA AND STRAIN AGEING.

Detailed examination of the hot tensile data, (Fig. 55) revealed a
deviation in proof and tensile stress in the region of $250^{\circ}C$.
This suggested that strain ageing was exerting some influence upon
the loss of proof and tensile stress.

Baird (49) in surveying the published work on strain ageing,
particularly in considering dynamic strain conditions, (50) noted the
elements manganese, molybdenum and chromium reduce the mobility of
carbon and nitrogen atoms.        He arrived at this conclusion
because the combined effects of the interstitial (carbon or nitrogen)
together with the substitutional solute (manganese, molybdenum or
chromium) were greater than the summed effects of a single
interstitial, say carbon, and a single substitutional, say molybdenum.
Baird considered that these carbide forming elements (molybdenum or
chromium) could retain a high concentration of carbon in solid
solution through a "solid solution" binding effect. This he termed
interaction solid solution hardening.    The interaction solid
solution hardening is a possible explanation of high temperature
dynamic strain ageing effects. These effects can be clearly seen
as an increase in work hardening rate as temperature increases.
This gives rise to a peak when a 1% proof stress or a tensile stress
is plotted against temperature, as in Fig. 56.

6.    <u>DISCUSSION</u>.

# D I S C U S S I O N.

## 6.1    INSERTS.

### Mechanical and Metallographic Properties.

Though the toughnesses of the two inserts were not compared on the
basis of $K_{1c}$, plane strain values, the comparison on the basis of Kc.
values at a fixed thickness of 1.25 in. is valid. In fact
the local surface cracking on die inserts, which leads to their
withdrawal from service, occurs in areas of thickness from
below 1 in. to above 1 in. as shown in Fig 8.

In general the material taken from insert B. had superior Kc.
values, as far as longitudinal specimens were concerned, in the working
temperature range $100^{o}$C. to $300^{o}$C.  This is consistent with the
longer service life of insert "B" as compared to insert "A".
It would therefore seem that fracture toughness is a good property
on which to base the relative suitability of a material for die
inserts when the failure mechanism is surface cracking. Of course it
is not yet clear whether the toughness itself is the best criterion
for material selection, or whether a fracture toughness approach
to fatigue properties would give a better correlation with service
life. The latter is beyond the scope of this project.

The normal tensile properties indicate that the insert "A" material
has greater proof stress and ultimate tensile stress, by about 5 t.s.i.
in comparison with insert "B". Thus, the greater strength properties
do not provide greater service life.

The metallographic structure is similar in both inserts, except that insert "A" has more pronounced banding. Further, insert "A" has less oxide inclusions but more manganese sulphide inclusions. It is not possible to make definitive interpretations of the effects of banding, oxide inclusions or manganese sulphide inclusions, on the high temperature toughness, though clearly this should be investigated more fully.

## 6.2 MECHANICAL AND METALLOGRAPHIC PROPERTIES OF THE STEPPED TEST BLOCK.

The effect of upset forging, together with incorporating a water quenching cycle in the heat treatment of No. 5. die steel has demonstrated that the transverse tensile properties  and notch impact properties are superior to the transverse properties of the inserts.  The ratio of proof to ultimate tensile stress has been increased to that present with the two direct forged oil hardened and tempered inserts. The acicular tempered martensitic structure of the stepped test block differs from the mixed transformation structure present with the two inserts. The total non-metallic inclusion content of the stepped test block is higher than that present with the inserts.

## 6.3 FRACTURE TOUGHNESS.

For the first time fracture toughness of No. 5. die steel has been assessed at elevated temperatures. A rather surprising feature can be observed by comparing the ambient temperature fracture toughness to that existing at elevated temperatures, in that a decrease in toughness is present at temperatures greater than $300^{o}$C. but from ambient to $200^{o}$C. a significant rise in toughness takes place.

This improvement in toughness in the ambient to approximately $100^{o}C.$ range has often been recorded in published literature for a general variety of low alloy steels. No. 5. die steel follows this same pattern but, contrary to the generally held view that by still further increasing the test temperature an increase in toughness takes place with steels, basically irrespective of alloy composition, has been disproved for No. 5. hot work die steel.

On the basis that all the high temperature results are readily comparable because of the use of constant thickness specimens, the Kc. values approach the true $K_{1c}$ for this nickel-chromium-molybdenum die steel. The elevated fracture toughness data of the "A" and "B" inserts is compared on the basis of Kc. values for 1.25 in. thickness since $K_{1c}$ criteria were not met at all temperatures. This situation did not arise in the case of the stepped test block in which acceptable validity requirements were met. From the data obtained with the eight small notch bend specimens, (Tables 8 & 9) there does not appear to be any basis for reducing the thickness limitation in the fracture toughness test method for No. 5. die steel.

In comparing the fracture toughness in terms of Kc. for 1.25 in. thickness of the two inserts obtained from identical sampling positions, the room temperature fracture toughness of insert "B" is clearly superior. The transverse properties for both inserts have a maximum toughness at $100^{o}C.$ thereafter, a decay occurs : it can additionally be observed that the transverse toughness of insert "B" is less erratic than that associated with sample "A".

In the past the assessment of toughness has placed emphasis upon notch impact toughness data. Transition data for No. 5. die steel has demonstrated that using the notched test bar method an improvement in toughness does occur. With increasing temperature, however, crack propagation data shows this not to be the case.

## The Effect of Non-Metallic Inclusions on Fracture Toughness.

Some (23) consider that low sulphur content helps to promote cleaner steels and, in consequence, better fracture toughness. Others (29) disagree and observe no difference in toughness between 5% chromium hot work die steels processed either by air cast or electro-slag melting.

This investigation has shown, on the basis of cleanliness, when comparing insert"B" containing a total area count of 0.190% non-metallic inclusions, to insert "A" possessing 0.206%, that the latter has inferior ambient fracture toughness, but critical non-destructive testing examination proved, overall, that insert "B" contained more inclusions than insert "A"; it must be recognised that the metallographic examination had less total area assessment compared to that carried out when ultrasonically examining the inserts.
As sample "B" has better fracture toughness, it must be concluded that such inclusions, although not significantly different between each insert, have not had the expected deleterious effect.

## 6.4    STEPPED TEST BAR.

The upset forged test block on which totally valid $K_{1c}$ results
were obtained received a varying amount of hot working, ranging
from 6.8:1 for the larger section to 17:1 for the smaller end,
and demonstrated that the longitudinal properties are reasonably
constant, but the transverse toughness of the smaller section,
which received the very severe amount of forging, has been
drastically reduced.

A similar toughness pattern exists with the test block to that
with the inserts, in that an increase in toughness from ambient to
$100^{o}$C. takes place; thereafter, the similarity ends, as the
improved test block toughness is maintained at $300^{o}$C. before any
reduction occurs. Assessing these results, it is apparent that the
upset forged test bar suffers less reduction in toughness than
that corresponding to the two direct forged inserts.
Additionally, it should be noted that the heat treatment of this
test block consisted of water/oil quenching and tempering.

The hot tensile data of specimens obtained from the stepped test
block confirmed that the ductility, (as measured by the reduction
in area), shows a gradual fall-off from ambient tempersture
to $200^{o}$C. and a trough exists between $200^{o}$C. and $400^{o}$C. before an
improvement occurs.  The elongation shows little variation with
temperature.

## 6.5 LOSS OF FRACTURE TOUGHNESS.

No simple explanation for decreasing toughness with increasing temperature is forthcoming, though it may be connected with variation of the strain ageing peak seen in Fig 56.

General low magnification Stereoscan examination has failed to reveal any distinct change from ductile to cleavage modes associated with temperature change, although at high resolutions a structural difference was observed which can be correlated to the $250^{\circ}C$. peaking noted with the hot tensile data.

## 6.6 STEREOSCAN EXAMINATION.

With the present state of the art in evaluating structures it is generally considered that dimple fracture patterns are representative of ductile materials such as low carbon steels, whilst a cleavage conditions denotes a tendency to brittle fracture. On this basis the Stereoscan analysis of No. 5. die steel, a material possessing not a simple ferritic structure but transformation products does not conform, as fracture toughness is at a maximum when a predominently cleavage structure is present, whilst a dimple ductile condition is associated with falling toughness.

This evidence may appear contradictory to recently published work ( 51 ) on low carbon alloy steels which stated that the increase in $K_{1c}$ with increasing temperature (up to $120^\circ$C) results in a change in the microscopic mode of fracture from cleavage to ductile tear. It should not be overlooked that the materials used (51) and the structures obtained, with maximum testing temperatures, are totally dissimilar to the work now under review. The measurement of actual dimple size was difficult to interpret based upon the intercept method, but no other metallographic assessment was possible.

It has recently been considered (48) that the matrix/particle cohesive bond relationship sustains the inducement of ductile failure, and that differing second phase particles would effect the cohesive bond strength for the same equivalent volume fracture. The difference in structure observed in Figs. 52 and 53, and with the specimen 1B9L (Fig. 47) must be examined based upon the matrix/ particle relationship ( 48).

For No. 5. die steel the finer dimple structure shows small nucleation cavities compared to those existing with the larger cleavage structure – thus the cohesive strength would be at its greatest with the latter condition.

In consequence, fracture toughness would also be in its maximum state. This is particularly evident with the toughness structure in that measurement of dimple size shows high river lines, whilst falling toughness, particularly that measured at $500^\circ$C. indicates a flat plane ductile–type structure.

## 7.   CONCLUSIONS.

1.  Due to production requirements in the drop forge the use of relatively
    small section insert size was employed, and the toughness examined.
    Additionally, the fracture toughness of a stepped test block was
    assessed. In consequence, it may be considered that the conclusions
    reached need not apply to die blocks whose weight and cross section
    are more substantial. Nevertheless, for the material examined,
    it has been demonstrated that of the two inserts on which industrial
    performance data was obtained, the insert with the highest fracture
    toughness produced the largest number of crankshaft drop forgings.
    Although the production increase was only 402 crankshafts, it was the
    opinion of the Forge Management that if this relatively small die life
    could be maintained, the financial and production contribution would
    be highly beneficial, even though the toughness data on which this
    observation is based does not conform to $K_{1c}$ specification acceptance
    criteria though they are valid Kc. values. It is contended that the
    data presented does form a basis in comparing the fracture toughness
    between the two inserts. Additionally, it should be recalled that
    "B" insert possessed a reduced tensile stress compared with the "A"
    insert.

2.  The difference between direct and an upset forging technique, when
    applied to No. 5. die steel, shows that the fracture toughness of
    the direct forged inserts is inferior; however, it should be
    remembered that a different type of austenitizing treatment was carried
    out with the upset forged material. Furthermore, the difference
    between longitudinal and transverse properties is minimised by
    utilising the upset forged method. The valid $K_{1c}$ stepped test bar results
    conform to specification criteria.  It should additionally be recalled

that a different cast was required to manufacture the stepped test block.

3. The fracture toughness of No. 5. die steel has been established at ambient and elevated temperatures. A surprising result has been obtained in that an increase in toughness from ambient to $300^{o}C$. occurs, thereafter a reduction is observed.

4. The influence of limiting the sulphur content of hot work steels in order to promote cleaner steels, which assists in improving toughness, is not universally accepted. Furthermore, it must be recalled that such evidence applies to hot work steels other than No. 5.

Insert "B" which contained the highest non-metallic inclusions, as measured by a N.D.T. method, possessed the highest ambient fracture toughness which tends to support the view that for No. 5. die steel the observed inclusion contents are not deleterious to toughness.

It must not be overlooked that the majority of nickel-chromium-molybdenum No. 5. die steel is purchased in the fully hardened and tempered condition, at which stage die impression machining is carried out. It is fully recognised in the drop forging industry that the lower the sulphur content the greater is machinability impaired.

5. Further work would be required to relate the decay in the fracture toughness of No. 5. hot work die steel.

A combination of factors must be considered when assessing the cause for the loss of fracture toughness at elevated temperatures. Undoubtedly this investigation has shown that dynamic strain ageing is present. A

change is observed by Stereoscan analysis in that a cleavage type structure is associated with the highest toughness, whilst falling toughness exhibits a ductile dimple pattern. Such factors, whilst being shown to play an important part in the reduction of toughness at elevated temperatures, are difficult to quantify. Future work might include, if the apparatus is available, the total assessment of dynamic strain ageing, as would a detailed study upon what effect dislocations and carbide spacings have based upon Stereoscan analysis.

6. A possible practical implication for the drop-forger using No. 5. die steel has been established, in that if premature cracking of the die tools is being experienced, and all accepted remedial measures have not improved the conditions, then die block pre-heating schedules should be re-examined using the compiled toughness data.

This investigation has shown that maximum fracture toughness is attained in the region of $100^{o}C$. It is therefore logical to use this as a pre-heating temperature for the die tools prior to actual drop forging. Additionally, it has been demonstrated that some previously claimed ideas, whereby increasing such preheating temperatures will automatically lead to better toughness, have been refuted when examined in light of fracture toughness criteria - in fact, a possible reverse situation may apply. The drop-forger, by judicious application of the coolant, should aim to limit in service the die surface temperatures attaining $400-500^{o}C.$, as this is the temperature zone where fracture toughness is reduced.

7. It is readily acknowledged that no single test can be used to assess potential die steels. Such parameters must include factors such as hardenability, adequate wear assessment, mechanical properties, both at

ambient and elevated temperatures, and resistance to mechanical and thermal fatigue. To this standard type testing of hot work die steels should now be added fracture toughness assessment.

The two inserts examined show that the "B" sample, which produced the largest number of drop forgings also possesses the highest fracture toughness, measured at ambient temperature, but at elevated temperatures the fracture toughness results of both inserts followed a similar pattern. Therefore, by compiling data on No. 5. die steel, relative to mass effect, structure and manufacturing techniques, it may be possible by even measuring room temperature toughness to be more able to quantitatively assist the practical wear of die steels. This investigation has demonstrated that fracture toughness assessment has direct everyday relevance to the metal forming industries.

8.  The method of using either conventional Charpy or Izod notch data, to predict the die steel pre-heating temperature to be employed, should be approached with caution. The conventional notch toughness of No. 5. die steel shows no energy loss at elevated temperatures, which differs entirely to the fracture toughness results, in which a significant change in crack propagation resistance characteristics is noted. The employment of fracture toughness data to assess die block preheating and operating conditions is to be recommended.

9.  The art of die design, as yet, does not include detailed stress analyses (commonly employed in the majority of general engineering component design). In consequence, until this art is transformed into a more scientifically-based subject, factors such as critical flow size estimations, using fracture mechanics, may not yield a totally fruitful result.

## REFERENCES.

1.      BAYLISS R.N.
M.Sc. Thesis. October 1967.

2.      ASTON J.L. & MUIR A.R.
Iron & Steel Institute. 1969. 207 (2) p. 167-176.

3.      TIPPER C.F.
"Testing for Brittleness in Steels".
p. 132-150. Report No. Pe H M 50. 1962.

4.      WELLS A.A.
"Brittle Fracture Mechanics - A Survey of
Published Work".
Report No. P3 p. 106-117.  H M 50.
Admiralty Advisory Committee Structural Steel.

5.      IRWIN G.R.
Discussion - Report No. P3 p. 118. H M 50.
Admiralty Advisory Committee Structural Steel.

6.      IRWIN G.R. & WELLS A.A.
Metallurgical Reviews. 1965. Vol. 10. No. 38.
p. 223-270.

7.      GRIFFITH A.A.
Phil. Trans. Roy. Soc. 1920. 221 p. 163.

8.      INGLIS G.R.
Trans. Inst. Naval Arch. 1913. 55. 219 and
"Fracturing of Metals" A.S.M. Symposium 1947.
p. 147. Metals Park. Ohio.

9.      IRWIN G.R.
Trans A.S.M.E. J. Applied Mech 1957. p. 361-365.

10.     OROWAN E.
Rep. Progress Physics. 1949. 12. 185.

11.     BARNBY J.T.
Welding - Metal Fabrications.
February 1969. p. 71-75.

12.     KNOTT J.F.
Iron & Steel Journal. March 1968.
p. 93-99. J.I.S.I. 1966. 204. p. 1014.

13.     Linear Fracture Mechanics. N.E.L. Report No.
465. August 1970.

14.     STEIGERWALD E.A.
Metal Progress 92. 1967. p. 96-101.

15. WINNE D.H. & WUNDT B.H.
Trans. A.S.M.E. 80. 1643. 1958.

16. WESSELL E.T.
A.S.M. Trans. Vol. L.11 1960. p. 277-296.

17. YEN & PENDLEBERRY.
A.S.M. Trans. Vol. 55. 1962. p. 214-229.

18. BIRKLE A.J., WEI P.R., & PELLISSIER G.E.
Trans. Act. A.S.T.M. Vol. 59. 1961. p. 981-998.

19. COTTRELL C.L.M. & LANGSTONE P.F.
J.I.S.I. November 1968. Vol. 206 (2) p. 1077-1087.

20. BARNBY J.T. & BAYLISS R.N.
Metal Forming. June 1969. 36. p. 157-162.

21. HOLLOWAY J.R. & HOPKINS A.D.
"The Effect of Cobalt on the Fracture Toughness
of a Nickel-Molybdenum Hot Work Die Steel".
J.I.S.I. October 1971. p. 813-818. Vol.209. Pt.19.

22. FIRTH K. & GARWOOD R.D.
I.S.I. 120. 1970. p. 81-89.

23. YOUNKIN C.N. & JACOBSEN W.A.
"Factors Affecting the Service Life of Cast Dies".
A.S.M. Technical Report C7-20-5. 1967.

24. BAYLISS R.N.
"Modern Manufacture of Die Blocks for the Metal
Forming Industries".
Metal Forming 1967. 34. p. 229-233 & 276-278.

25. WEISS & YUKAWA.
A.S.T.M. Special Technical Report 381. p. 84.

25a. SRAWLEY J.E.
Proc. Practical Fracture Mechanics Symposium. Risley.
April 1969. p. A3-A13.

26. PELLINI W.S., STEEL L.E., & HAWTHORNE J.R.
U.S. Navy Research Lab. Report 5780. 1962.

27. PELLINI W.S. & LOSS F.J.
N.R.L. Report No. 6900. 1969.

28. BROWN W.F. & SRAWLEY J.E.
A.S.T.M. Special Report No. 410. 1966.

29.    MAY M.J. & WALKER E.F.
B.I.S.R.A. Open Report MG/E/307/67.

30.    BROTHERS A.J. & YUKAWA S.
"Application of Fracture Toughness Parameters to
Structural Metals".
Society of A.E.M.E. Publishers – Gordon & Beech.
Vol. 31. 1966. p. 35–68.

31.    LUBAHN J.D.
Proc. A.S.T.M. 59. 1959. p. 885.

32.    SRAWLEY J.E. & BROWN W.F.
N.A.S.A. Technical Memo. TM-X-52030.
Symposium on Fracture Testing. Chicago June 1964.

33.    WESSELL R.T.
"State of the Art of the W.O.L. Specimen for $K_{1c}$ Fracture
Toughness Testing". J. Eng. Fracture Mech 1968.
Vol. 1. p. 77–103.

34.    British Standard Institution : Draft for Development.
3. 1971. Methods for Plane Strain Fracture Toughness
Testing.

35.    Recommended A.S.T.M. Toughness Testing for Plane
Strain Fracture Toughness Testing.
B.I.S.R.A. Open Report MG/EB/312/67.

36.    British Standard 1500.
Fusion Welded Pressure Vessel Steels for Use in the
Chemical Petroleum & Allied Industries 1958.
A.S.M.E. Unfired Pressure Vessel Code.

37.    HOFER K.E.
Machine Design. February 1968. p. 109–113.

38.    POOK L.P.
"Fracture Mechanics & The Steelmaker".
Iron & Steel – June 1971. p. 197–202.

39.    THORNTON D.V.
"Fracture Toughness of Alloy Steels Used in Turbo-
Generator Components".
Eng. Fracture Mech. 1970. Vol 2. p. 125–141. Paragon Press.

40.    LOGAN J.G. & CROSSLAND B.
London Conference on Pressure Vessel Technology. 1971.
Institution of Mechanical Engineers. p. 148–155.

41.    NICHOLSS R.W.
"The Status of the Application of Fracture Mechanics to
Pressure Vessels" 1971. Conference on Pressure Vessel
Technology. Institution of Mechanical Engineers. p. 307–312.

42.  SUSUKIOA H., ANDO T., TSUJI I. & HIBARU V.
     Mitsubishi Technical Review. Vol. 6. No. 1. 1969 p. 50-61.

43.  BONISZEWSKI T., & RENDALL J.H.
     Discussions. I.S.I. 114. Special Report p. 241-2.

44.  KRAUTKRAMER J.V.H.
     Ultrasonic Non-Destructive Testing of Material.
     Gesellschaftt fur Elektrophysik. p. 259-269. Cologne.

45.  LIVERSIDE D.B. & FERN G.A.
     The Origin Detection and Identification of Defects in
     Steel Forgings.
     British Journal of Non-Destructive Testing.
     March 1967. Vol 9. No. 1.

46.  KRAFFT J.M.
     Applied Materials Research. Vol. 3. 1964.

47.  McCLINTOCK F.A. & IRWIN G.R.
     A.S.T.M.    S.T.P.381. p. 84-5.

48.  THOMASON P.F.
     Metal Science Journal.
     Vol. 5. March 1971. p. 64-67.

49.  BAIRD J.D.
     Metals & Materials. Vol. 5. Review 149. February 1971.

50.  BAIRD J.D.
     Private communication based upon ASM Seminar -
     Homogeneity of Plastic Deformation.

51.  BARSOM J.M. & PELLERGRIND J.V.
     Relationship between $K_{1c}$ and Plane Strain and
     Microscopic Mode of Fracture.
     Engineering Fracture Mechanics. 1973. Vol. 5. p. 209-221.

...
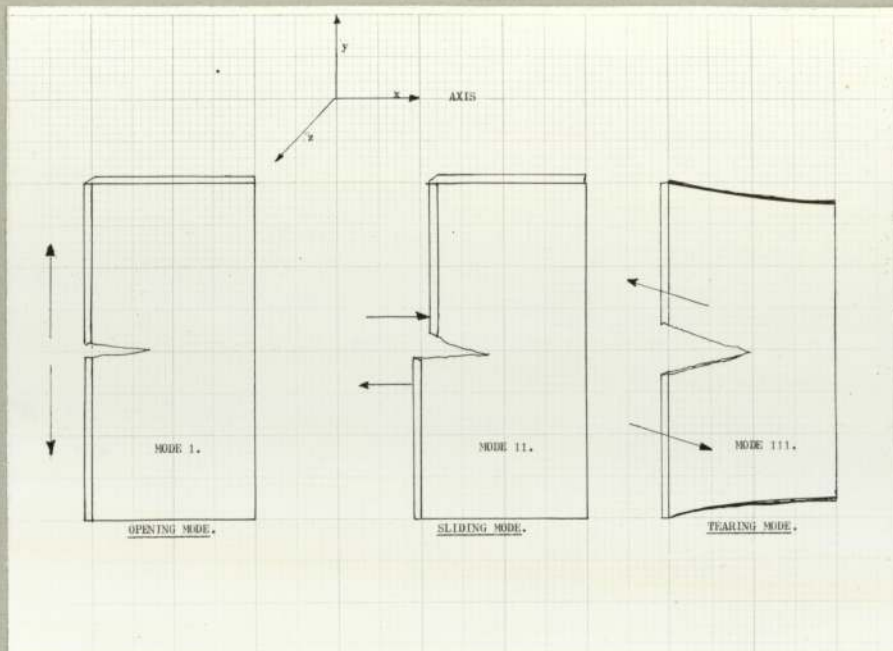
Fig -1-

Displacement modes for crack surfaces.
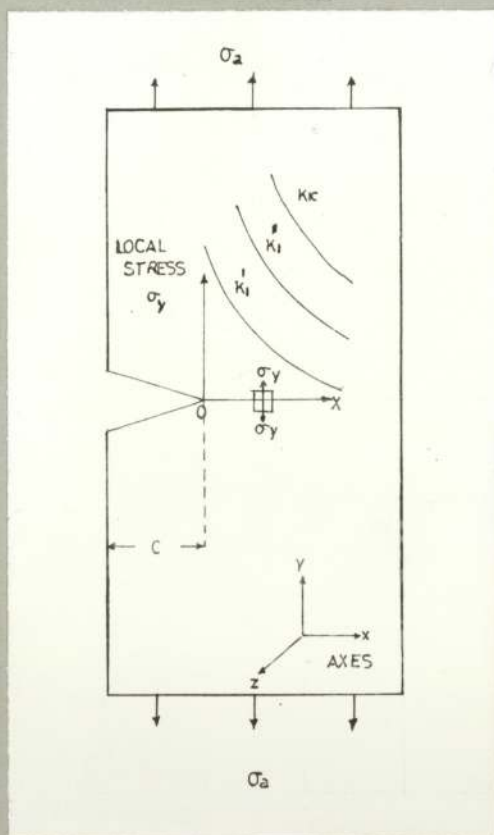


Fig -2a-

Stress distribution
near the root of a notch.
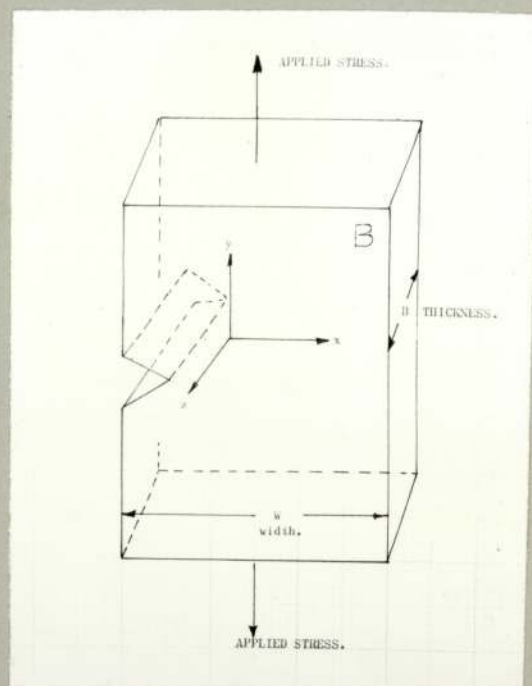


Fig -2b-

Three-dimensional stress
systems under applied load.
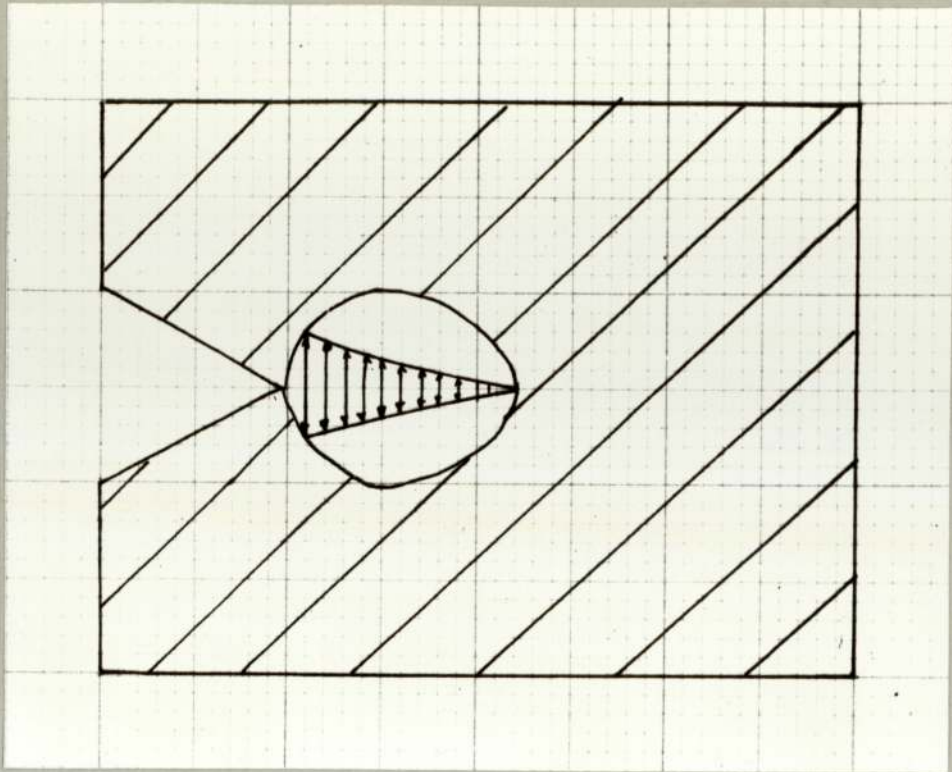
Fig –3a–

THREE DIMENSIONAL STRESS SYSTEM.
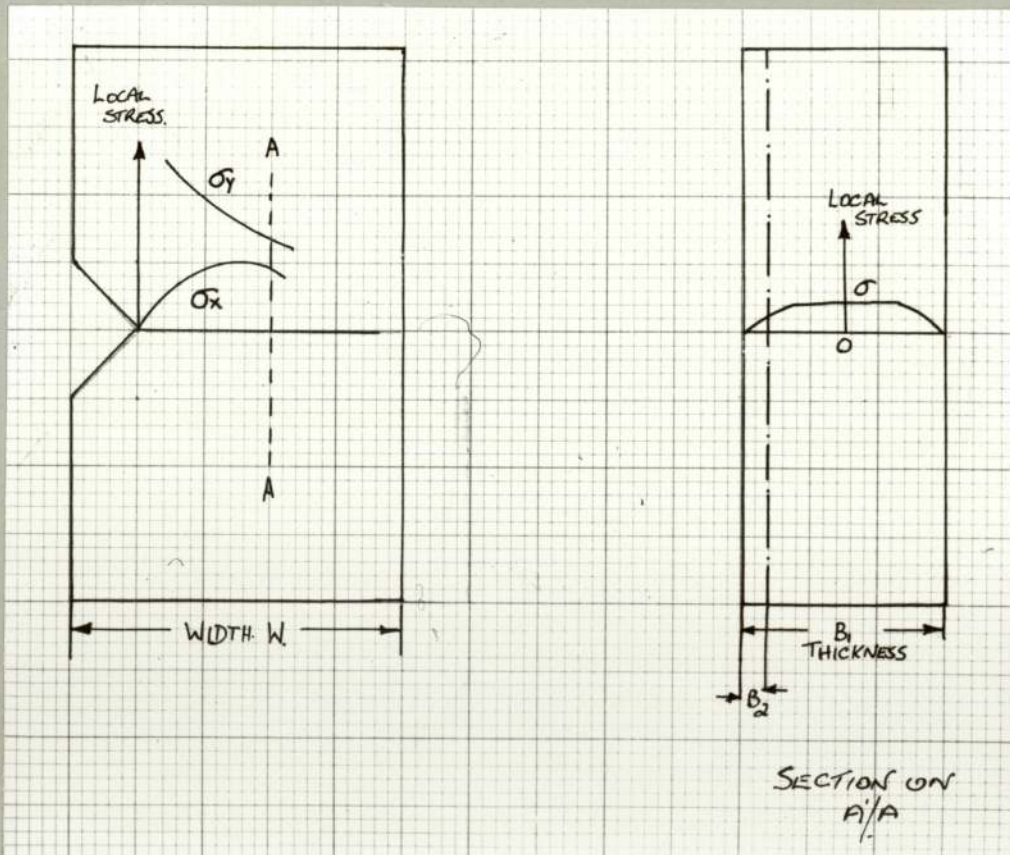


VARIATION OF $\sigma_y$ AND $\sigma_x$ ACROSS
WIDTH. ELASTIC CONDITION.

Fig –3b–

Through crack in plate.
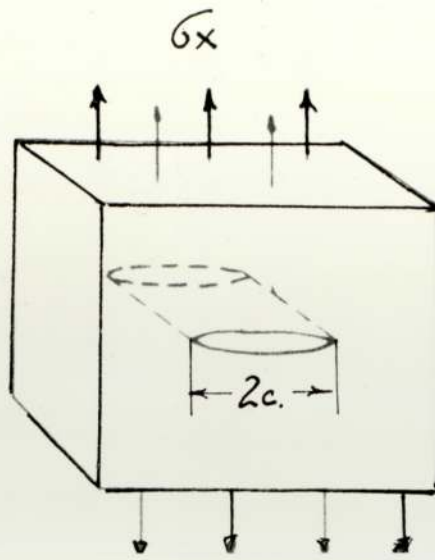
Fig -4-
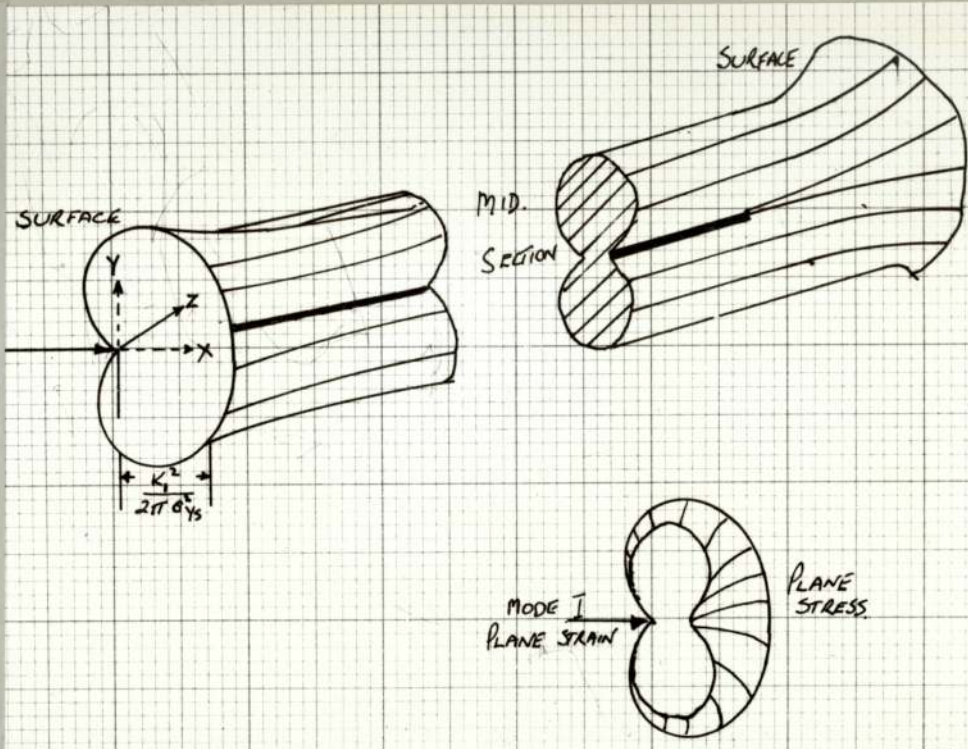
Fig -4a-
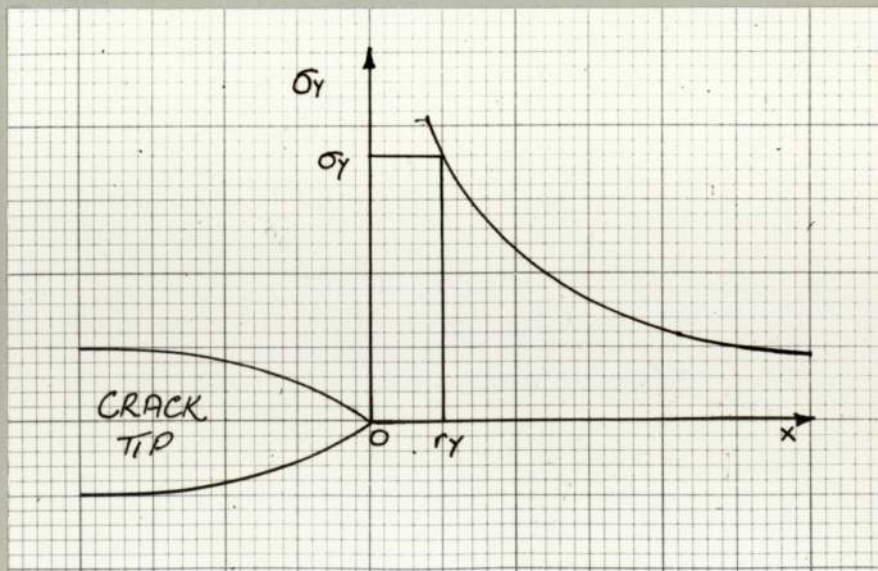


Fig -4b-

PLASTIC YIELDING FROM THE CRACK TIP.

A = Notch.
B = Fatigue notch.
C = Central flat plane strain crack.
D = Plane strain plastic zone.
E = Plane stress plastic zone.
F = Shear lips of the crack.
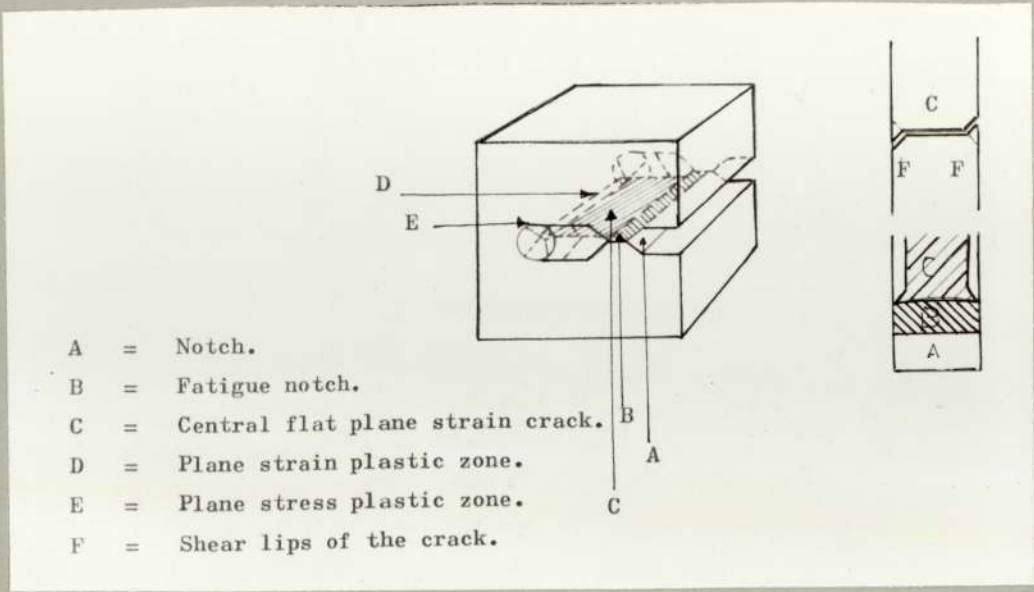
Fig -5-

Freacture Toughness specimen.
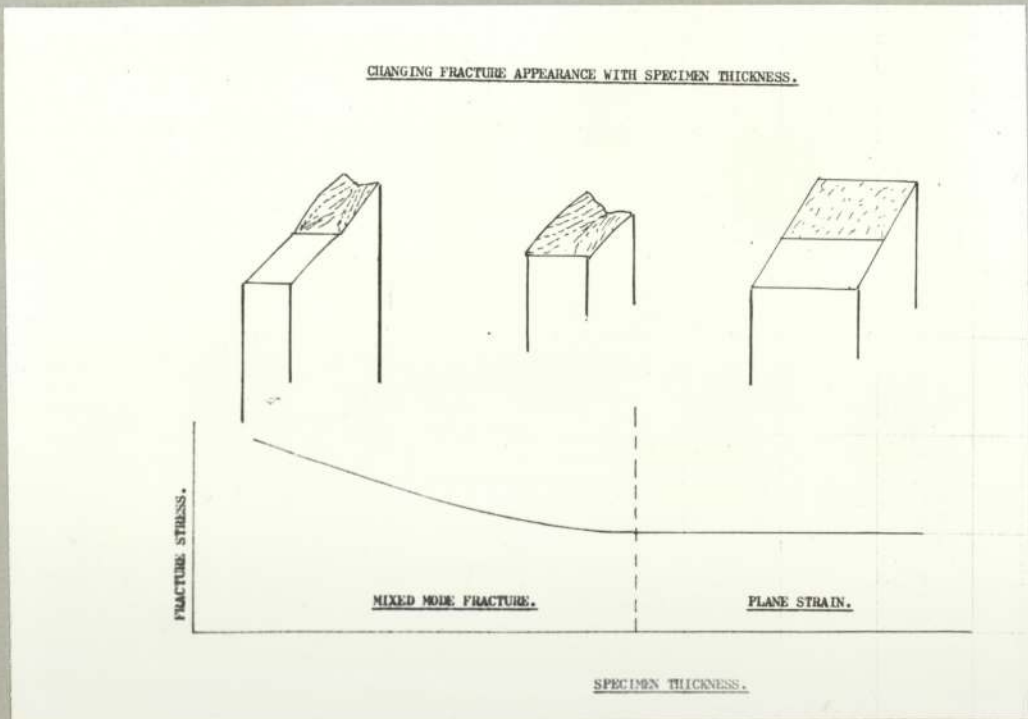


Fig -6-

Fracture Appearance Change.
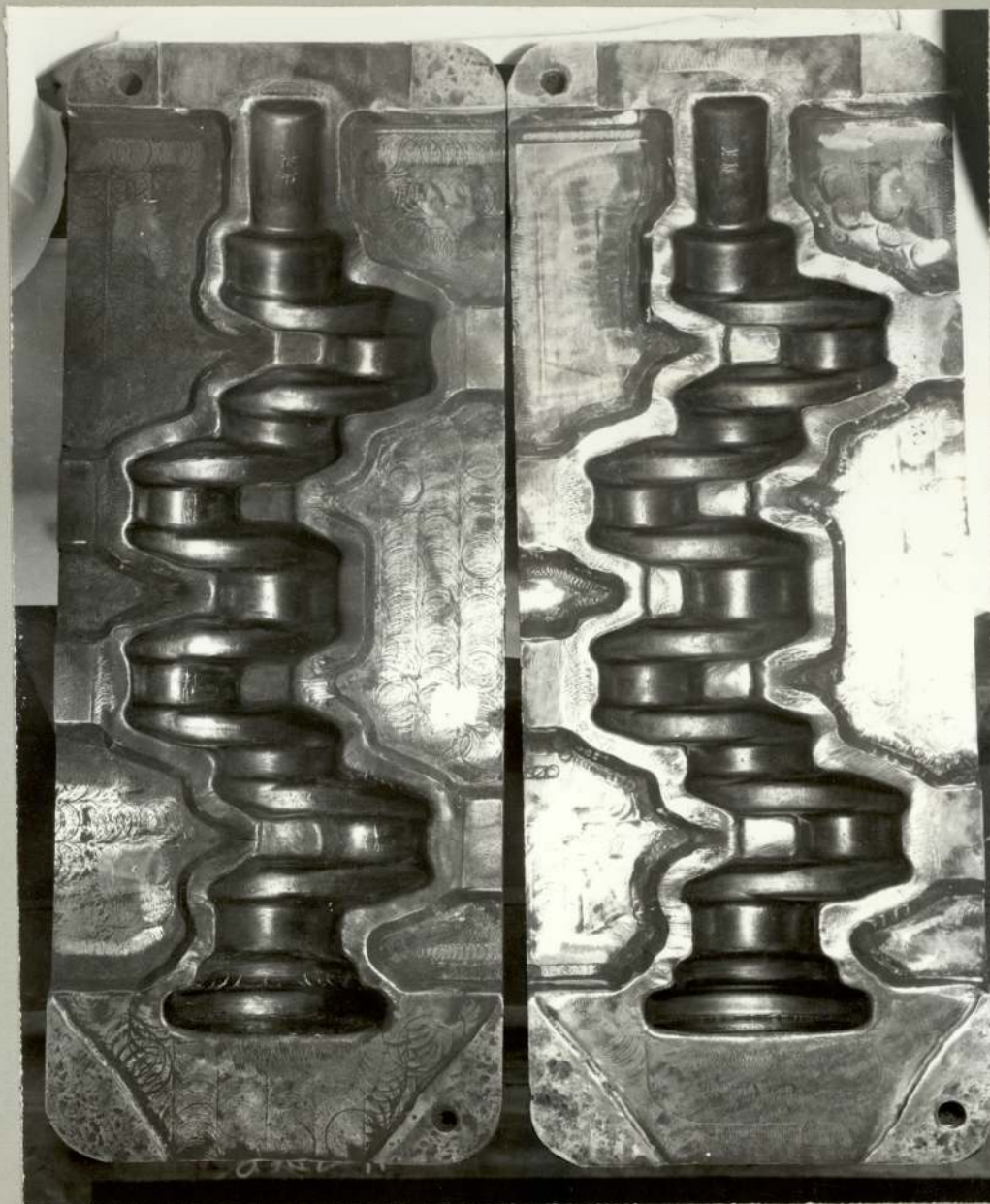
(A)                                        (B)

<u>Crankshaft Inserts.</u>

Fig -7-
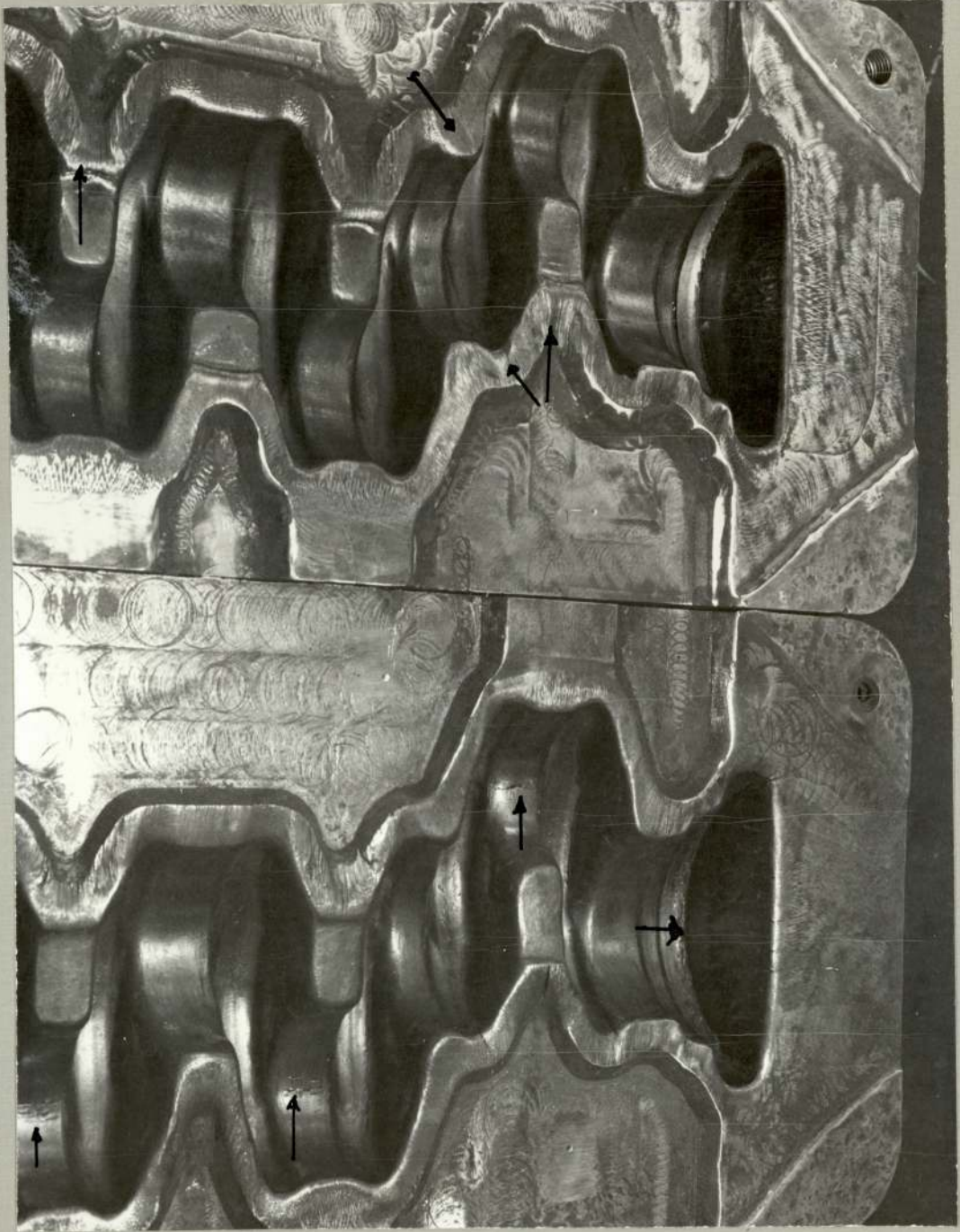
CRANKSHAFT INSERT "A".

Fig -8-

STEPPED TEST BLOCK.

Fig -9-

ULTRASONIC TRACE.        INSERT "B".

Fig -10-

ULTRASONIC TRACE.                    INSERT "A".

Fig -1b=
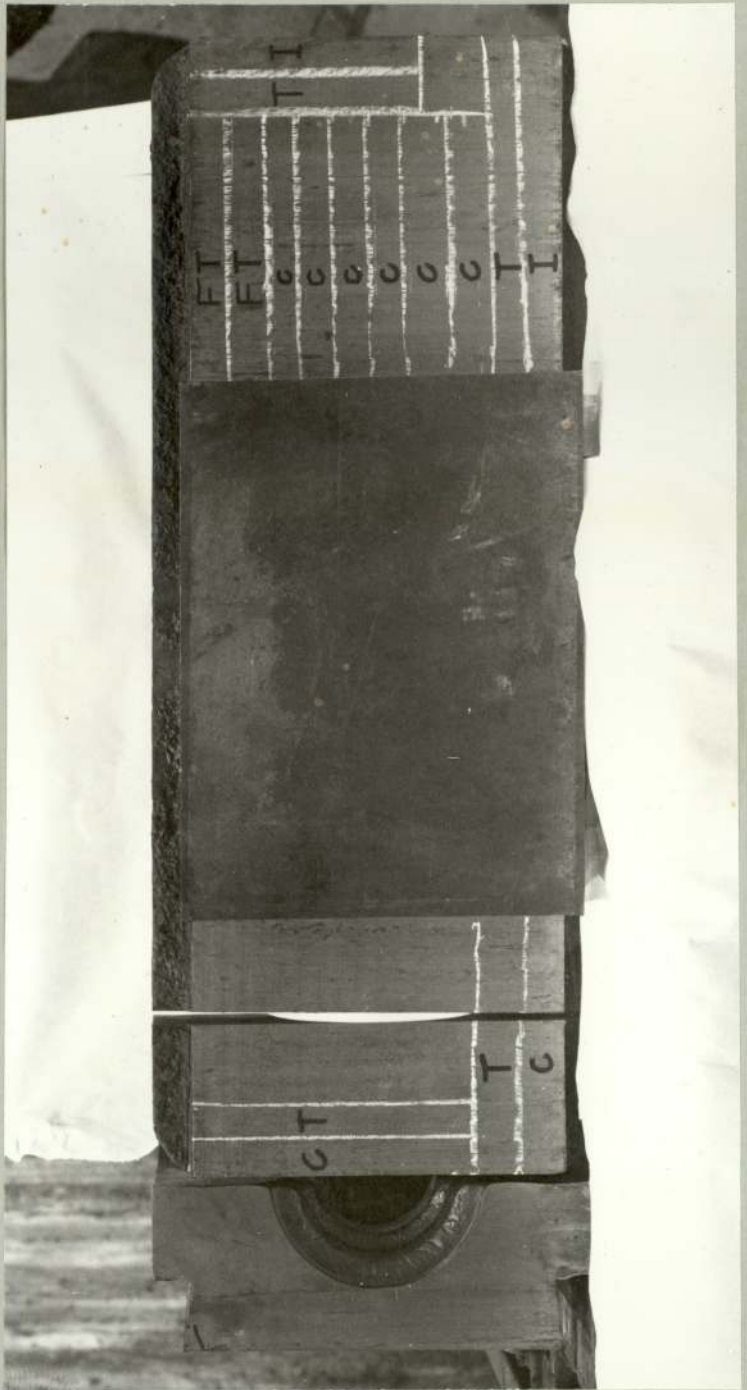
INSERT SAMPLING POSITIONS.

C   =   Charpy.
T   =   Tensile.
I   =   Izod.
FT  =   Fracture toughness.

Fig =12-
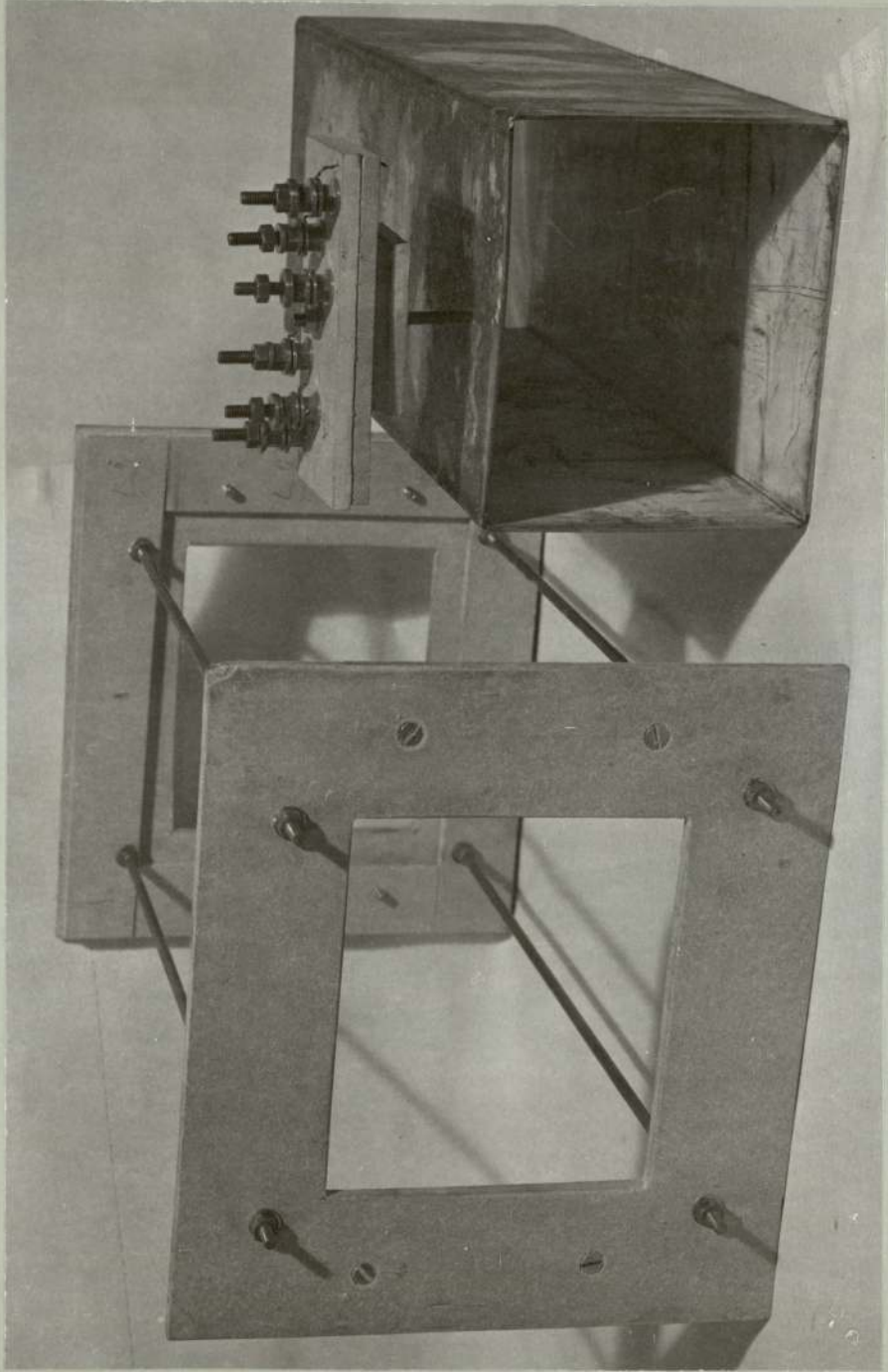
FURNACE CONSTRUCTION.

Fig -13-
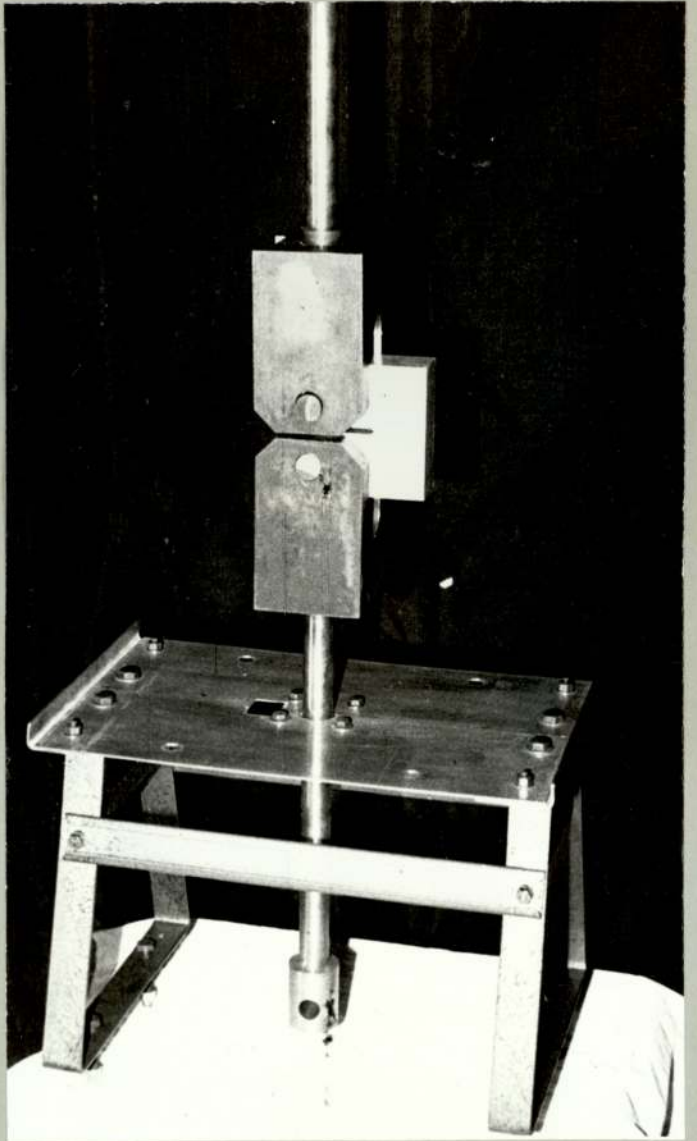
FURNACE TABLE CONSTRUCTION.

Fig -14-

# INSTRON LOADING RIG FOR HIGH TEMPERATURE
## TOUGHNESS TESTING.



FRAME / BOTTOM

1¼ DIA TO
SUIT FEMALE.

INSTRON
UNIVERSAL JNT.

⅝

⁵⁄₁₆

3¾"

TOP OF FURNACE

5"

4"

¼" APPROX

4"

22¼"

33" DAY LIGHT

A

15⅜"

16"

BOTTOM OF FURNACE

9"

3¼ DIA.

3"

B

¾"

CROSSHEAD TOP

2"
DIA.

4½"
DIA.

5" TRAVEL. LEF.
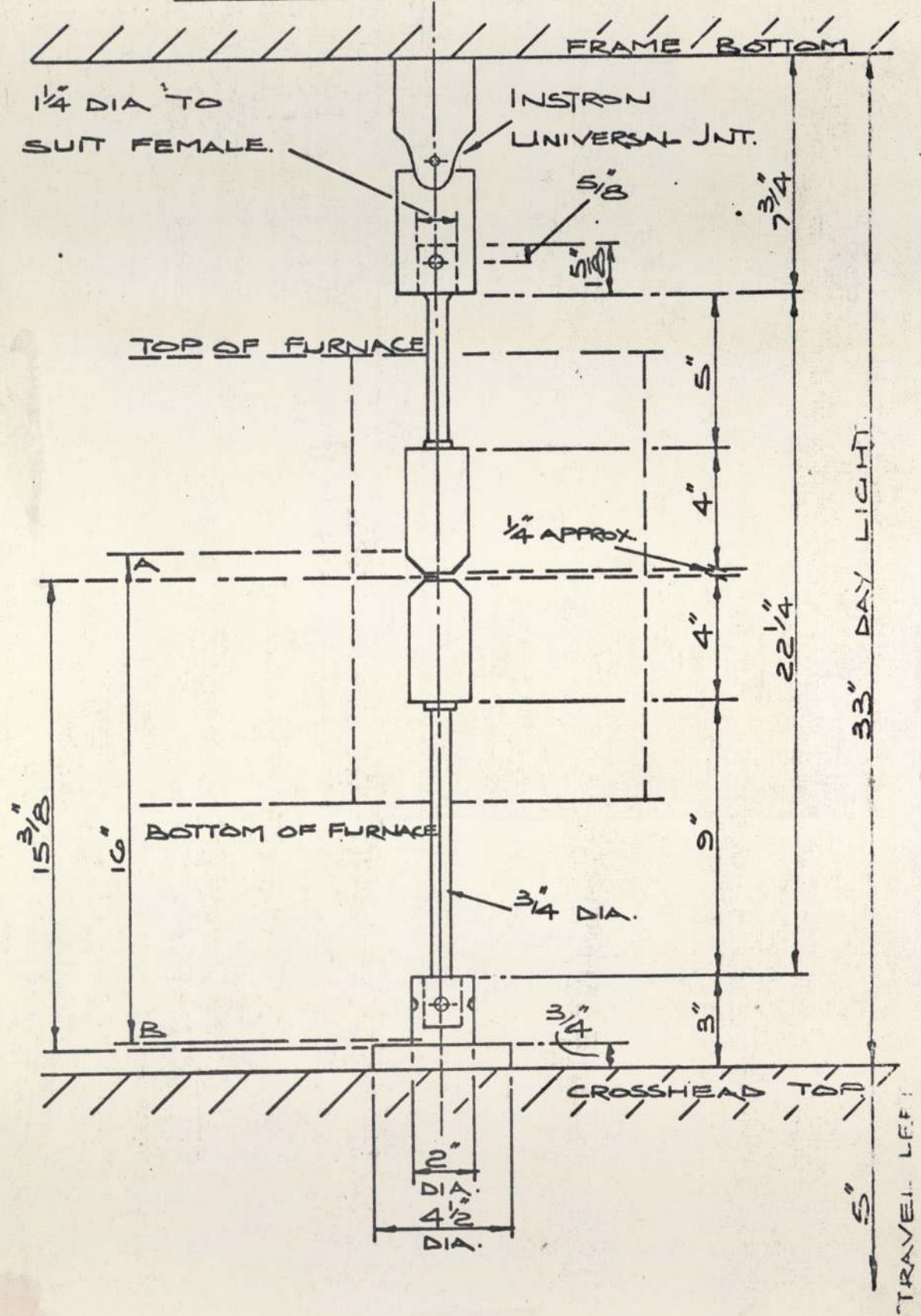
GENERAL ARRANGEMENT.

Fig -14s--

# GRIPPING JAWS.
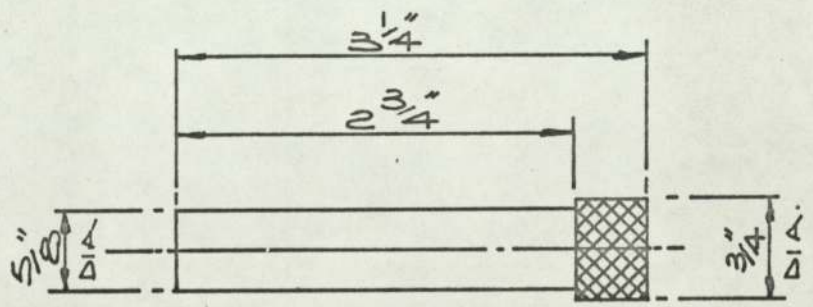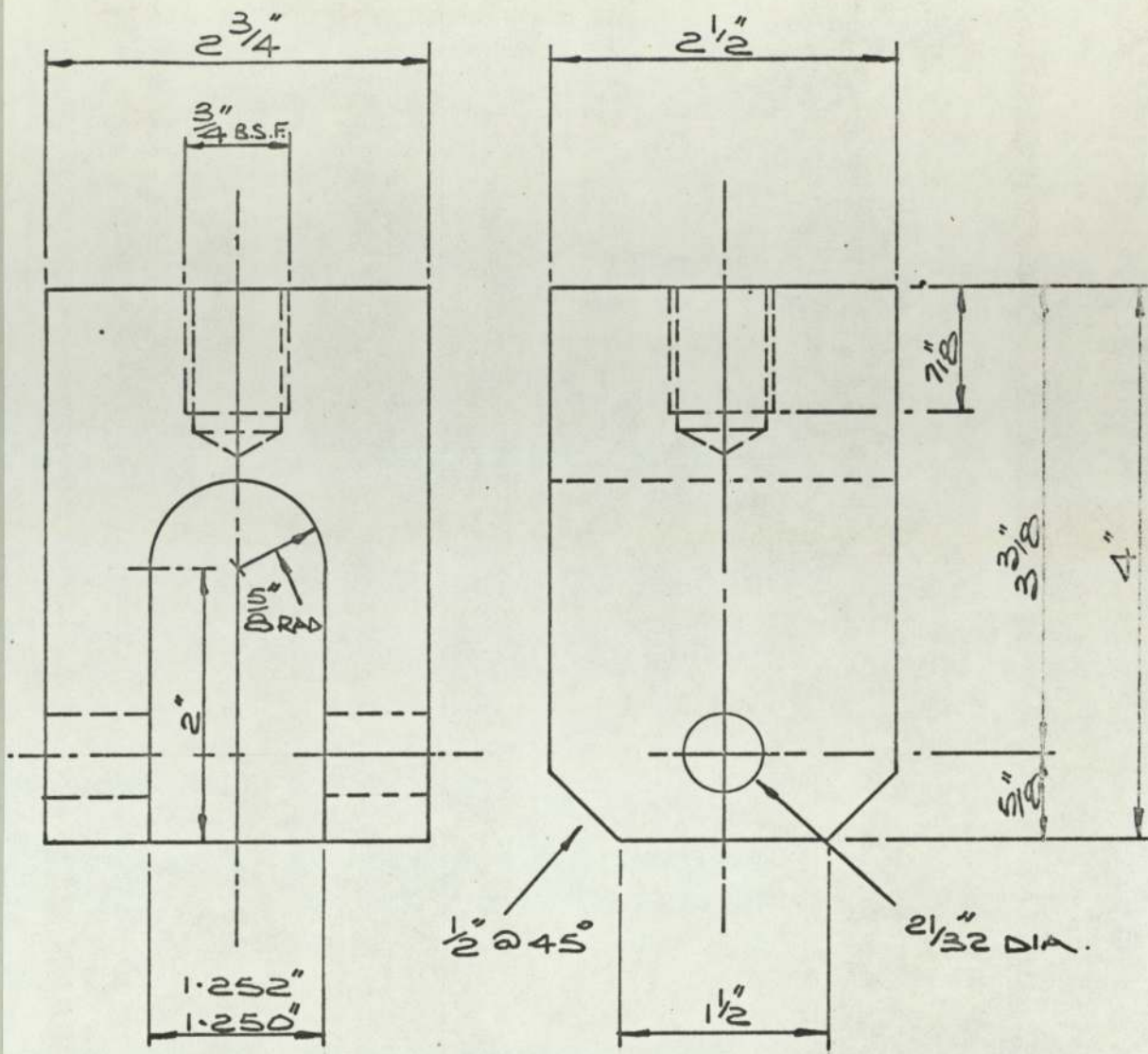


## LOADING PINS
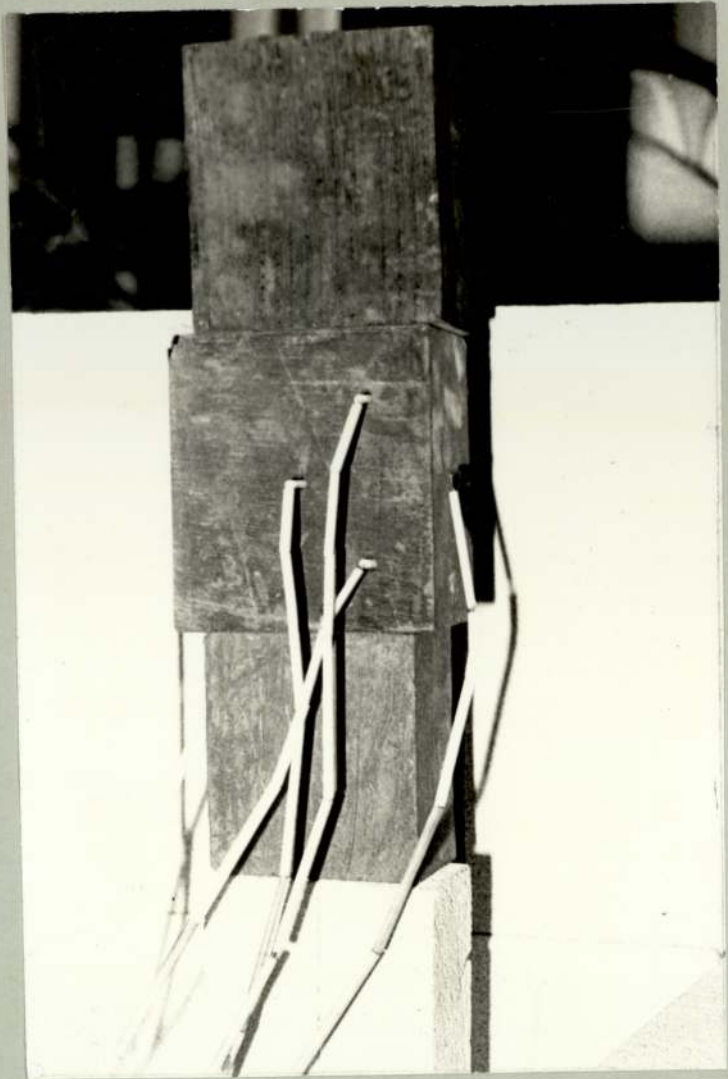
SIMULATION OF SPECIMEN TEMPERATURE
CONDITIONS.

Fig -15-

Left axis (top to bottom): 12, 11, 10, 9, 8, 7, 6, 5, 4, 3, 2, 1, 12, 11, 10, 9, 8, 7

Right axis (top to bottom): 12, 11, 10, 9, 8, 7, 6, 5, 4

DEGREES CENTIGRADE

0  100  200  300  400  500  600  700  800  900  1000  1100  1200  1300  1400

DEGREES CENTIGRADE

Reset for 500°C.

Reset for 400°C.

Surface Temp 80°C.

Reset for 300°C. Surface Temp 75°C.
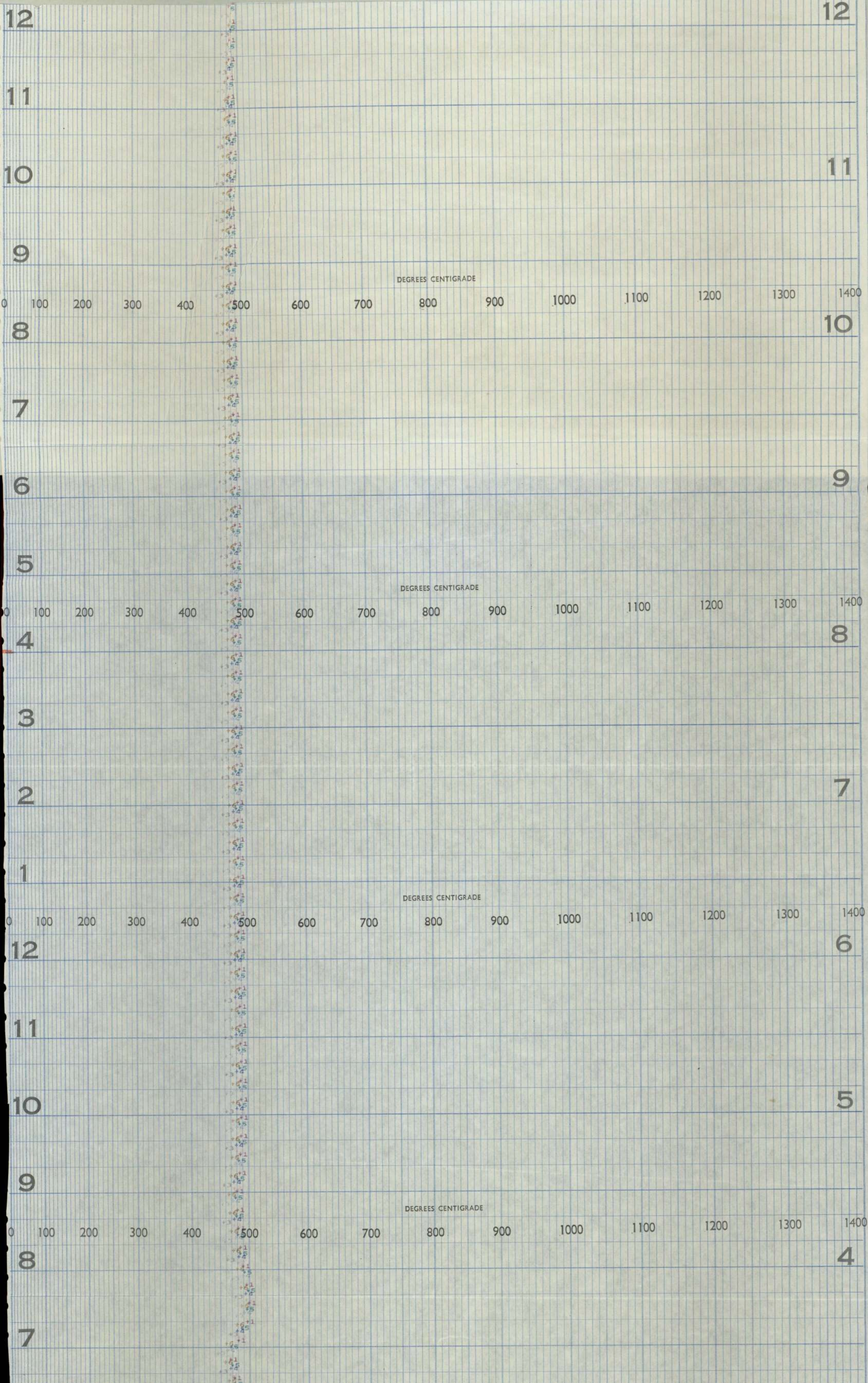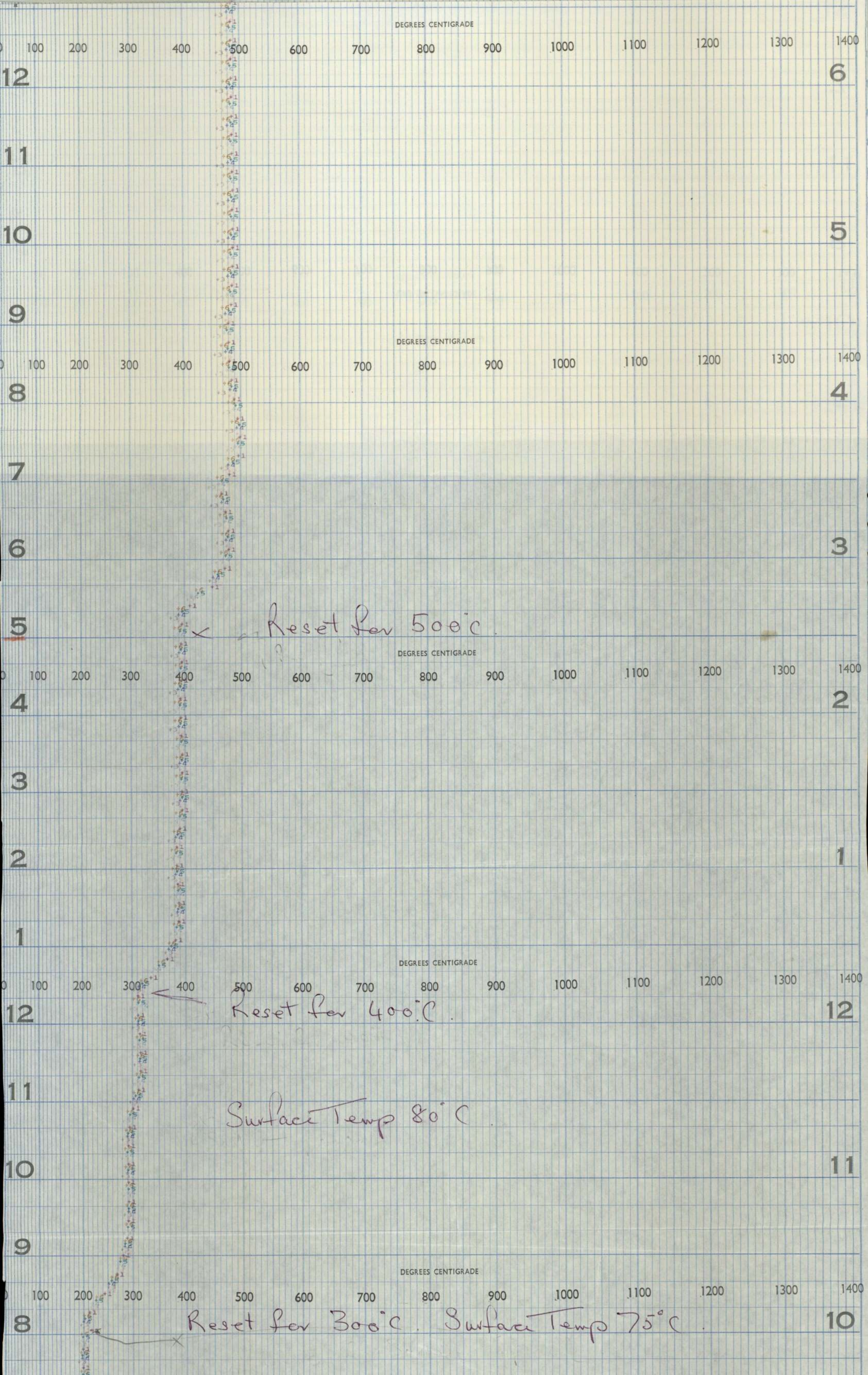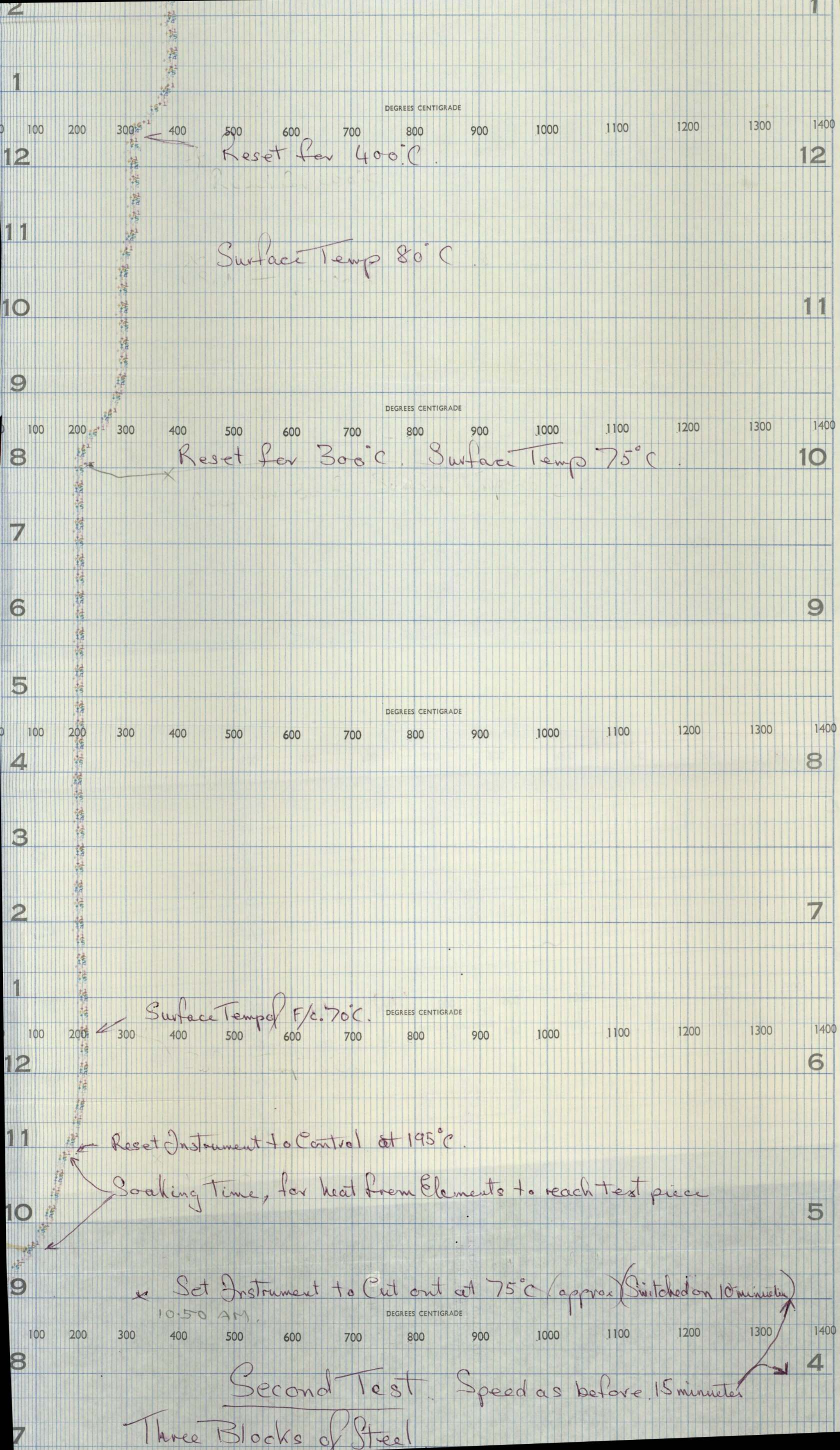
DEGREES CENTIGRADE

100   200   300   400   500   600   700   800   900   1000   1100   1200   1300   1400

Reset for 400°C.

Surface Temp 80°C

DEGREES CENTIGRADE

100   200   300   400   500   600   700   800   900   1000   1100   1200   1300   1400

Reset for 300°C.   Surface Temp 75°C.

DEGREES CENTIGRADE

100   200   300   400   500   600   700   800   900   1000   1100   1200   1300   1400

Surface Temp F/c. 70°C.

DEGREES CENTIGRADE

100   200   300   400   500   600   700   800   900   1000   1100   1200   1300   1400

Reset Instrument to Control at 195°C.

Soaking Time, for heat from Elements to reach test piece

Set Instrument to Cut out at 75°C (approx) (Switched on 10 minutes)

10.50 AM.

DEGREES CENTIGRADE

100   200   300   400   500   600   700   800   900   1000   1100   1200   1300   1400

Second Test. Speed as before 15 minutes

Three Blocks of Steel

SIMULATED TEST SPECIMEN.
THERMAL CHART.

DEGREE CENTIGRADE
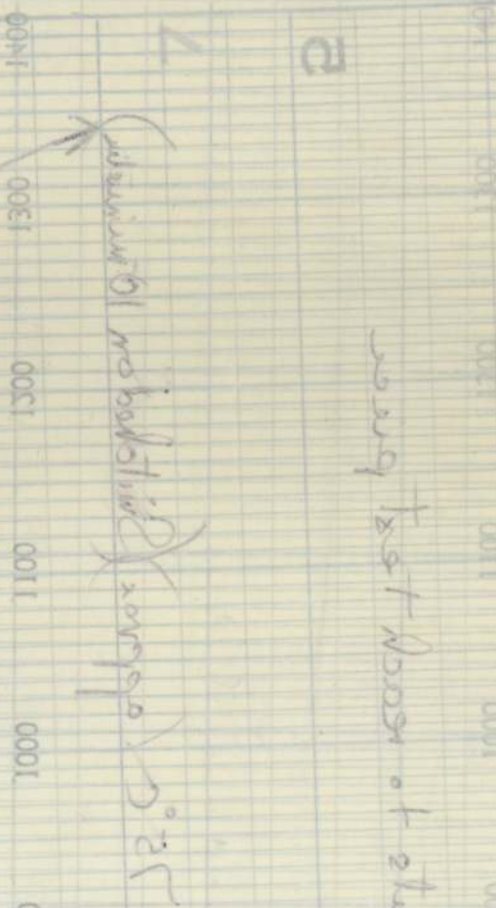
Fig =15a-
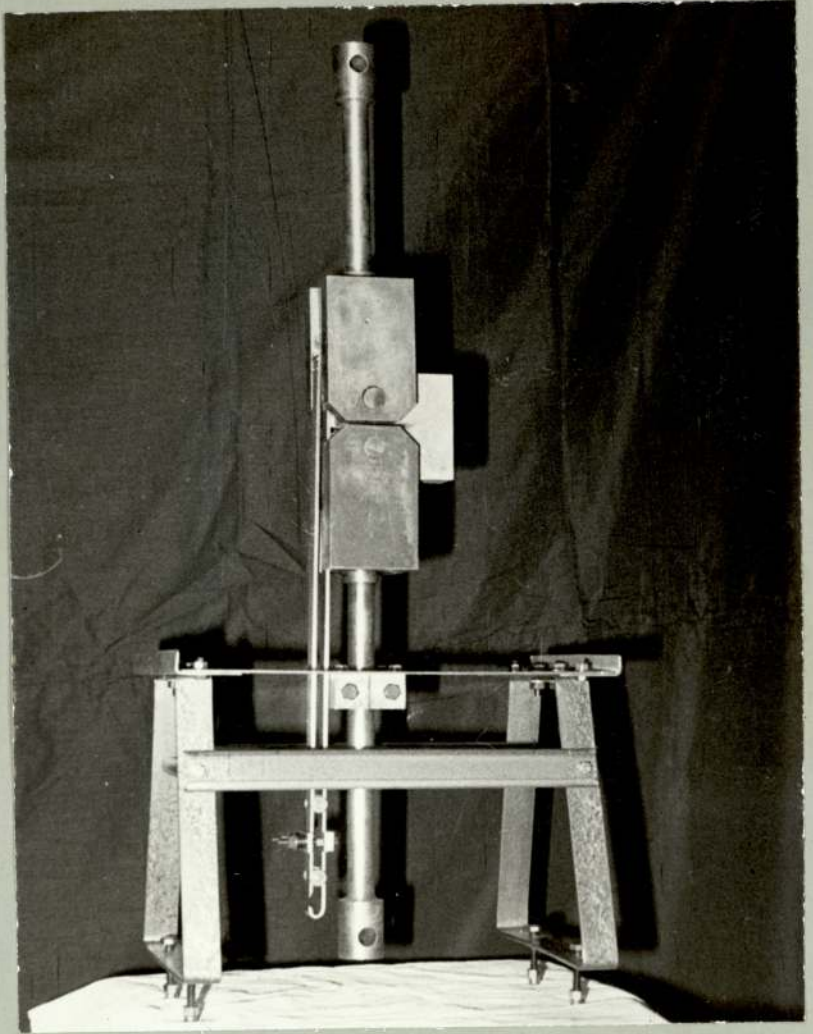
COMPACT TENSION SPECIMEN WITH EXTENSION ARMS.

Fig -16-

# LEGS FOR REMOTE CLIP GAUGE.

CLEARANCE HOLES TO SUIT 6 B.A. SCREWS

HOLES AS INNER LEG

DOWEL PINS.

BACK AND FRONT OF SPACER BLOCKS FINE GROUND FLAT AND PARALLEL (BOTH BLOCKS)

$\frac{1}{8}$" THK.

OUTER LEG

INNER LEG

COIL SPRINGS

ROLLERS

CLIP GAUGE

FINE GROUND KNIFE EDGES

OUTER LEG

INNER LEG

$16"$

$15\frac{3}{4}"$

$14\frac{7}{8}"$

$5\frac{1}{8}"$

$1"$

$\frac{1}{4}"$

$\frac{1}{4}"$

$5\frac{1}{32}"$

$5\frac{1}{32}"$

$\frac{3}{8}"$

$\frac{1}{4}"$

$1"$

$\frac{1}{4}"$ DIA.

GROUND STEEL ROLLER.

Fig -17-
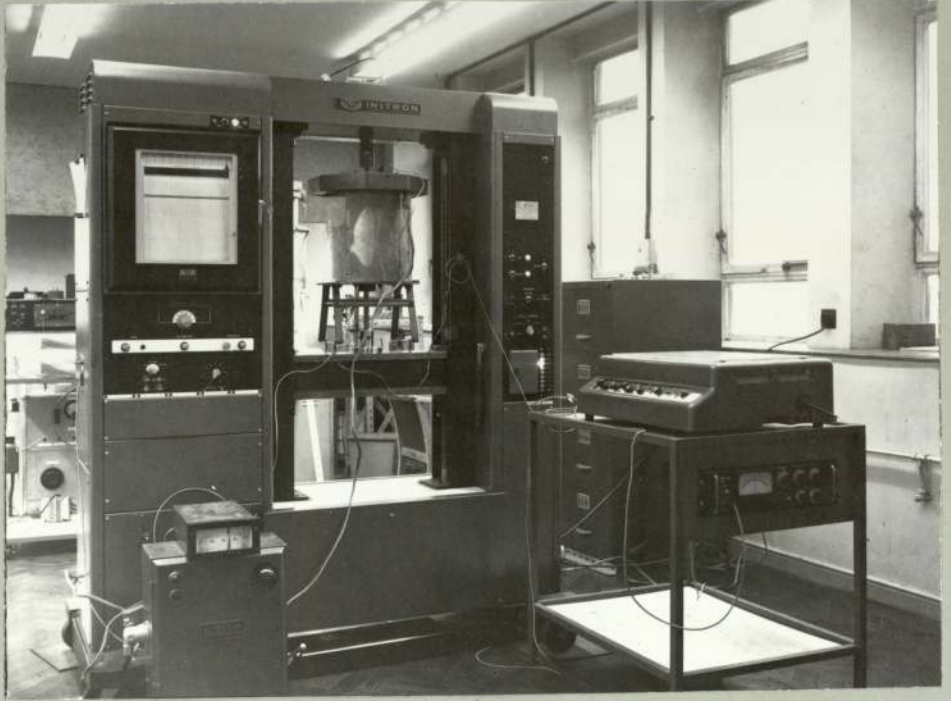
Fig -18-
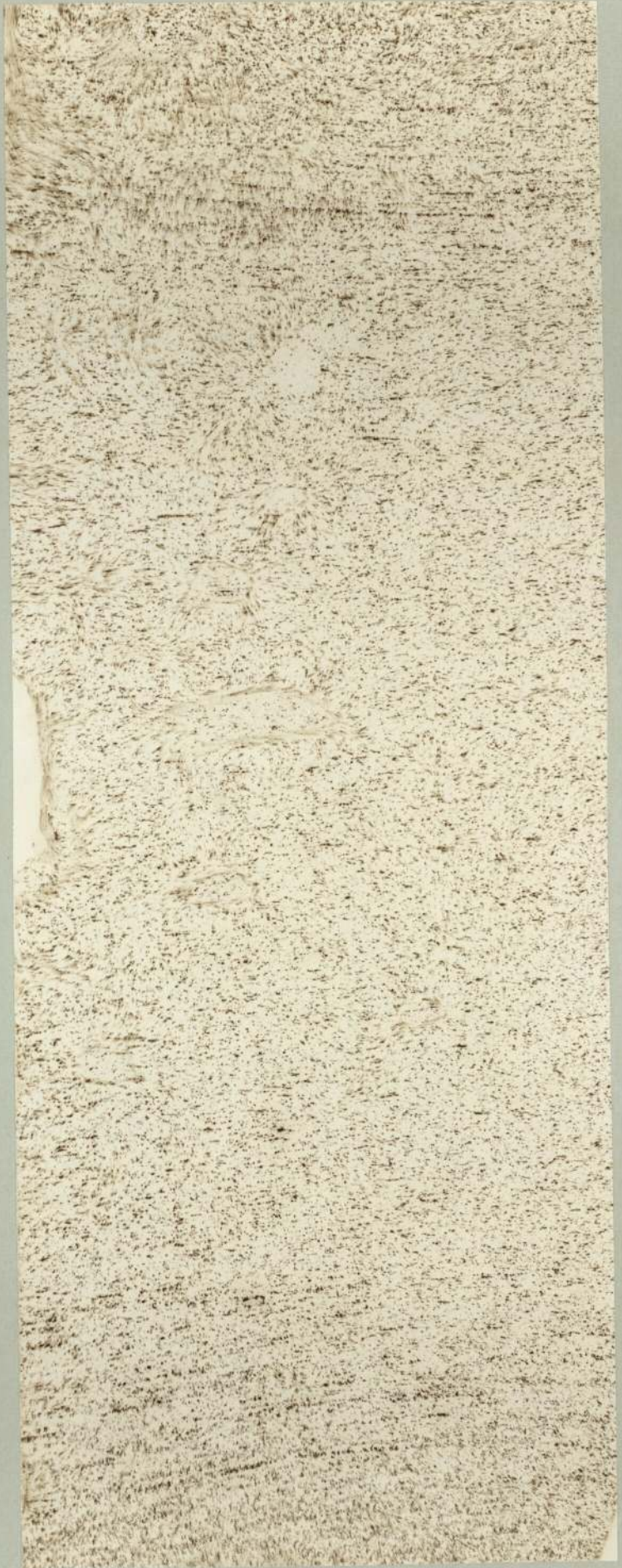
Sulphur print.

Fig -19-

Sulphur print.

Fig -20-

Insert "A".                    x 100

Insert "B".                    x 100

Fig -21-
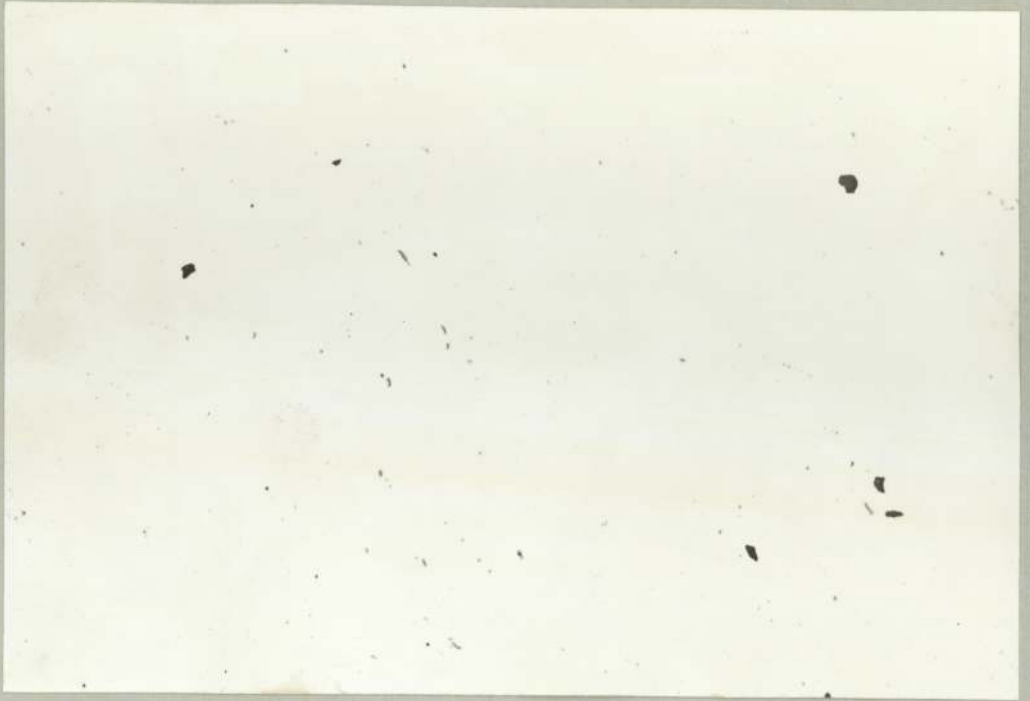
Stepped test block. Large section.          x 100.



Stepped test block. Small section.          x 100.

Fig -22-

x 100

Etched structure.



x 650

INSERT "A".

Fig =23-

Etched structure.                                              x 100



x 650

INSERT "B".

Fig =24-
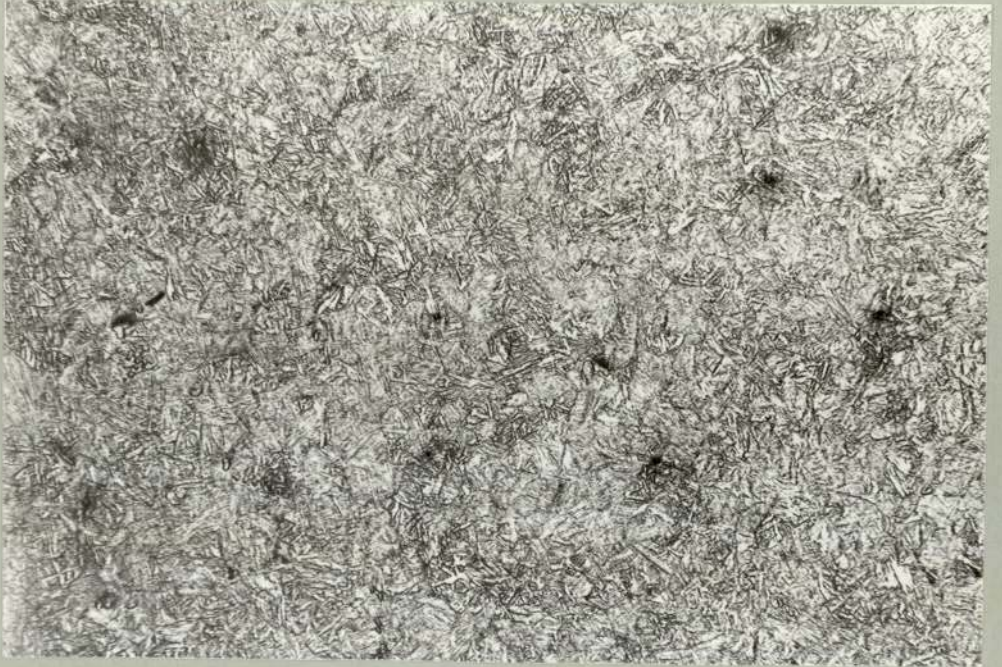
x 100

Etched structure.



x 650

STEPPED TEST BLOCK, LARGE SECTION.

Fig -25-

Etched structure.                                        x 100



x 650

STEPPED TEST BLOCK. SMALL SECTION.

Fig =26-
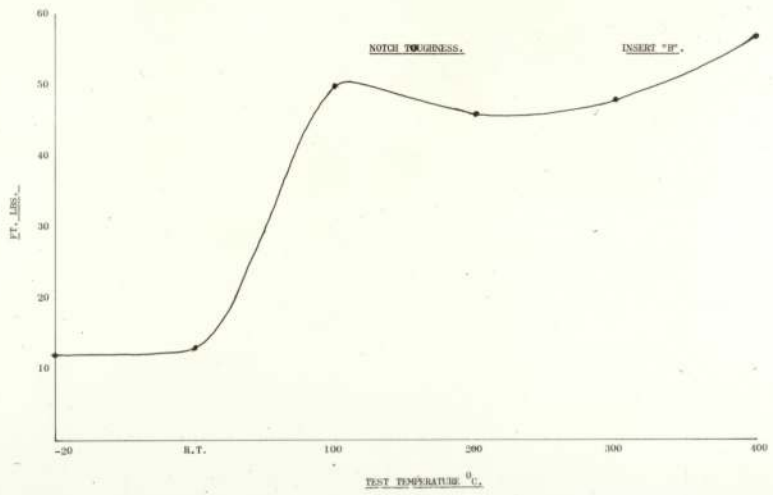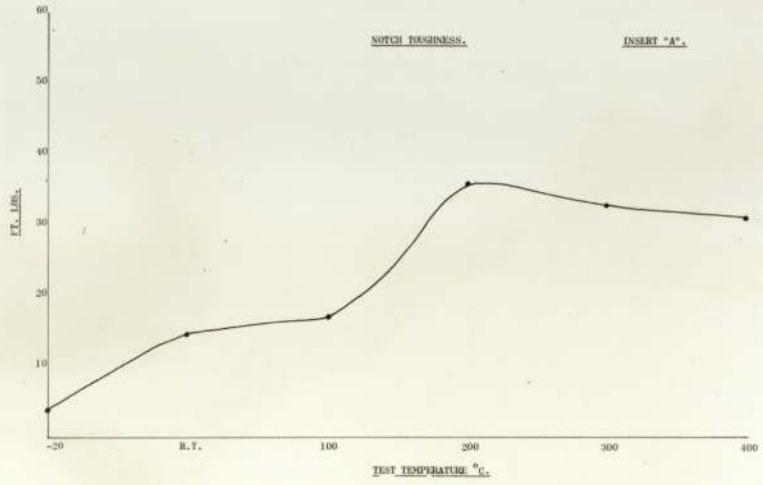
NOTCH TOUGHNESS.

Fig -27-
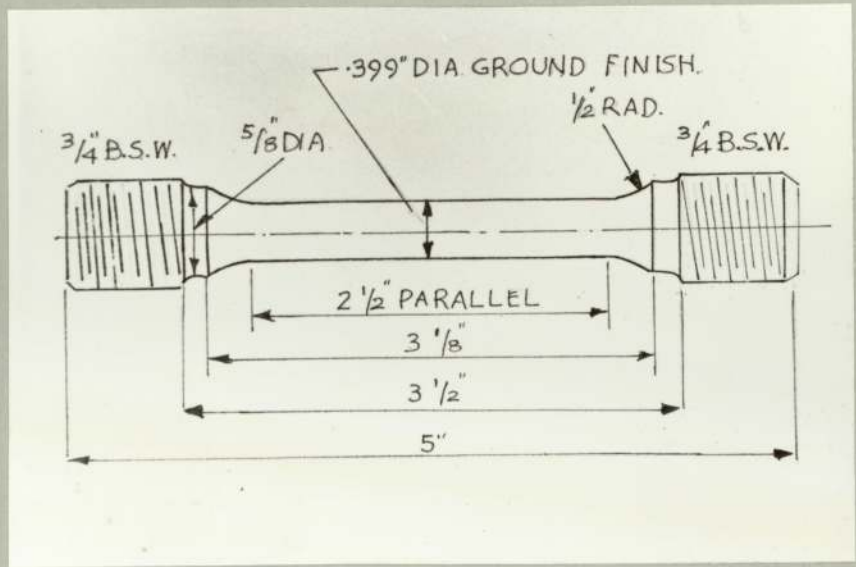
HOT TENSILE SPECIMEN.

Fig =28-
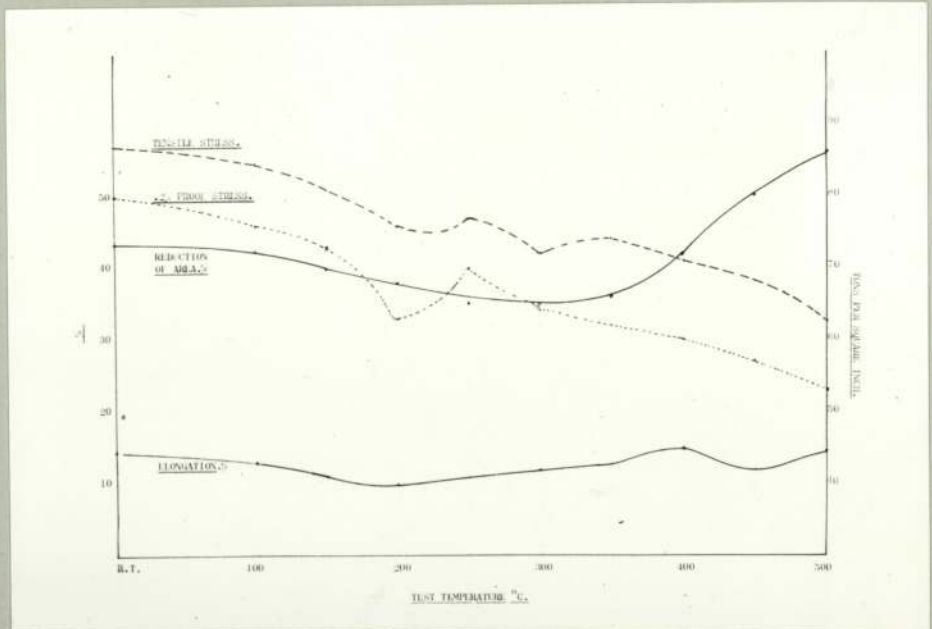


HOT TENSILE DATA OBTAINED FROM STEPPED
TEST BLOCK.

Fig -29-

Force P

Displacement Gauge Output.

A

$P_Q = P_5$

$P = 0.8 P_Q$

TYPE I

5%

O
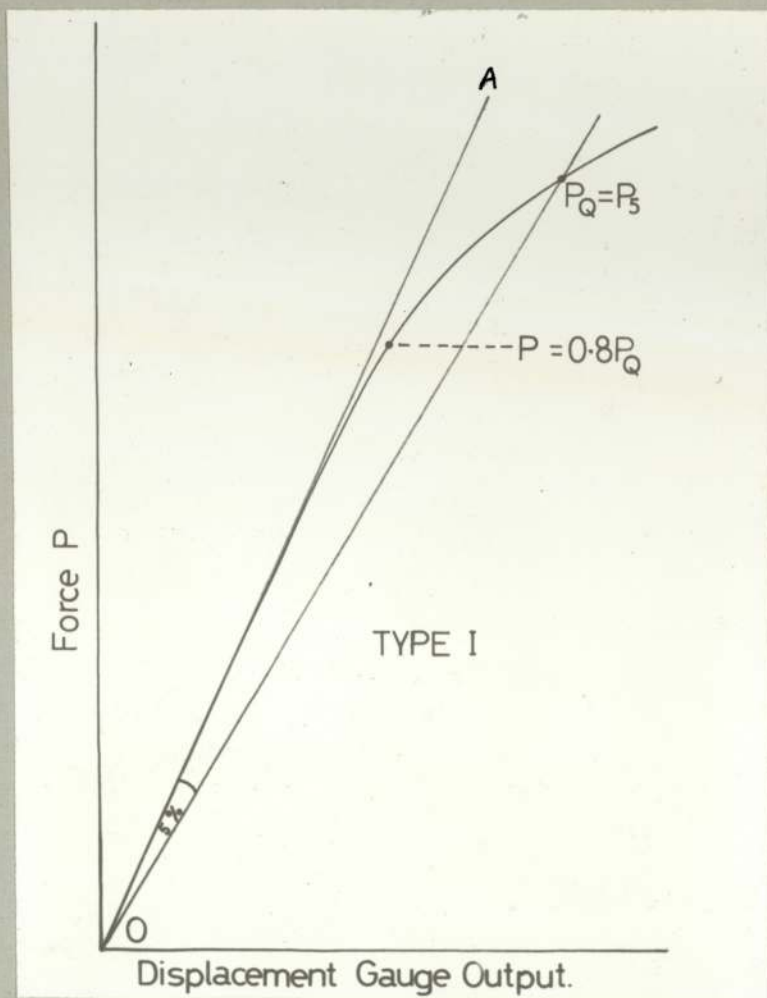
Fig –31–

Four drilled and tapped holes to suit dowels and screws.
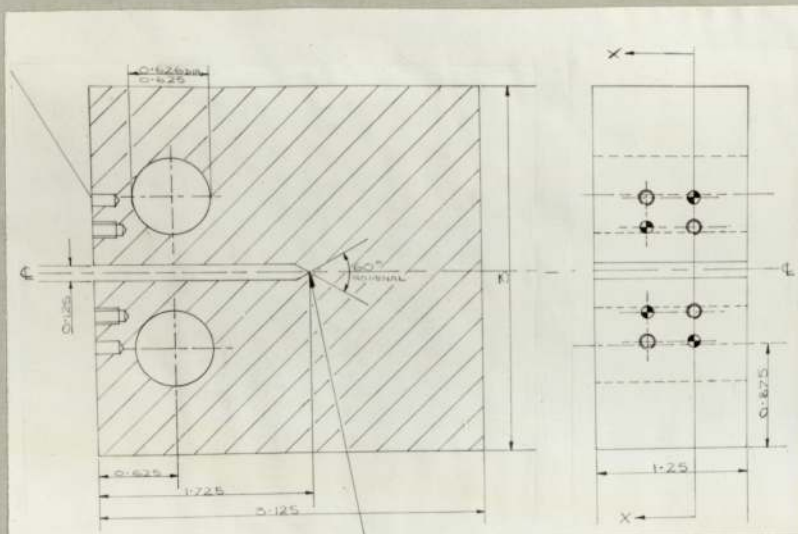


see detail "A". Surfaces parallel and perpendicular
to 0.001".

Root radius 0.010" maximum.
             0.005" preferred.
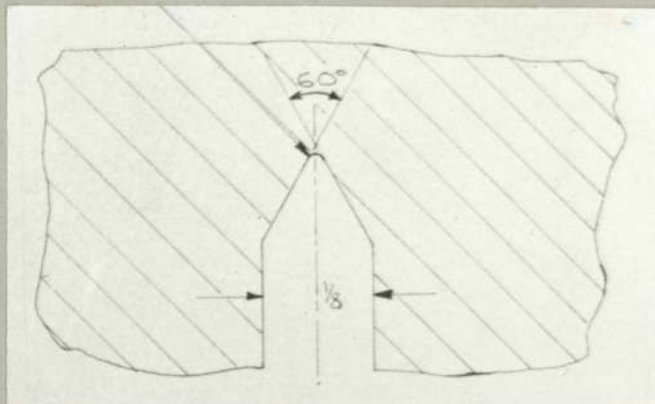


All final cuts to be small to minimise surface damage,
fine ground to observe fatigue crack surfaces true to
centre-line within 0.001".

FRACTURE TOUGHNESS W.O.L. OR COMPACT TENSION SPECIMEN.

Fig -32-

COMPACT TENSION SAMPLE INSERT "A".

INITIAL SAMPLE TESTED AT ROOM TEMPERATURE.
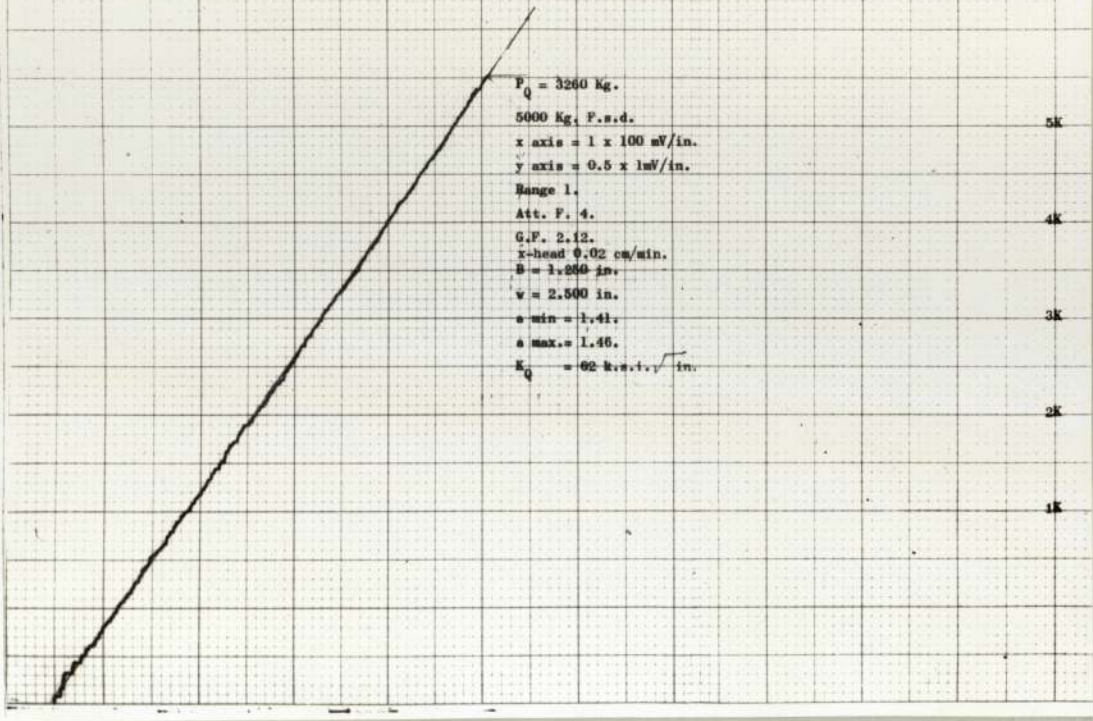
$P_Q$ = 3260 Kg.

5000 Kg. F.s.d.

x axis = 1 x 100 mV/in.

y axis = 0.5 x 1mV/in.

Range 1.

Att. F. 4.

G.F. 2.12.

x-head 0.02 cm/min.

B = 1.250 in.

w = 2.500 in.

a min.= 1.41.

a max.= 1.46.

$K_Q$ = 62 k.s.i.$\sqrt{\text{in.}}$
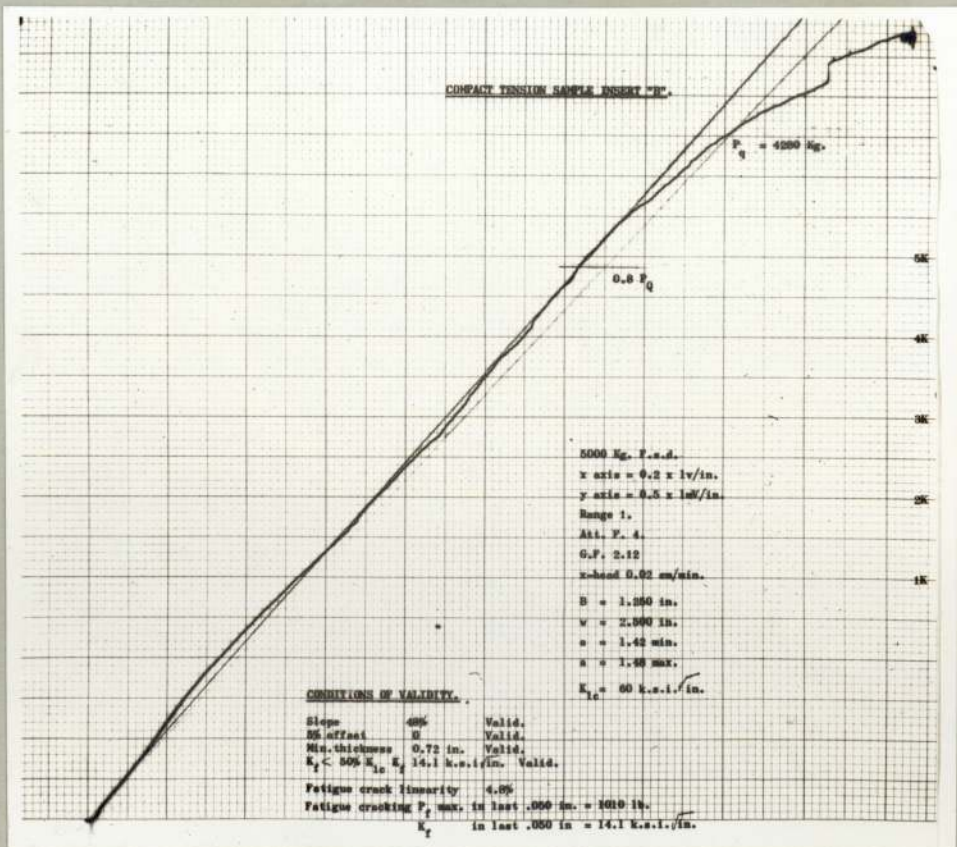


COMPACT TENSION SAMPLE INSERT "B".

$P_Q$ = 4280 Kg.

0.8 $P_Q$

5000 Kg. F.s.d.

x axis = 0.2 x 1v/in.

y axis = 0.5 x 1mV/in.

Range 1.

Att. F. 4.

G.F. 2.12

x-head 0.02 cm/min.

B = 1.250 in.

w = 2.500 in.

a = 1.42 min.

a = 1.46 max.

$K_{1c}$= 60 k.s.i.$\sqrt{\text{in.}}$

CONDITIONS OF VALIDITY.

Slope          40%          Valid.
5% offset       0           Valid.
Min.thickness  0.72 in.     Valid.
$K_f$ < 50% $K_{1c}$  $K_f$ 14.1 k.s.i/in.  Valid.

Fatigue crack linearity    4.8%
Fatigue cracking $P_f$ max. in last .050 in. = 1610 lb.
$K_f$ in last .050 in = 14.1 k.s.i.$\sqrt{\text{in.}}$

X-Y RECORDER EXTENSION.
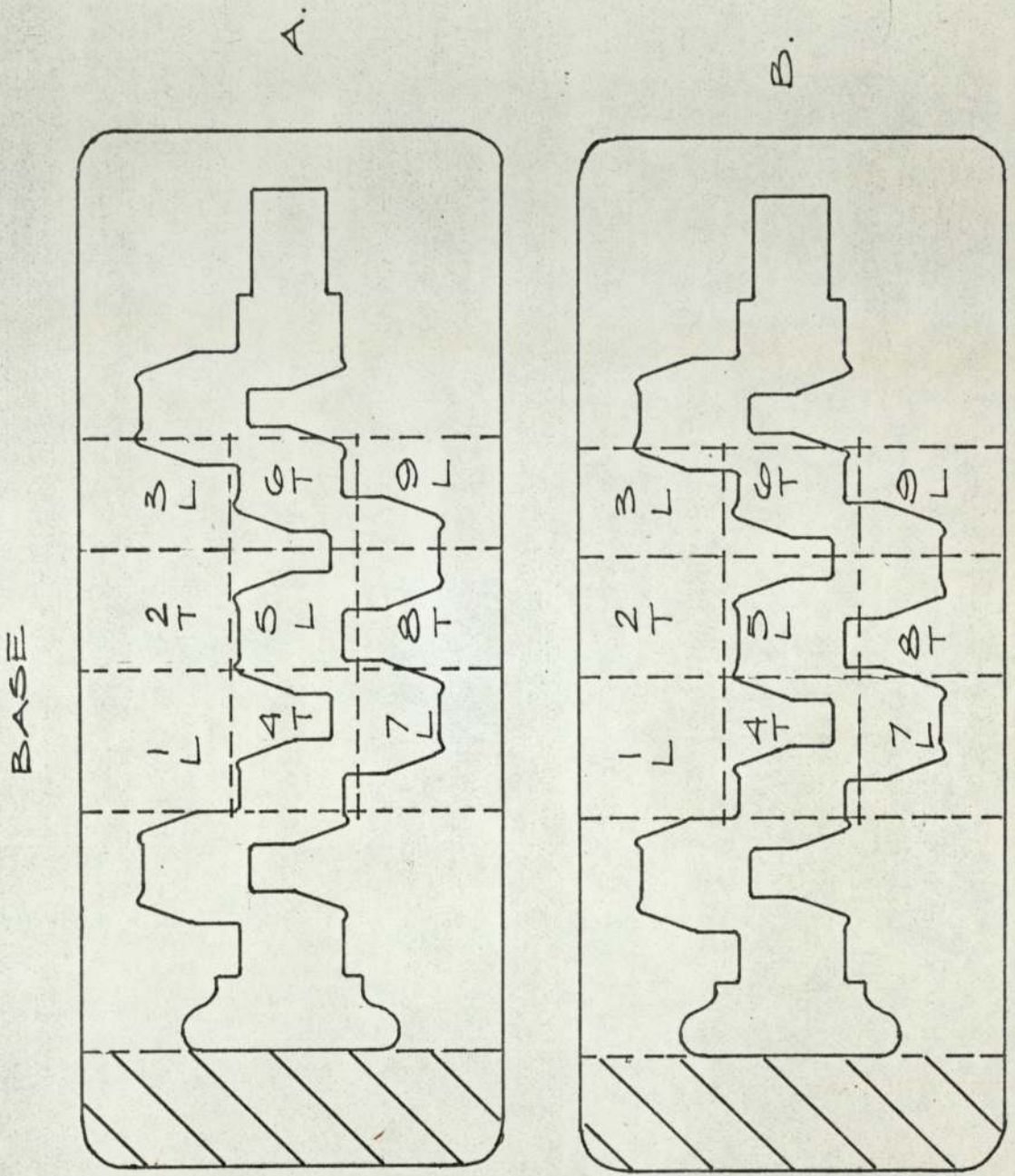
Fig -33-

INSERT FRACTURE TOUGHNESS SAMPLING POSITIONS.

Fig -34-

INSERT FRACTURE TOUGHNESS SAMPLING POSITIONS.

Fig –35–
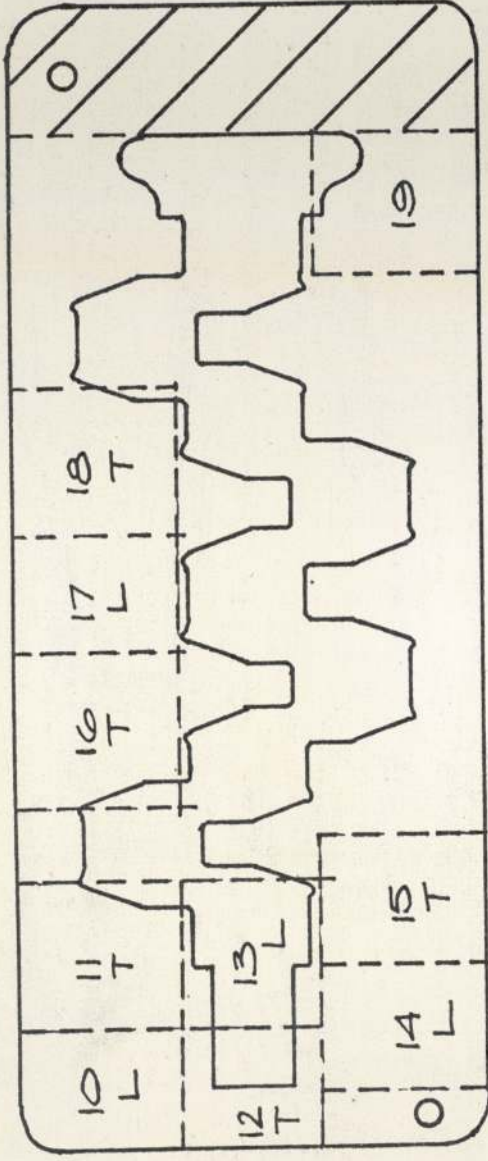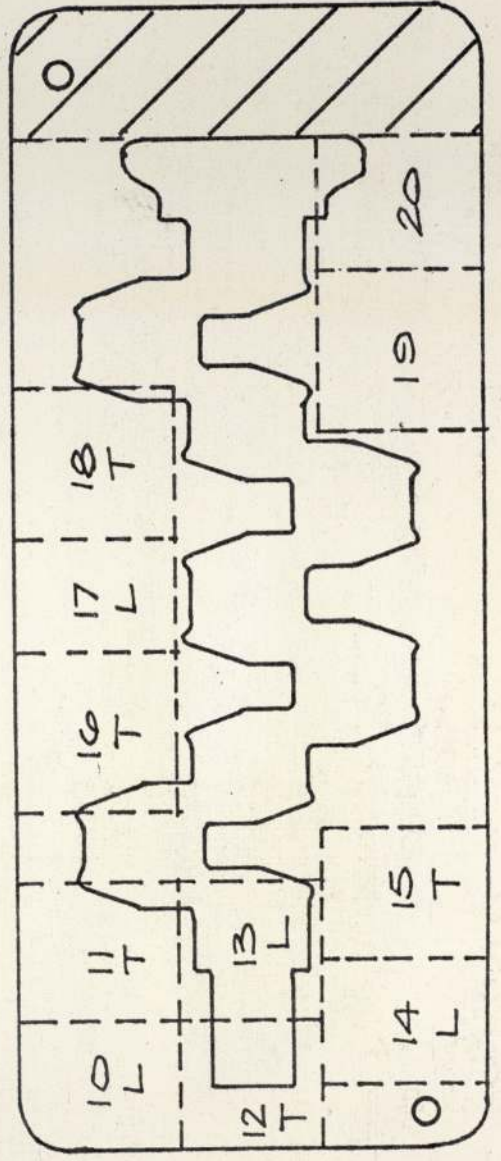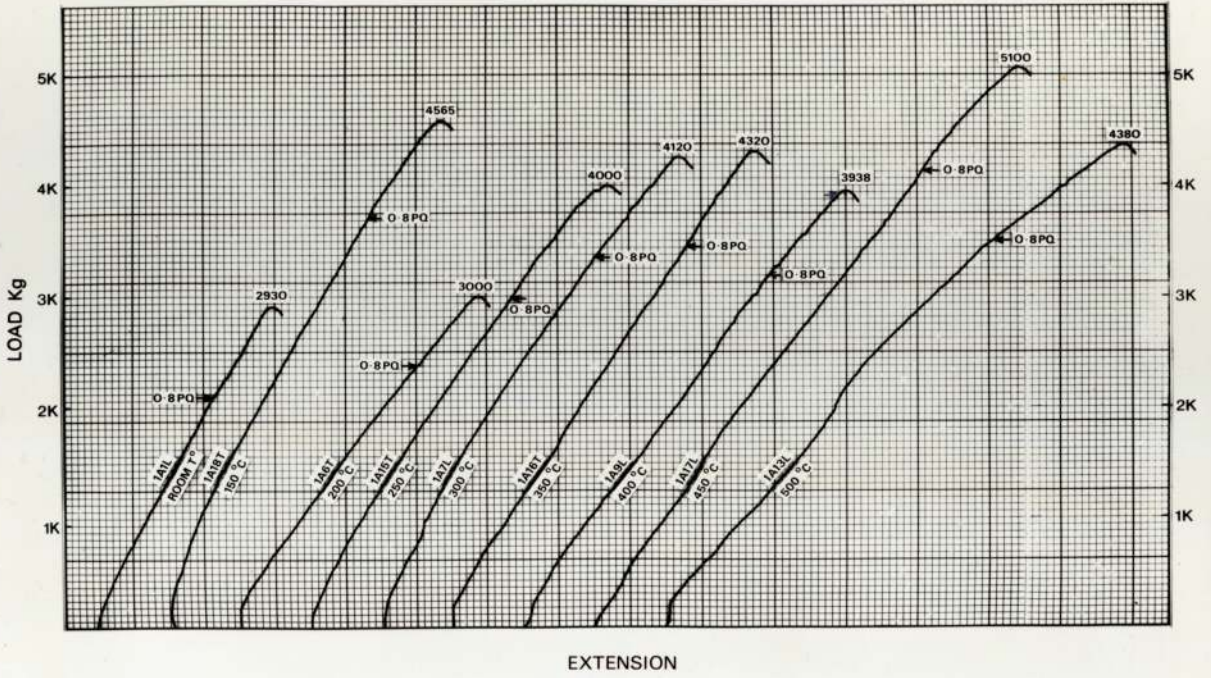
"A" INSERT

TYPICAL FORCE/DISPLACEMENT RECORDS.

"B" INSERT
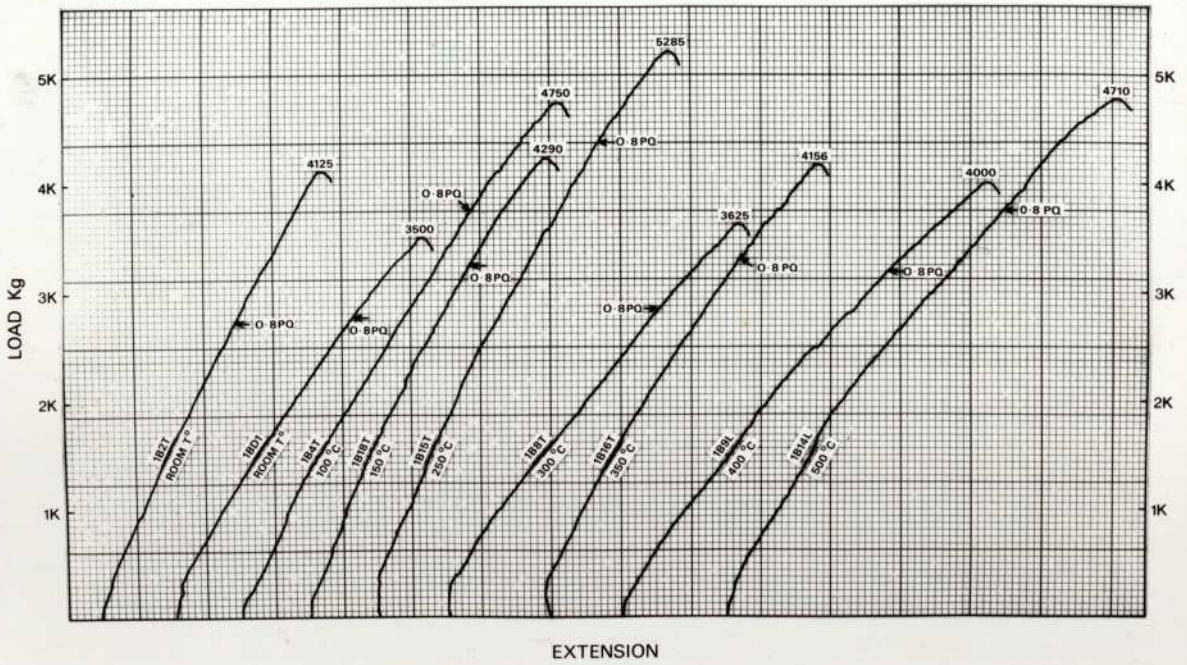
Fig -36-
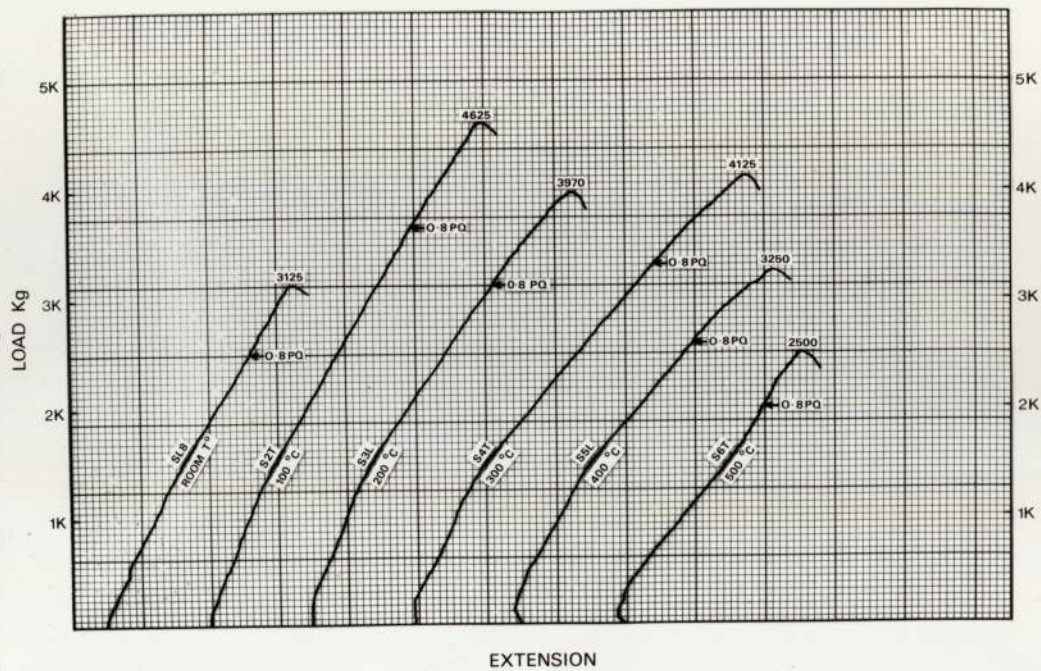
FORCE/DISPLACEMENT RECORD.

Fig -37-

INSERT "A".
FRACTURE TOUGHNESS.
LONGITUDINAL.

FRACTURE TOUGHNESS.



INSERT "A".
TRANSVERSE FRACTURE TOUGHNESS.

Fig -38-

INSERT "B".
FRACTURE TOUGHNESS.
LONGITUDINAL PROPERTIES.

● VALID.

▲ INVALID.

TEST TEMPERATURE °C.

FRACTURE TOUGHNESS.



INSERT "B".
TRANSVERSE FRACTURE TOUGHNESS.

● VALID

▲ INVALID

TEST TEMPERATURE °C.
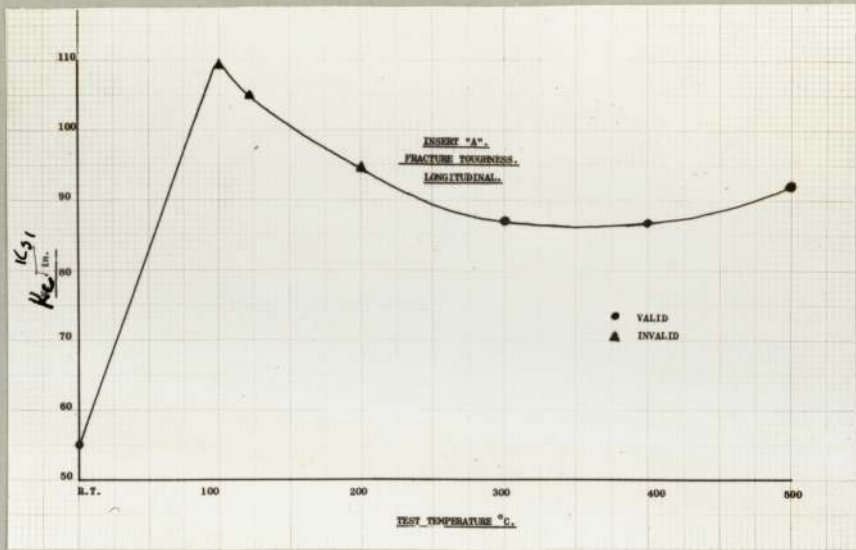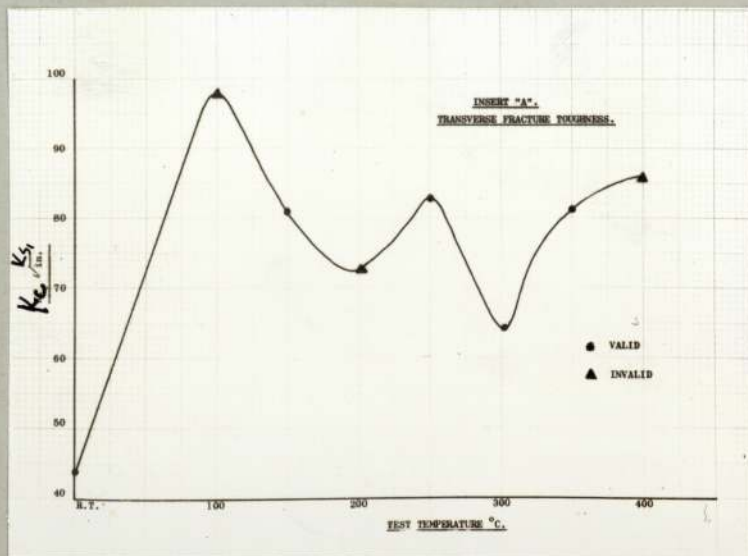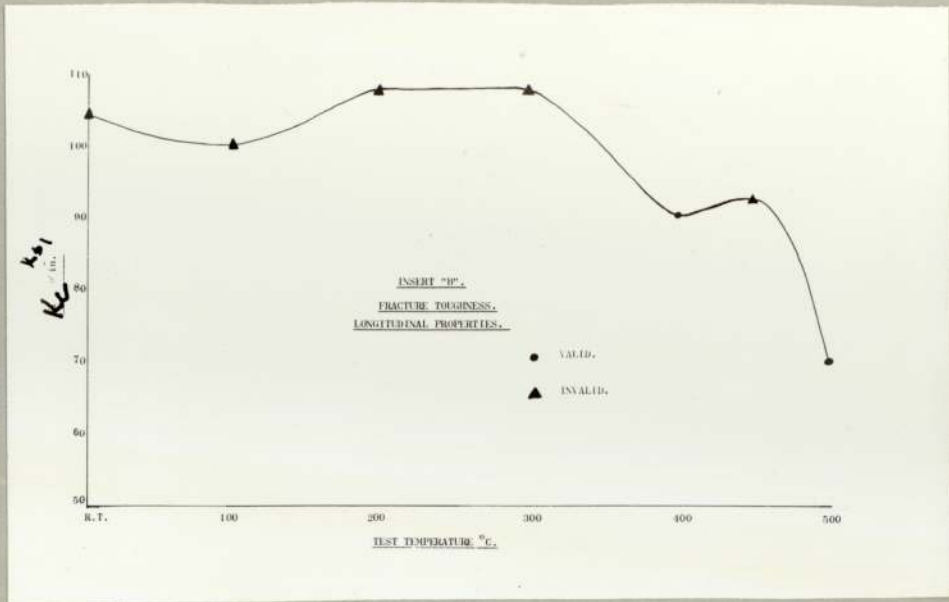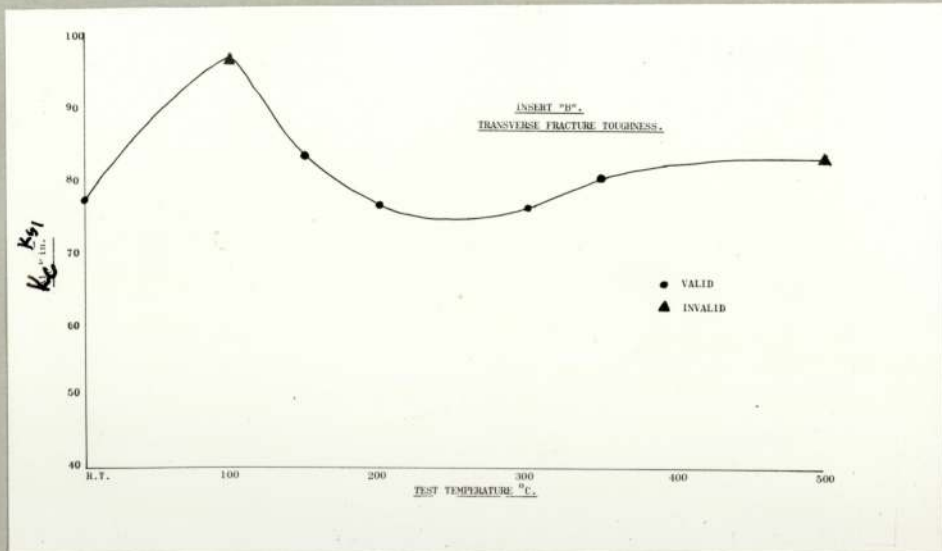
Fig -39-

FRACTURE TOUGHNESS.



Fig -40-

Sample S12T
Tested at 500°C.

P.Q. = 2765 kg./f
= 6083 lb./f.

Fig –41a–



Sample S1L
Tested at
Room
Temperature.

P.Q. = 4750 kg/f.
= 10,450 lb./f.

Fig –41b–

FIG -A-

INSERT "A"    LONGITUDINAL ROOM TEMPERATURE PROPERTIES.

$2.5\left(\frac{Kq}{Gy}\right)^{2}$

X= DATA FROM BEND TESTS.

(X)= DATA FROM C K S TEST.

Kq
k.s.i.
√in.



FIG - B-

INSERT "A"   TRANSVERSE ROOM TEMPERATURE PROPERTIES

$2.5\left(\frac{Kq}{Gy}\right)^{2}$

X = DATA FROM BEND TESTS.

(X)= DATA FROM C K S TEST.

Kq
k.s.i.
√in.
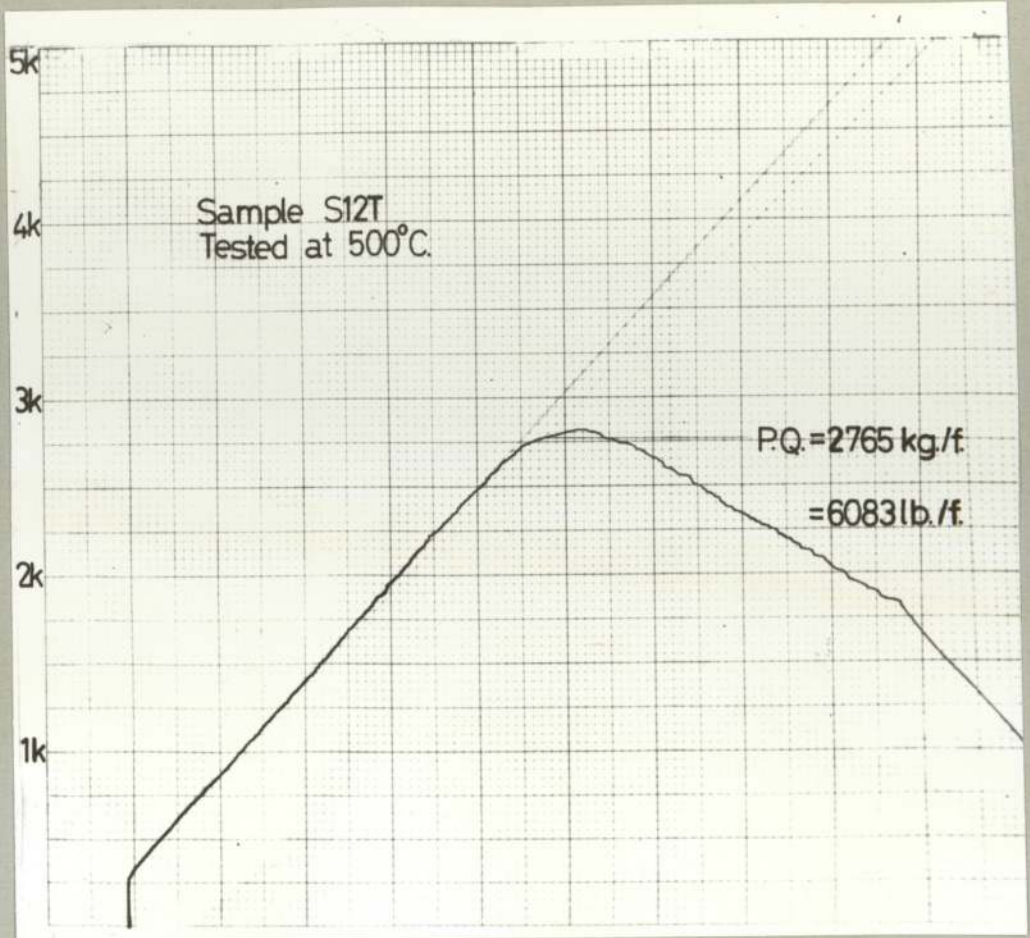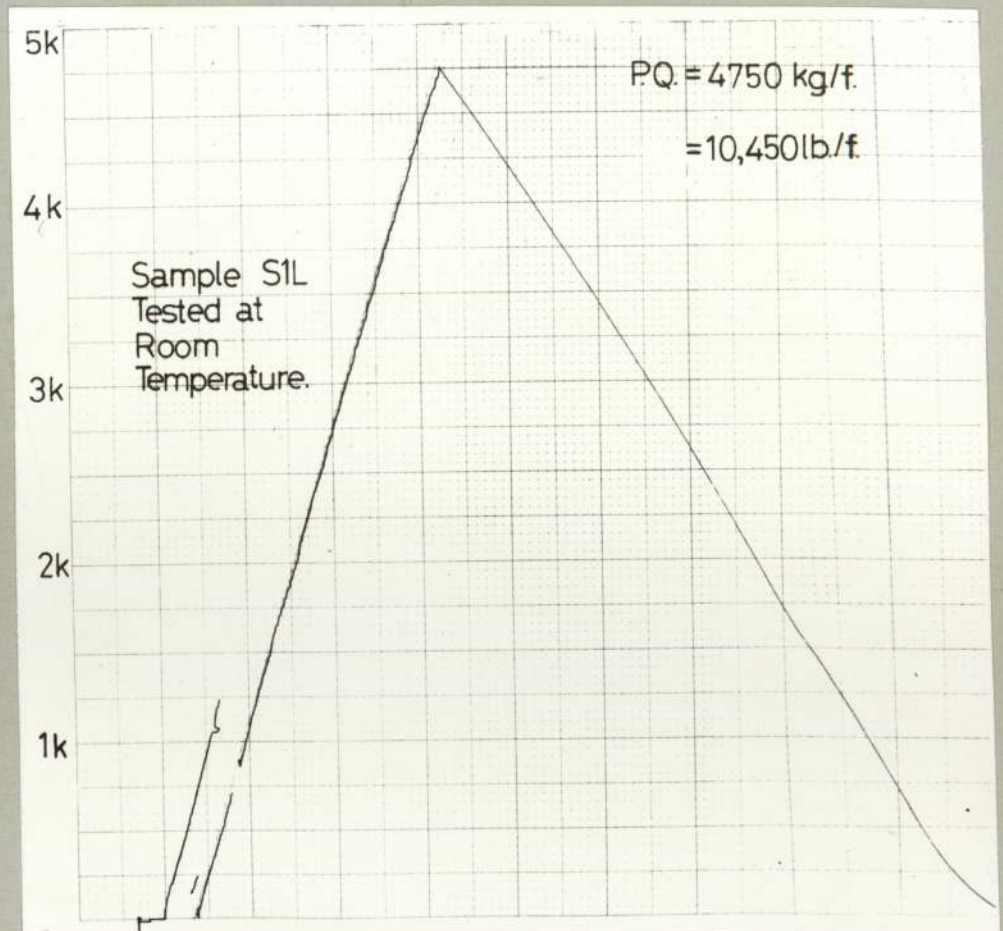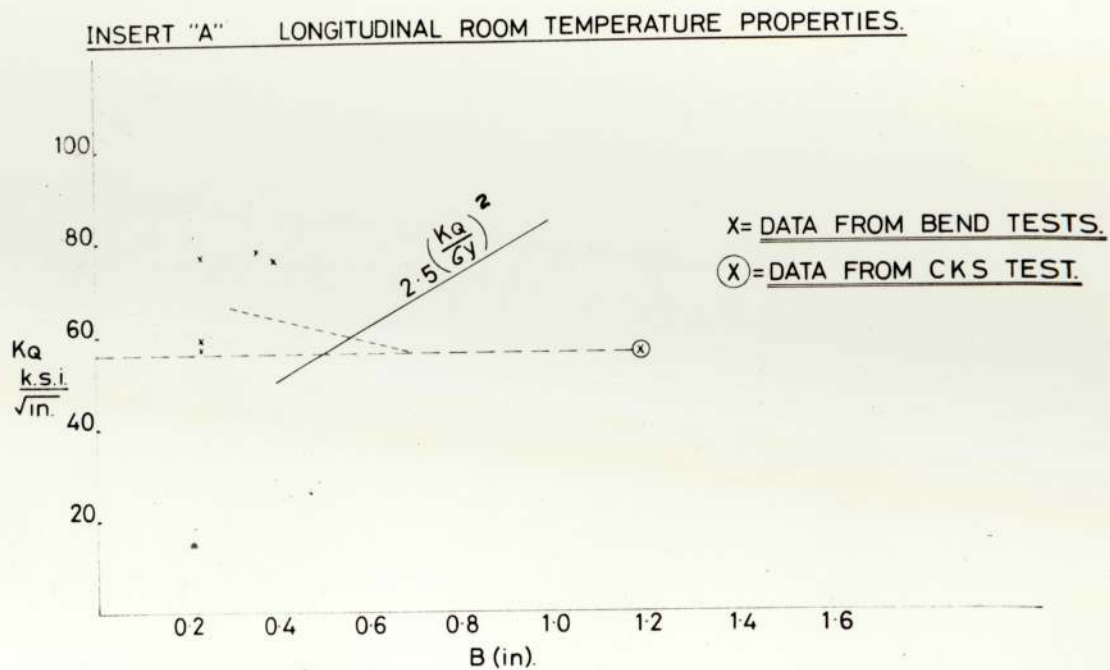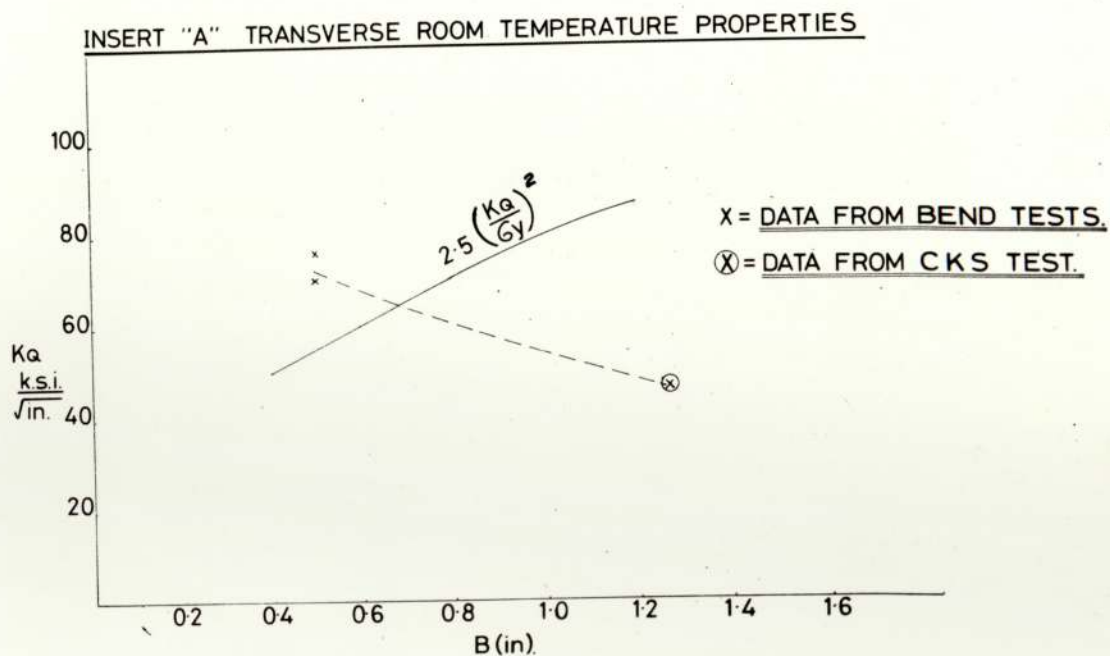
COMPARISON OF OBTAINED TOUGHNESS WITH
SPECIFICATION THICKNESS REQUIREMENTS.

Fig -42-

COMPACT TENSION FRACTURE TOUGHNESS SAMPLES.

Fig —43—
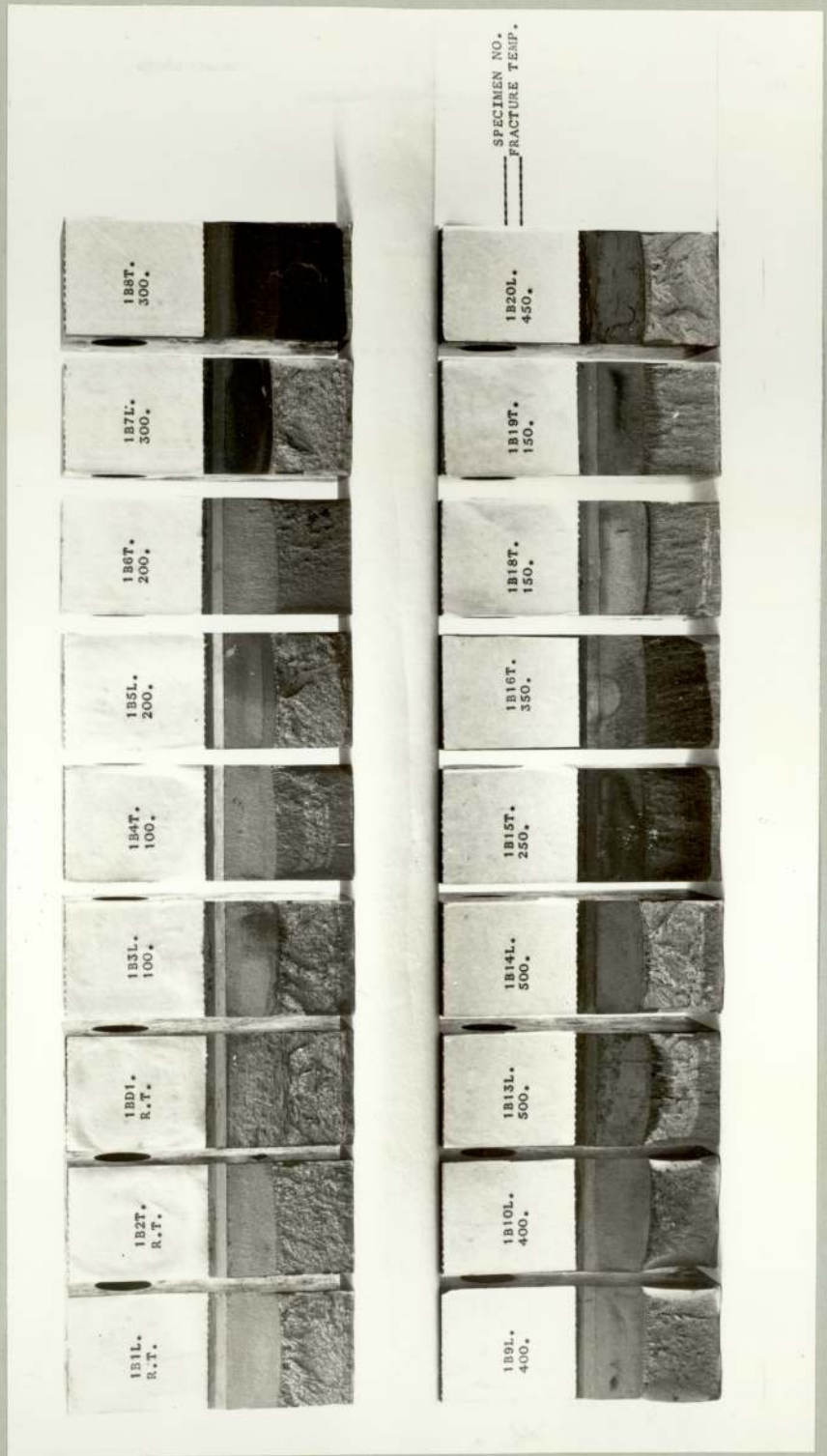
COMPACT TENSION FRACTURE TOUGHNESS SAMPLES.

Fig -44-

COMPACT TENSION FRACTURE TOUGHNESS SAMPLES.

Fig -45-
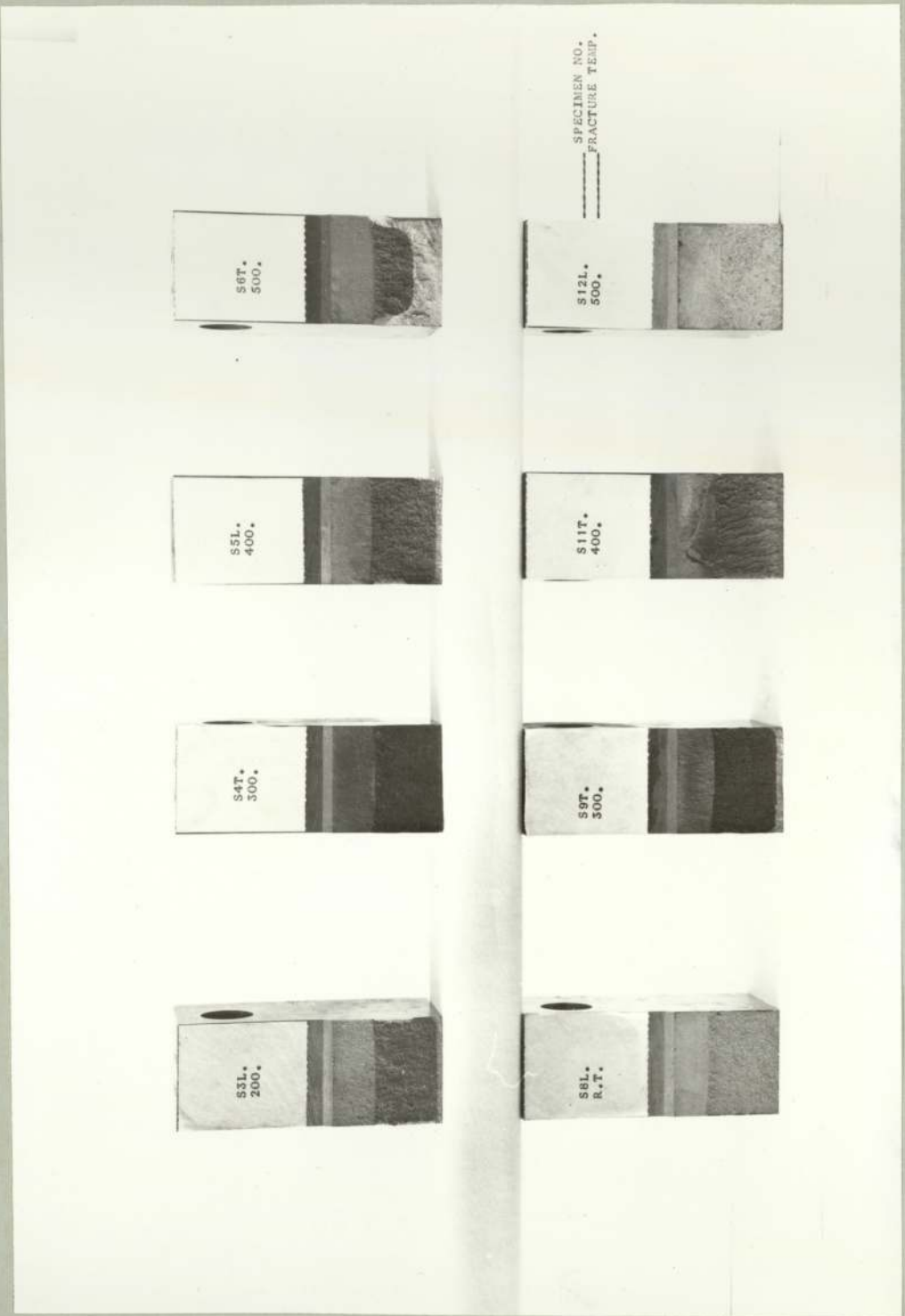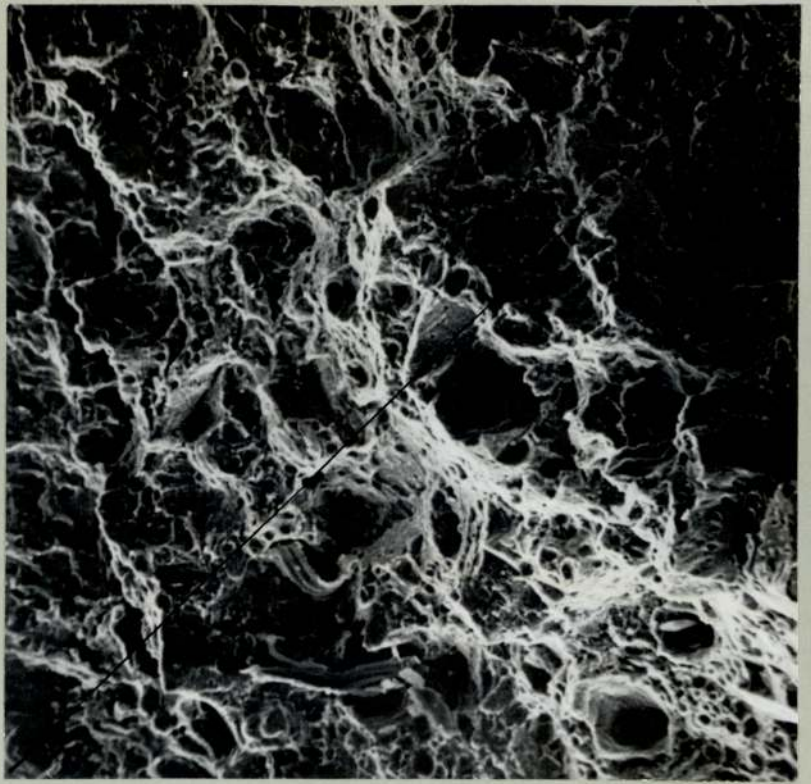
Sample 1B1L.    Room temperature        x 300



Sample 1B5L.    Tested at $200^{o}$C.        x 300

Fig -46-

Sample 1B7L.

Tested at 300°C.          x 300
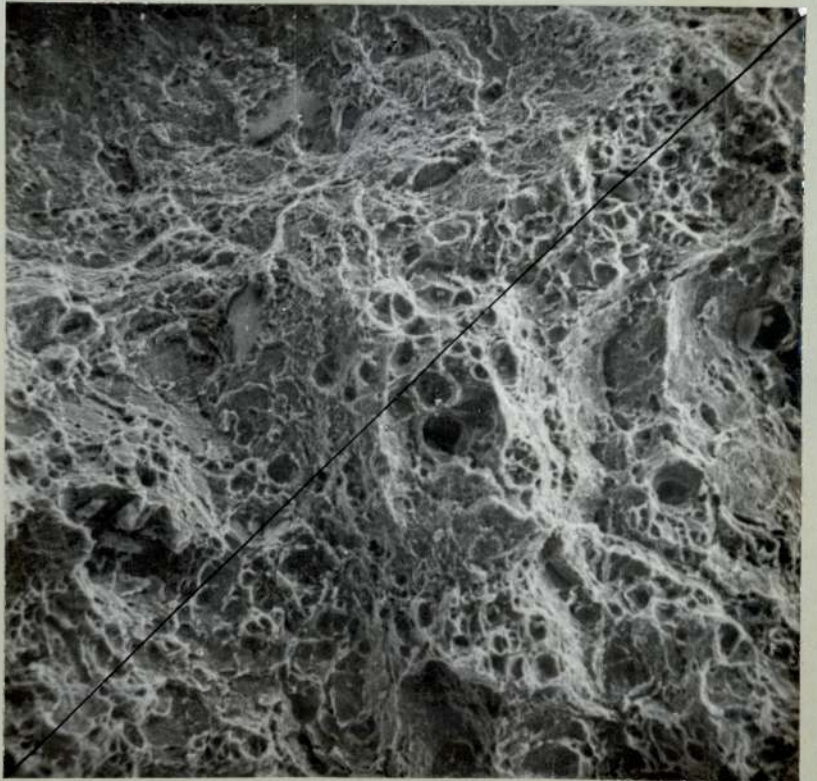


Sample 1B9L.

Tested at 400°C.          x 300

Fig -47-

Sample 1B1L.

Tested at room temperature.
x 120.



Sample 1B5L.

Tested at 200°C.

x 70
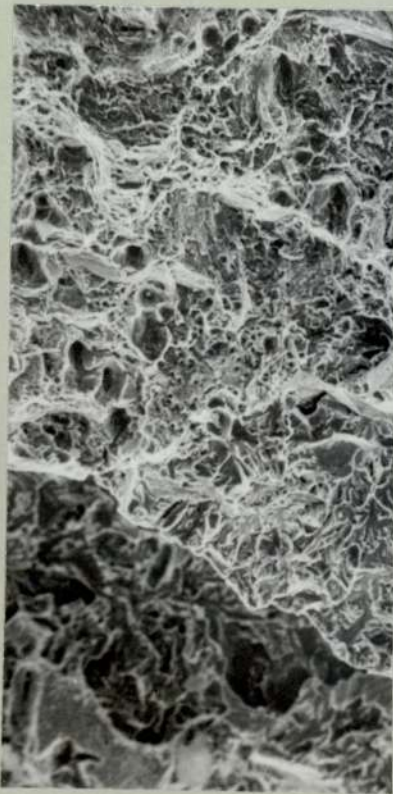


Sample 1B7L.

Tested at 300°C.
x 210



Sample 1B9L.

Tested at 400°C.

x 120

Fig -48-

Sample 1B2T.

Tested at room temperature.
x 240.



Sample 1B4T.

Tested at 100°C.     x 240



Sample 1B6T.

Tested at 200°C.    x 130

Fig -49-

Sample 1A1L.

Tested at room temperature.
x260



Sample 1A5L.

Tested at 200°C.

x 120
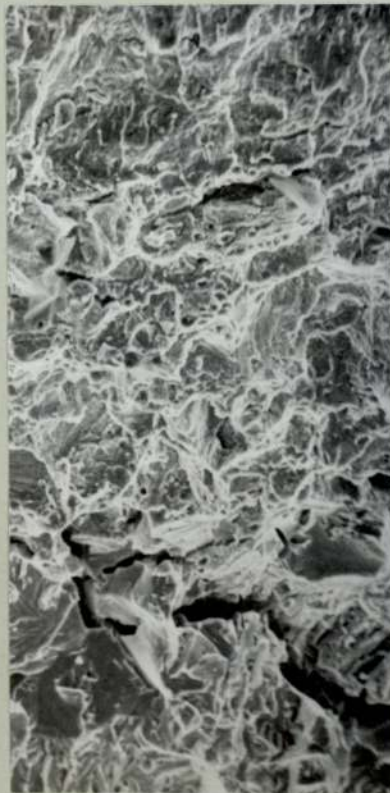


Sample 1A3L.

Tested at 100°C.    x 270



Sample 1A5L.

Tested at 200°C.    x 130

Fig -50-
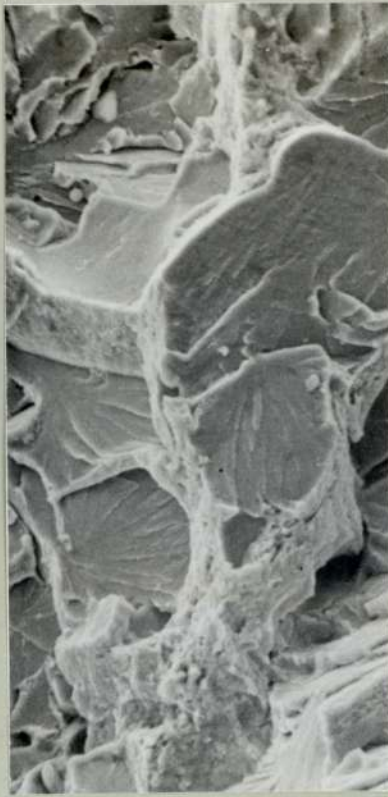
Sample 1A2T.
Tested at room temperature.
x 650.



Sample 1A4T.
Tested at 100°C.
x 240.
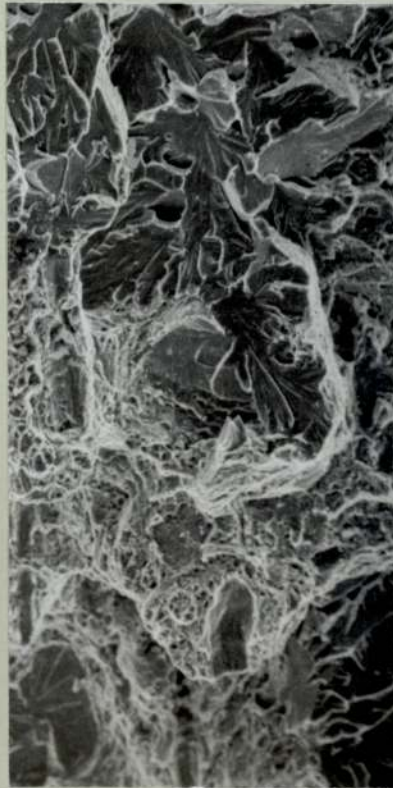


Sample 1A4T.
Tested at 100°C.
x 240.



Sample 1A6T.
Tested at 200°C.
x 70.

Fig -51-

Specimen S3L.

Tested at $200^{\circ}$C.

x 600

Fig -52-



Specimen S2T.

Tested at $100^{\circ}$C.

x 650

Sample 1A1L.
Tested at
room
temperature.

x 2,700



Sample 1B1L.
Tested at
room
temperature.
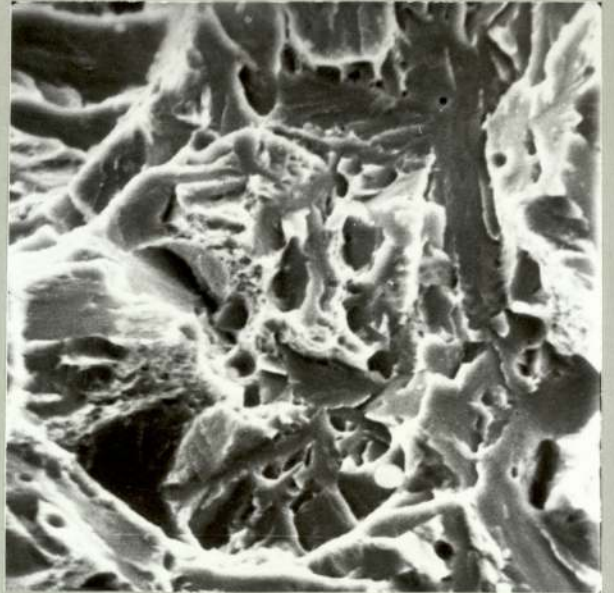
x 2,700



Sample 1B5L.
Tested at
200°C.

Fig -53-
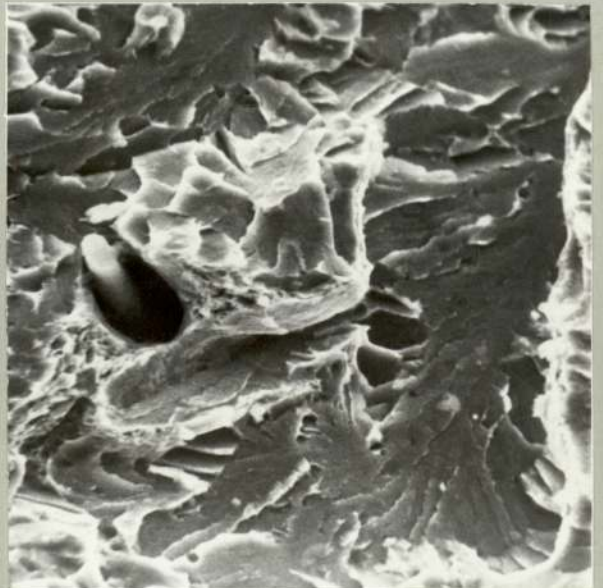
x 2,700

Sample 1B7L.
Tested at
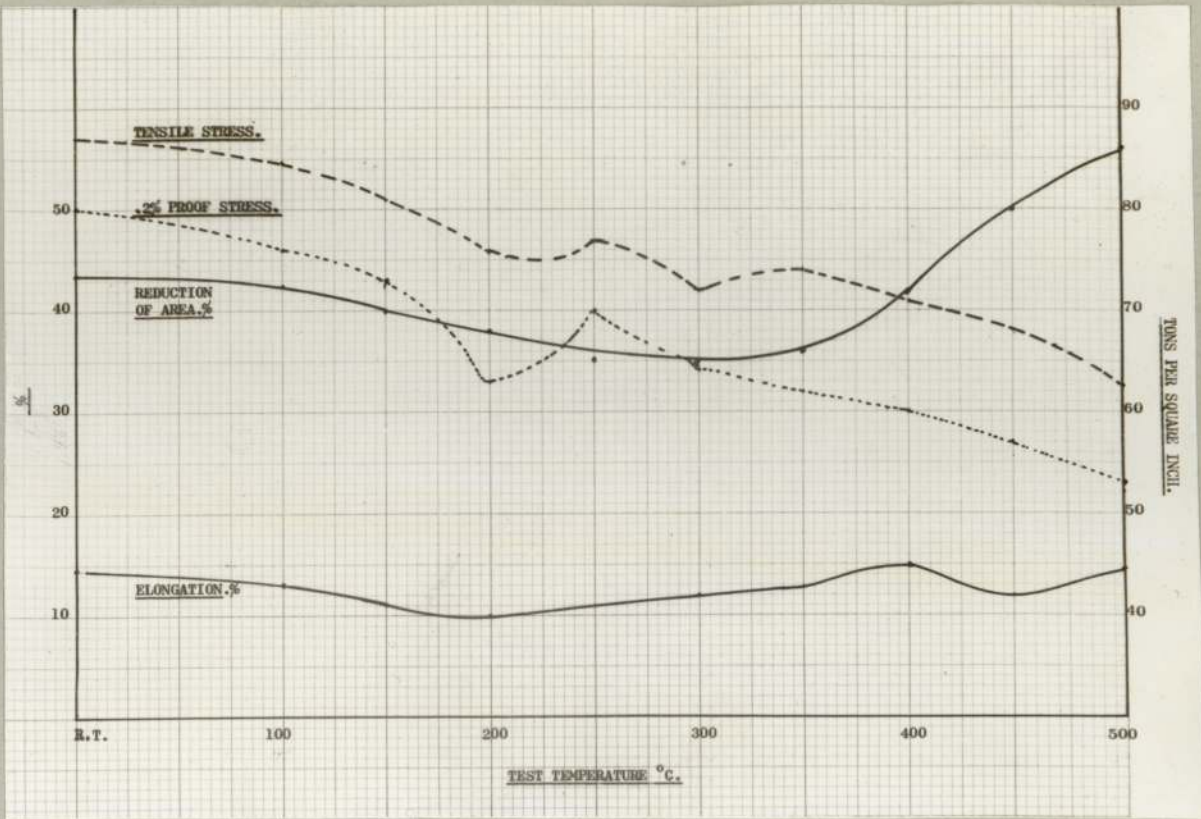300°C.
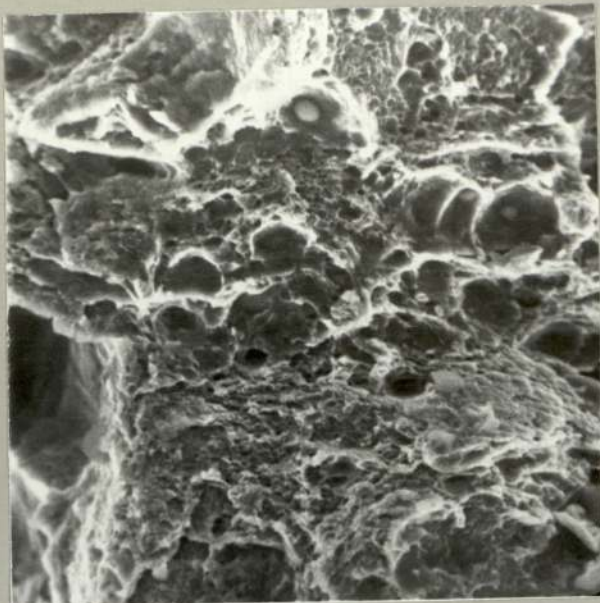
x 2,700



Sample 1B9L.
Tested at
400°C.

x 2,700



Round notch
tensile.
Tested at
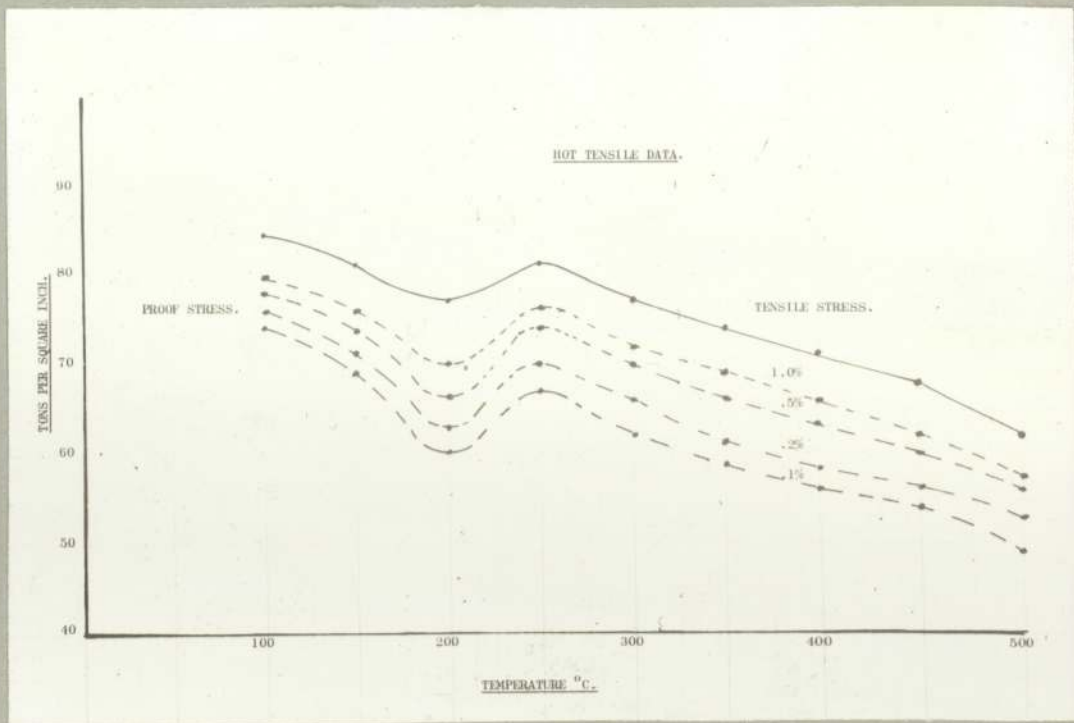500°C.

x 2,700

Fig -54-

HOT TENSILE DATA.

Fig -55-



Fig -56-